APPLICATIONS OF VINE COPULAS IN COMMODITY RISK MANAGEMENT AND PRICE ANALYSIS

A Dissertation

by

KUNLAPATH SUKCHAROEN

Submitted to the Office of Graduate and Professional Studies of
Texas A&M University
in partial fulfillment of the requirements for the degree of

DOCTOR OF PHILOSOPHY

Chair of Committee,	David J. Leatham
Co-Chair of Committee,	David A. Bessler
Committee Members,	Henry L. Bryant
	James W. Kolari
Head of Department,	C. Parr Rosson III

August 2017

Major Subject: Agribusiness and Managerial Economics

ABSTRACT

This dissertation consists of three studies that focus on applications of vine copulas, a relatively new class of multivariate copula approach, in commodity risk management and price analysis. The first study proposes a vine copula approach to estimate multiproduct hedge ratios that minimize the risk of refining margin erosion – the downside risk facing a typical oil refinery whose profit greatly depends on its refining margin or the difference between the prices of its refined products and the cost of crude oil. The out-of-sample hedging effectiveness of two popular classes of vine copula models – canonical (C-) and drawable (D-) vine copula models – are evaluated and compared with that of a widely used nonparametric method and three standard multivariate copula models. The empirical results reveal that the D-vine copula model seems to be a good and safe choice in managing the downside risk of the refinery.

The second study explores the importance of modeling heterogeneous dependence structures between different pairs of energy commodity returns with vine copulas in improving one-step-ahead density forecasts of these returns. The value of modeling heterogeneous dependence structures is measured by comparing the performance of density forecasts based on vine copulas with density forecasts based on standard copulas that assume homogeneous dependence structures. The empirical results suggest that modeling heterogeneous dependence structures using vine copulas does not help improve quality of multivariate density forecasts of energy commodity returns.

The third study applies a vine copula approach to analyze the dependence structure and tail dependence patterns among daily prices of three agricultural commodities (corn, soybean, and wheat) and two energy commodities (ethanol and crude oil) from June 2006 to June 2016. Our findings suggest that the prices of corn and crude oil are linked through the ethanol market. We also find that crude oil and agricultural commodity prices are statistically dependent during the extreme market downturns but independent during the extreme market upturns. Moreover, the results from our sub-sample analysis show that both the upper and lower tail dependence between crude oil and other commodity markets become weaker in the recent years when the ethanol market became more mature.

DEDICATION

To my mother, Praparut Sukcharoen, and my father, Pison Sukcharoen

ACKNOWLEDGEMENTS

First and foremost, I would like to express my deepest gratitude to my advisor, Dr. David Leatham, for seeing my potential and for supporting me during these past four years. I am thankful for his invaluable support, guidance and understanding. I would also like to thank my committee co-chair, Dr. David Bessler, and my committee members, Dr. Henry Bryant and Dr. James Kolari, for their guidance and feedback throughout the course of this research. I am also indebted to Dr. Ximing Wu, Dr. Henry Bryant, Dr. Dmitry Vedenov, Dr. Reid Stevens, and Dr. Desmond Ng for their encouragement and support during my job searching process. In addition, my special thanks go to Dr. Frederick Boadu for giving me the opportunity to teach a course while at Texas A&M University, and for supporting me in the toughest times during my Ph.D. journey.

I thank Panit Arunanondchai for his constant support, immense understanding, and endless encouragement. Thank you for always being there for me and for helping me through difficult times. I would like to express my thanks to my lifelong friends: Pailin Ngamchutham and Pasita Chaijaroen for their unfailing moral support. Thanks also go to my fellow friends in the Ph.D. program and the department faculty and staff for making my time at Texas A&M University a great experience.

Last but not least, I would like to thank to my mother, my father and my brother for their unconditional love and support. I consider myself the luckiest in the world to have such an understanding family, giving me the strength and support to pursue my dreams. For that I am forever thankful.

CONTRIBUTORS AND FUNDING SOURCES

Contributors

This work was supervised by a dissertation committee consisting of Dr. David Leatham [advisor], Dr. David Bessler [co-advisor] and Dr. Henry Bryant of the Department of Agricultural Economics and Dr. James Kolari of the Department of Finance.

All work for the dissertation was completed by the student, under the advisement of Dr. David Leatham and Dr. David Bessler of the Department of Agricultural Economics.

Funding Sources

Graduate study was supported by a graduate assistantship from the Department of Agricultural Economics at Texas A&M University.

TABLE OF CONTENTS

Page

ABSTRACT ii

DEDICATION iv

ACKNOWLEDGEMENTS v

CONTRIBUTORS AND FUNDING SOURCES vi

TABLE OF CONTENTS vii

LIST OF FIGURES ix

LIST OF TABLES xi

CHAPTER I INTRODUCTION 1

CHAPTER II HEDGING DOWNSIDE RISK OF OIL REFINERIES WITH VINE COPULAS 4

- 2.1 Introduction 4
- 2.2 Methodology 11
- 2.3 Data and Preliminary Analysis 21
- 2.4 Empirical Results 27
- 2.5 Conclusions 50

CHAPTER III FORECASTING THE DISTRIBUTIONS OF ENERGY COMMODITY RETURNS: THE IMPORTANCE OF MODELING HETEROGENEOUS DEPENDENCE STRUCTURES 54

- 3.1 Introduction 54
- 3.2 Data 57
- 3.3 Methodology 60
- 3.4 Empirical Results 78
- 3.5 Conclusions 96

CHAPTER IV MEASURING TAIL DEPENDENCE BETWEEN AGRICULTURAL AND ENERGY COMMODITY MARKETS: A REGULAR VINE COPULA METHOD 99

4.1 Introduction 99
4.2 Data 103
4.3 Methodology 105
4.4 Empirical Results 114
4.5 Conclusions 121

CHAPTER V SUMMARY 124

REFERENCES 127

APPENDIX A SUPPLEMENTARY RESULTS FOR CHAPTER II 143

APPENDIX B SUPPLEMENTARY RESULTS FOR CHAPTER III 146

LIST OF FIGURES

Page

Figure 2.1. Weekly crude oil spot prices, gasoline spot prices, heating oil spot prices, and 3:2:1 refining margin (unhedged) 5

Figure 2.2. Six-dimensional C-vine trees 17

Figure 2.3. Six-dimensional D-vine trees 18

Figure 2.4. Weekly changes in petroleum spot and futures prices for the period January 7, 1987 to December 30, 2015 23

Figure 2.5. Time-varying Kendall's Tau (Kendall's rank correlation) between weekly price changes in spot and its corresponding futures markets (estimated with 261-week rolling window) 26

Figure 2.6. Out-of-sample hedging effectiveness: percentage reductions in Semivariance 35

Figure 2.7. Out-of-sample hedging effectiveness: percentage reductions in Lower Partial Moment 37

Figure 2.8. Out-of-sample hedging effectiveness: percentage reductions in Value at Risk at the 90% confidence level 40

Figure 2.9. Out-of-sample hedging effectiveness: percentage reductions in Value at Risk at the 95% confidence level 41

Figure 2.10. Out-of-sample hedging effectiveness: percentage reductions in Value at Risk at the 99% confidence level 43

Figure 2.11. Out-of-sample hedging effectiveness: percentage reductions in Expected Shortfall at the 90% confidence level 44

Figure 2.12. Out-of-sample hedging effectiveness: percentage reductions in Expected Shortfall at the 95% confidence level 46

Figure 2.13. Out-of-sample hedging effectiveness: percentage reductions in Expected Shortfall at the 99% confidence level 47

Figure 3.1. Time-varying linear correlation between weekly crude oil and other energy commodity returns (estimated with a 104-week rolling window) 61

Figure 3.2. Four-dimensional canonical vine copula (CVC) 65

Figure 3.3. Four-dimensional drawable vine copula (DVC) 66

Figure 3.4. Four-dimensional regular vine copula (RVC) 67

Figure 3.5. Calibration plots for the density forecasts of crude oil returns based on the canonical vine copula (CVC), drawable vine copula (DVC), regular vine copula (RVC), standard Gaussian copula (SGC), and standard Student's t copula (SSC) models with Student's t marginal distributions 80

Figure 3.6. Calibration plots for the density forecasts of diesel fuel returns based on the canonical vine copula (CVC), drawable vine copula (DVC), regular vine copula (RVC), standard Gaussian copula (SGC), and standard Student's t copula (SSC) models with Student's t marginal distributions 81

Figure 3.7. Calibration plots for the density forecasts of gasoline returns based on the canonical vine copula (CVC), drawable vine copula (DVC), regular vine copula (RVC), standard Gaussian copula (SGC), and standard Student's t copula (SSC) models with Student's t marginal distributions 82

Figure 3.8. Calibration plots for the density forecasts of heating oil returns based on the canonical vine copula (CVC), drawable vine copula (DVC), regular vine copula (RVC), standard Gaussian copula (SGC), and standard Student's t copula (SSC) models with Student's t marginal distributions 83

Figure 3.9. Calibration plots for the density forecasts of jet fuel returns based on the canonical vine copula (CVC), drawable vine copula (DVC), regular vine copula (RVC), standard Gaussian copula (SGC), and standard Student's t copula (SSC) models with Student's t marginal distributions 84

Figure 3.10. Calibration plots for the density forecasts of natural gas returns based on the canonical vine copula (CVC), drawable vine copula (DVC), regular vine copula (RVC), standard Gaussian copula (SGC), and standard Student's t copula (SSC) models with Student's t marginal distributions 85

Figure 3.11. Calibration plots for the density forecasts of propane returns based on the canonical vine copula (CVC), drawable vine copula (DVC), regular vine copula (RVC), standard Gaussian copula (SGC), and standard Student's t copula (SSC) models with Student's t marginal distributions 86

Figure 4.1. Estimated R-vine copula structure with 1 = Ethanol, 2 = Corn, 3 = Soybean, 4 = Oil, and 5 = Wheat 110

LIST OF TABLES

Page

Table 2.1. Summary statistics and correlation analysis on weekly changes in spot and futures prices 24

Table 2.2. Average log-likelihood (LLH), Akaike Information Criterion (AIC), and Bayesian Information Criterion (BIC), and number of parameters for the multivariate copula models 29

Table 2.3. Average optimal hedge ratios (with standard deviations in parentheses) of different hedging models and hedging objectives 32

Table 2.4. Out-of-sample hedging effectiveness of different hedging models and hedging objectives 33

Table 3.1. Summary statistics and correlation analysis on weekly spot returns for crude oil (CO), diesel fuel (DF), gasoline (GL), heating oil (HO), jet fuel (JF), natural gas (NG), and propane (PP) 58

Table 3.2. Average log-likelihood (LLH), Akaike Information Criterion (AIC), Schwarz's Bayesian Information Criterion (BIC), and number of parameters for the five multivariate copula models 77

Table 3.3. Pearson's chi-square test statistic 87

Table 3.4. Anderson-Darling (AD) test of normality 89

Table 3.5. Test of independence of the probability integral transform (PIT) series 91

Table 3.6. Berkowitz (2001) likelihood ratio (LR1) test of independence 92

Table 3.7. Tests of equal predictive accuracy between two copula models 93

Table 3.8. Tests of equal predictive accuracy between two copula models for two sub-periods 94

Table 4.1. Summary statistics and correlation analysis on daily log returns on the futures contracts of corn, soybean, wheat, ethanol, and oil 104

Table 4.2. Results for the marginal distributions 113

Table 4.3. Tests of the marginal distribution specifications 115

Table 4.4. Results for the regular vine copula models 116

Table 4.5. Upper and lower tail dependence coefficients 120

CHAPTER I

INTRODUCTION

Accurate and realistic modeling of multivariate distributions is commonly perceived to be of great importance for reliable risk assessments and sound risk management strategies. For a long time, the modeling of high-dimensional joint distributions has been limited to the use of elliptical distributions (mainly multivariate normal and multivariate Student's t distributions) due to the lack of suitable alternative multivariate distributions. However, these elliptical distributions are not able to capture features such as asymmetric and heterogeneous dependence among multiple risk factors.

Over the last decade, vine copulas have been touted as the most promising and flexible tool for modeling multivariate distributions. This is particularly due to their ability to describe complex dependence relationships among multiple data series. Given the potentially complex (asymmetric and heterogeneous) dependence patterns among commodity markets, this dissertation considers the applications of vine copulas in the field of risk management. In particular, this dissertation consists of three stand-alone but related empirical studies on applications of vine copulas in the context of commodity risk management and price analysis.

The first study (Chapter II), titled "Hedging Downside Risk of Oil Refineries with Vine Copulas," examines the use canonical and drawable vine copulas in deriving optimal multiproduct hedge ratios for oil refineries in a downside risk framework. Focusing on the problem of hedging downside risk of oil refineries, we ask if the more

advanced vine copula models can produce better out-of-sample hedging outcomes than a widely used nonparametric method and three standard multivariate copula models. We answer this question by evaluating the hedging effectiveness of each model based on its ability to reduce downside risk over a number of out-of-sample test windows. To ensure the robustness of the results, four alternative measures of downside risk, including Semivariance, Lower Partial Moment, Value at Risk and Expected Shortfall, are considered.

The second study (Chapter III), titled "Forecasting the Distributions of Energy Commodity Returns: An Importance of Modeling Heterogeneous Dependence Structures," explores the potential of vine copulas in forecasting the distributions of multiple energy commodity returns. More specifically, this study analyzes the value of modeling heterogeneous dependence structures between different pairs of energy commodity returns using vine copulas in improving one-step-ahead density forecasts of these returns. The importance of heterogeneous dependence structures for density forecasting is then measured by comparing the performance of density forecasts based on three types of vine copulas – canonical, drawable, and regular vine copulas – with density forecasts based on two standard copulas that assume homogeneous dependence structures – Gaussian and Student's t copulas. The forecast quality of the competing density models is assessed and compared based on both calibration and equal predictive accuracy tests.

The third study (Chapter IV), titled "Measuring Tail Dependence between Agricultural and Energy Commodity Markets: A Regular Vine Copula Method," uses a

regular vine copula method to analyze the price dependence patterns among agricultural and energy commodity markets. In particular, the regular vine copula method is used to study the dependence structure and tail dependence patterns of daily futures prices of three agricultural commodities – corn, soybean, and wheat – and two energy commodities – ethanol and crude oil from June 2, 2006 to June 30, 2016. This study also examines whether and how the dependence structure and degree of tail dependence evolve between the two periods of ethanol production: the rapid growth (June 2006 to June 2011) and slowing growth (June 2011 to June 2016). The findings from the three studies should provide valuable information for practitioners, academics, and policy makers regarding the use of vine copulas in commodity risk management and price analysis.

CHAPTER II

HEDGING DOWNSIDE RISK OF OIL REFINERIES WITH VINE COPULAS

2.1 Introduction

A typical oil refinery purchases crude oil (the primary input in refinery operations) and sells refined products (e.g., gasoline and heating oil). Its refining margin (or the profit margin) is then related to the spread between the prices of refined products and the price of crude oil. There is, however, no clear relationship between the refining margin and the prices of petroleum. Rising crude oil price does not necessarily tighten the refining margin if the prices of refined products also increase proportionally to the rise in crude oil price. In such an environment, the refinery suffers from the increase in the crude oil price (downside risk) but at the same time benefits from the rise in refined product prices (upside risk). As a result, hedging does not seem to be necessary.

Unfortunately, it is also possible that, for example, the prices of refined products remain static or (even worse) decline when the price of crude oil increases. In this case, the refinery faces significant downside risks in both crude oil and refined product markets. In particular, since late 2005, a large decline in the refining margin (due to the simultaneous adverse movements in the petroleum prices) has appeared to be more common (Figure 2.1). The risk of losses because of unfavorable petroleum price movements clearly signifies the importance of hedging the joint downside risks of input and output prices. Accordingly, the goal of this chapter is to develop a multiproduct

futures hedging model that minimizes the downside risk of the refinery (or the risk of profit margin erosion)[1].

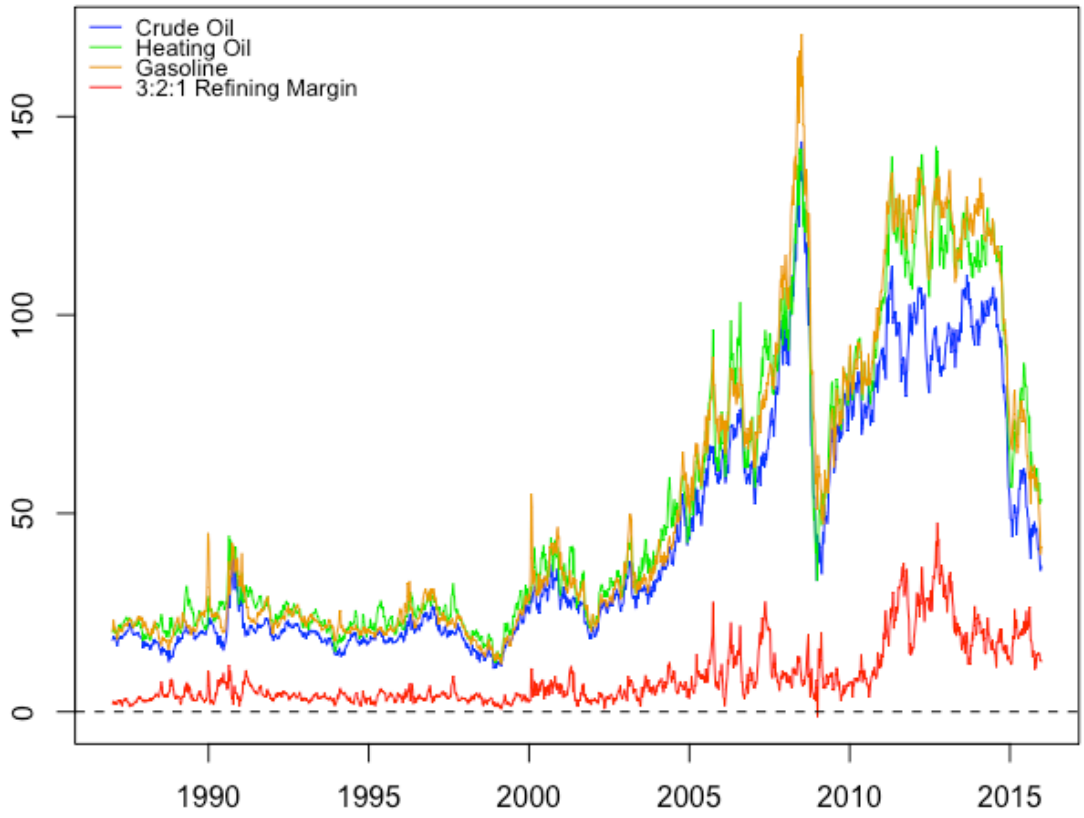

Figure 2.1. Weekly crude oil spot prices, gasoline spot prices, heating oil spot prices, and 3:2:1 refining margin (unhedged)

[1] Multiproduct hedging involves the use of multiple futures contracts to hedge exposures to price risks in multiple commodities. In this study, crude oil, gasoline, and heating oil futures are used simultaneously to hedge the refining company's exposures to adverse price movements in the crude oil, gasoline, and heating oil spot markets. In contrast, single-product hedging uses a single futures contract to hedge a spot position in a particular commodity market.

Solving for the minimum-downside risk hedge ratios requires the estimation of the entire joint distribution of spot and futures price changes (or returns). For single-product hedging, the standard practice is to rely on a nonparametric method – in particular, the empirical distribution or historical simulation method (Lien and Tse 2000, 2001; Demirer and Lien 2003; Harris and Shen 2006). This approach is very flexible and could be easily extended to the case of multiproduct hedging[2]. However, it often produces inaccurate estimates of extreme quantiles due to its heavy dependence on historical data (McNeil and Frey 2000; Pritsker 2006; Cao, Harris, and Shen 2010). Recently, Barbi and Romagnoli (2014) propose a standard bivariate Archimedean copula model for estimating downside-risk hedge ratios in a single-product setting. They show that their proposed method produces superior hedging performance to the nonparametric approach. The superior performance of the Archimedean copula model may be attributed to its ability to capture both univariate and dependence asymmetries typically found in the asset returns[3]. Such asymmetries are also found in crude oil and refined product markets (Hammoudeh, Li, and Jeon 2003; Grégoire, Genest, and Gendron 2008; Chang, McAleer, and Tansuchat 2010; Ji and Fan 2011; Serra and Gil 2012; Aloui et al. 2014).

Against this background, we believe that modeling the joint distribution more realistically is crucial for hedging the downside risk of the refinery. As such, we propose to combine a vine copula model with Monte Carlo simulation to construct the joint

---

[2] See, for example, Harlow (1991), Agarwal and Naik (2004), Gaivoronski and Pflug (2005), Adam, Houkari and Laurent (2008), and Quaranta and Zaffaroni (2008) for studies on portfolio optimization in a downside-risk framework that apply the nonparametric method.

[3] The evidence of asymmetries in asset returns has been well documented in many studies, including Ang and Chen (2002), Patton (2006), Ammann and Süss (2009), and Reboredo (2012b).

distribution of spot and futures price changes[4]. The vine copula model, initially introduced by Joe (1996) and first estimated by Kurowicka and Cooke (2006), is a relatively new class of multivariate copula models. Similar to the standard multivariate copula models (e.g., the standard Gaussian, Student's t, and Archimedean copula models), the vine copula model is able to account for the asymmetry in the univariate distributions. This is because the model allows one to separate the modeling of the marginal distributions from the dependence structure that links these marginal distributions to form a joint distribution. However, while the standard copula models require all pairs of variables to have the same dependence structure, the vine copula model permits different dependence specifications for different pairs of variables[5]. It thus provides greater flexibility in capturing the complex dependence structure in the petroleum markets[6].

In particular, the proposed hedging model builds the joint distribution of multiple variables using an empirical distribution function for the marginal distributions and two different classes of vine copulas – the canonical (C-) and drawable (D-) vine copulas (Kurowicka and Cooke 2005) – for the dependence structure[7]. The C- and D-vine copula models are estimated using a sequential maximum likelihood procedure proposed by Aas

---

[4] Following Haigh and Holt (2002) and Alexander, Prokopczuk, and Sumawong (2013), our hedging analysis is based on the price changes instead of the log returns or percentage returns. The reasons for why the price changes should be used are discussed in Alexander, Prokopczuk, and Sumawong (2013).

[5] Details about the limitations of the standard multivariate copula models are discussed in Czado (2010) as well as Brechmann and Schepsmeier (2013).

[6] The advantages of the vine copula model for modeling complex dependence patterns have been emphasized by Aas et al. (2009), Czado (2010), and Kurowicka and Joe (2011).

[7] This study uses an empirical distribution function to estimate the marginal distribution of each price change series to allow for the univariate asymmetry while avoiding univariate distribution misspecification.

et al. (2009), and the joint distribution is generated using Monte Carlo simulation. The optimal hedge ratios are then derived through a numerical optimization method for four alternative downside-risk hedging objectives: the minimization of Semivariance (SV), Lower Partial Moment (LPM), Value at Risk (VaR), and Expected Shortfall (ES) of the refinery's hedged margin.

We examine the usefulness of the proposed model through out-of-sample hedging exercises. Specifically, a rolling window approach of Conlon and Cotter (2012, 2013) and Barbi and Romagnoli (2014) is employed. This approach tests the model's hedging effectiveness over a number of out-of-sample test windows, and also allows us to track the evolution of the hedging effectiveness of the proposed model over time. For each hedging objective, the model's hedging effectiveness is defined as its ability to reduce the respective downside risk of the refinery with no-hedging strategy. Overall, both C- and D-vine copula models provide good out-of-sample hedging effectiveness across all hedging objectives, and the D-vine copula model is superior to the C-vine copula model. We also compare the out-of-sample hedging effectiveness of the vine copula models to that of the widely used nonparametric method and three standard multivariate copula models (namely, the standard Gaussian, Student's t, and Clayton copula models)[8]. As expected, the D-vine copula model, on average, provides the largest downside-risk reductions. This is possibly due to its ability to better capture complex (tail) dependence between different pairs of price changes than the other models.

[8] The standard Clayton copula model is a commonly used Archimedean copula model due to its ability to capture lower tail dependence among variables.

This chapter contributes to two main strands of literature. First, it contributes to the literature on multiproduct hedging by estimating multiproduct hedge ratios in a downside-risk framework. Most previous studies in this field have focused on deriving either minimum-variance or mean-variance hedge ratios[9]. However, it is well-known that the variance is not a proper risk measure when asset returns are non-normal because businesses and investors are only concerned with downside risks but not upside risks (Lien and Tse 1998; Unser 2000; Veld and Veld-Merkoulova 2008). Despite the widespread awareness of the non-normality of asset returns, the literature on downside risk hedging in a multiproduct setting is still scarce[10]. One of the few studies is Power and Vedenov (2010) who estimate the minimum-LPM hedge ratios for a feedlot operator (whose profit depends on the prices of corn, feeder cattle, and fed cattle) and compare them with the minimum-variance hedge ratios. Another is Awudu, Wilson, and Dahl (2016) who consider a hedging problem of a corn-based ethanol producer and derive the mean-VaR hedge ratios based on two distributional specifications: multivariate normal and Gaussian copula distributions. This study also develops a multiproduct hedging model in a downside-risk framework. However, we focus on the oil refining industry. Also, we consider four (not only one) alternative measures of downside risk. This allows us to examine the sensitivity of the results vis-à-vis the downside risk measures used.

[9] See, among many others, Leuthold and Peterson (1987), Noussinov and Leuthold (1999), and Tejeda and Feuz (2014) for multiproduct hedging of a cattle feeder; Tzang and Leuthold (1990), Collins (2000), and Tejeda and Goodwin (2014) for multiproduct hedging of a soybean processor; Haigh and Holt (2002), Ji and Fan (2011), and Alexander, Prokopczuk, and Sumawong (2013) for multiproduct hedging of an oil refinery; and Sarassoro and Leuthold (1991), Haigh and Holt (2000), and Wilson, Nganje, and Wagner (2006) for multiproduct hedging of other commodity-based businesses.

[10] Non-normality of petroleum prices and returns are documented in many studies such as Hammoudeh, Li, and Jeon (2003), Chang, McAleer, and Tansuchat (2010), Ji and Fan (2011).

Besides, while none of the two studies evaluate the out-of-sample hedging effectiveness of the methods used, this study analyzes the usefulness of the proposed model through out-of-sample hedging exercises.

Second, this chapter contributes to the growing literature on vine copula models by examining the use of these models in the context of downside-risk hedging. Heretofore, the vine copula methodology has been mostly applied to analyze the dependence structures of financial and commodity markets (e.g., Aas and Berg (2011), Allen et al. (2013), Zhang (2014); Loaiza Maya, Gomez-Gonzalez, and Melo Velandia (2015), and Zimmer (2015)), to forecast VaR and ES of financial portfolios (e.g., Hofmann and Czado (2010), Weiß and Supper (2013), Brechmann, Czado, and Paterlini (2014), Zhang et al. (2014), and Siburg, Stoimenov, and Weiß (2015)), and to analyze asset allocation problems (e.g., Grothe and Schnieders (2011), Low et al. (2013), Riccetti (2013), Wei et al. (2013), and Bekiros et al. (2015)). However, to our best knowledge, no study has examined the use of the vine copula approach in the context of hedging. We address this here. Our findings would benefit oil refineries (as well as other multiproduct hedgers), and provide a richer understanding of the usefulness of vine copulas in risk management.

The remainder of this chapter is organized as follows. Section 2.2.1 presents a hedging problem of an oil refinery. Section 2.2.2 describes the four downside risk measures employed in this study. Section 2.2.3 provides an overview of the empirical procedure. Section 2.3 presents data and preliminary analysis. Section 2.4 reports and

discusses the empirical results, including the model fit, estimated hedge ratios, and out-of-sample hedging effectiveness. Section 2.5 concludes the chapter.

2.2 Methodology

2.2.1 Oil Refinery's Hedging Problem

In the empirical analysis, the stylized problem of a typical oil refinery whose profit depends on the refining margin is considered. We focus on a 3:2:1 refining margin, which approximates the profitability of a typical U.S. refinery that converts 3 barrels of crude oil to 2 barrels of gasoline and 1 barrel of heating oil. The refinery may hedge its exposures to downside risks in the three petroleum markets using crude oil, gasoline and heating oil futures.

Following Haigh and Holt (2002), we assume that the refinery takes futures positions in period $t-1$ (long crude oil futures, and short gasoline and heating oil futures) and liquidates all futures positions in period t (when the purchase of crude oil and the sales of refined products occur). Accordingly, the refinery's hedged margin (or profit per barrel) at time t is:

$$\pi_t(\boldsymbol{b}) = -S_t^C + \frac{2}{3}S_t^G + \frac{1}{3}S_t^H + b_C \Delta F_t^C - \frac{2}{3}b_G \Delta F_t^G - \frac{1}{3}b_H \Delta F_t^H \quad (2.1)$$

where superscripts and subscripts C, G and H refer to crude oil, gasoline and heating oil, respectively; S_t and F_t denote spot and futures prices at time t, respectively; $\Delta F_t = F_t - F_{t-1}$ denotes the changes in futures prices; and $\boldsymbol{b} = \{b_C, b_G, b_H\}$ are hedge ratios determined at time $t-1$. For simplicity, we assume that other costs (e.g., transactions

costs) are deterministic and thus do not affect hedging decisions. Prices at time $t-1$ are known at time t, whereas prices at time t are random (stochastic) variables.

The hedged margin in equation (2.1) can be rewritten in terms of spot and futures price changes:

$$(2.2) \quad \pi_t(\boldsymbol{b}) = -\Delta S_t^C + \frac{2}{3}\Delta S_t^G + \frac{1}{3}\Delta S_t^H + b_C \Delta F_t^C - \frac{2}{3} b_G \Delta F_t^G - \frac{1}{3} b_H \Delta F_t^H + S_{t-1}^{CS}$$

where $\Delta S_t = S_t - S_{t-1}$ denotes the changes in spot prices, and $S_{t-1}^{CS} = -S_{t-1}^C + \frac{2}{3}S_{t-1}^G + \frac{1}{3}S_{t-1}^H$. The last term in equation (2.2), S_{t-1}^{CS}, is known at the time the hedge is initiated, and hence does not cause a variation in the refiner's profit margin at time t. Therefore, similar to Haigh and Holt (2002) and Alexander, Prokopczuk, and Sumawong (2013), we base our hedging analysis on the changes in spot and futures prices. More specifically, we focus on hedging the risky portion of the hedged margin at time t, denoted by:

$$(2.3) \quad \mathrm{y}_t(\boldsymbol{b}) = -\Delta S_t^C + \frac{2}{3}\Delta S_t^G + \frac{1}{3}\Delta S_t^H + b_C \Delta F_t^C - \frac{2}{3} b_G \Delta F_t^G - \frac{1}{3} b_H \Delta F_t^H$$

where $\mathrm{y}_t(\boldsymbol{b}) = \pi_t(\boldsymbol{b}) - S_{t-1}^{CS}$. In Alexander, Prokopczuk, and Sumawong (2013), $\mathrm{y}_t(\boldsymbol{b})$ is known as the hedged (portfolio) profits and losses (P&Ls).

The refinery's objective is then to select the optimal hedge ratios $\boldsymbol{b}^*$ that minimize the downside risk of the hedged P&Ls. Mathematically,

$$(2.4) \quad \boldsymbol{b}^* = \arg\min_{\boldsymbol{b}} Risk\big(y_t(\boldsymbol{b})\big)$$

where $Risk\big(y_t(\boldsymbol{b})\big)$ is the measure of downside risk defined on $y_t(\boldsymbol{b})$. In this study, we consider four standard measures of downside risk: the SV, LPM, VaR, and ES, which we describe in more detail in the next section.

2.2.2 Downside Risk Measures

The first downside risk measure considered is the Semivariance (SV). The SV, introduced in Roy (1952), measures the variability of P&Ls that fall below the target level. It is defined as:

(2.5) $SV = \int_{-\infty}^{c} (c - y_t)^2 dF(y_t)$

where c is the target P&L; y_t is the random P&L; and F is the distribution function of y_t. As the basic goal of hedging is to avoid loss (i.e., y_t being less than zero), we select the target P&L equal to zero (that is, $c = 0$).

The second measure is the nth-order lower partial moment (LPM_n). The LPM_n, proposed by Fishburn (1977), is a generalization of the SV, and is defined as:

(2.6) $LPM_n = \int_{-\infty}^{c} (c - y_t)^n dF(y_t)$

where c is the target P&L; $n > 0$ is the level of hedger's risk tolerance; y_t is the random P&L, and F is the distribution function of y_t. Fishburn (1977) shows that $0 < n < 1$ reflects risk-seeking behavior, $n = 1$ captures risk-neutral behavior, and $n > 1$ corresponds to risk-averse behavior. For the similar reason as above, we assume $c = 0$. In addition, we consider $n = 3$ to focus on a risk-averse hedger.

The third measure is Value-at-Risk (VaR). The VaR measures the largest potential loss over a certain period of time (for this study, over one week) for a particular confidence level (p). More generally, VaR at the confidence level p is given by:

(2.7) $VaR_p = -F^{-1}(1 - p)$

where F is the distribution of y_t. In this study, the VaR is calculated for three different confidence levels: $p = 0.90$, 0.95 and 0.99. Two primary shortcomings of VaR are that it

does not account for losses beyond the VaR value, and that it does not have an additivity property, one of the desirable properties of a risk measure (Artzner et al. 1999).

The forth risk measure is Expected Shortfall (ES), which addresses the stated limitations of VaR. It measures the expected loss given that losses exceed the VaR. The ES at the confidence level p is given as:

(2.8) $ES_p = -E[\mathrm{y_t}|y_t \leq -VaR_p]$

Similar to the VaR, the ES is calculated for $p = 0.90$, 0.95 and 0.99.

2.2.3 Empirical Procedure

Solving for the minimum-SV, minimum-LPM, minimum-VaR, and minimum-ES hedge ratios is technically very demanding. This is because the calculation of SV, LPM, VaR, and ES depends on the entire joint distribution of the six random variables in equation (2.3). In this study, we use a multivariate copula approach to model the joint distribution of random variables.

From Sklar's theorem (Sklar 1959), any n-dimensional multivariate distribution can be constructed from n marginal distributions and a copula that describes the dependence structure. More formally,

(2.9) $F(x_1, x_2 \dots, x_n) = C(F_1(x_1), F_2(x_2), \dots, F_n(x_n))$

where F is a joint distribution of $x_1, x_2, \dots, x_n$ with marginal distributions $F_i = F_i(x_i)$ for $i = 1,2, \dots, n$, and $C: [0,1]^n \rightarrow [0,1]$ is a copula function. Suppose that F_i and C are differentiable. Then, the joint density function is defined as:

(2.10) $f(x_1, x_2 \dots, x_n) = f_1(x_1)f_2(x_2) \cdots f_n(x_n)[c(F_1(x_1), F_2(x_2), \dots, F_n(x_n))]$

where $f_i = f_i(x_i)$ is the (unconditional) density of F_i and c is the density of the copula.

This composition allows one to capture both the asymmetry in each individual marginal distribution and the complex (asymmetric) dependence structure of random variables. As for the choice of copula families, a natural starting point in the modeling of the joint distribution with asymmetric dependence might be any standard Archimedean copulas (typically, a standard Clayton copula). However, standard Archimedean copulas use only one or two parameters to describe the dependence structure among the n random variables and thus may not be able to adequately capture the dependence structure when $n \geq 3$. As a result, a common approach, when dealing with a joint distribution of more than two variables, is to ignore the asymmetric dependence and restrict attention to the elliptical copulas such as Gaussian and Student's t copulas. Nevertheless, the Gaussian and Student's t copulas assume a symmetric dependence structure for all pairs of variables. We could, however, go beyond these standard multivariate copulas by using a vine copula approach, which is a more advanced and flexible alternative method of modeling the dependence structure (Joe 1996; Bedford and Cooke 2001, 2002; Aas et al. 2009).

A vine copula is a multivariate copula that is generated via a cascade of (conditional) bivariate copulas (called pair-copulas) and marginal distribution functions. The idea of the vine copula construction (also known as the pair-copula construction) can be easily illustrated using a three-dimensional case. Without loss of generality, the multivariate density of x_1, x_2, and x_3 can be decomposed into a product of unconditional and conditional densities:

(2.11) $f(x_1, x_2, x_3) = f_1(x_1) f_{2|1}(x_2|x_1) f_{3|1,2}(x_3|x_1, x_2)$

where $f_{i|j,k} = f_{i|j,k}(x_i|x_j, x_k)$. Using the Sklar's theorem, the first conditional density function in equation (2.11) can be written as:

(2.12) $f_{2|1}(x_2|x_1) = \frac{f(x_1,x_2)}{f_1(x_1)} = c_{1,2}\big(F_1(x_1), F_2(x_2)\big) f_2(x_2)$

where $c_{1,2}$ is a copula function linking x_1 and x_2. In a similar manner, the second conditional density can be written as:

(2.13) $f_{3|1,2}(x_3|x_1, x_2) = \frac{f_{2,3|1}(x_2,x_3|x_1)}{f_{2|1}(x_2|x_1)} = c_{2,3|1}\left(F_{2|1}(x_2|x_1), F_{3|1}(x_3|x_1)\right) f_{3|1}(x_3|x_1)$

where $f_{3|1}(x_3|x_1) = c_{1,3}\big(F_1(x_1), F_3(x_3)\big) f_3(x_3)$. Accordingly, the joint density function in equation (2.11) can be decomposed further as:

(2.14) $f(x_1, x_2, x_3) = f_1 f_2 f_3 c_{1,2}(F_1, F_2) c_{1,3}(F_1, F_3) c_{2,3|1}\big(F_{2|1}, F_{3|1}\big)$

where the conditional distribution functions $F_{i|j}\big(x_i|x_j\big)$ can be solved from:

(2.15) $F(x|\boldsymbol{v}) = \frac{\partial C_{x,v_j|\boldsymbol{v}_{-j}}(F(x|\boldsymbol{v}_{-j}),F(v_j|\boldsymbol{v}_{-j}))}{\partial F(v_j|\boldsymbol{v}_{-j})}$

where $C_{x,v_j|\boldsymbol{v}_{-j}}$ is a conditional bivariate copula and $\boldsymbol{v}_{-j}$ is the vector $\boldsymbol{v}$ with the component v_j removed (Joe 1997).

As the decomposition in equation (2.14) is not unique, a difficulty lies in selecting a vine copula specification from a large number of possible vine copula constructions. In this study, we consider two popular classes of vine copula constructions: canonical (C-) and drawable (D-) vine (Kurowicka and Cooke 2005). An n-dimensional (C- or D-) vine is defined by a sequence of $n-1$ trees. The jth tree ($j = 1,2, \dots, n-1$), denoted as T_j, has $n+1-j$ nodes and $n-j$ edges. Edges in T_j

become nodes in T_{j+1}, and the two nodes in T_{j+1} are joined by an edge only if their corresponding edges in T_j share a common node. The last condition is known as the proximity condition (Bedford and Cooke 2001). C- and D-vines are different in how the density function is decomposed.

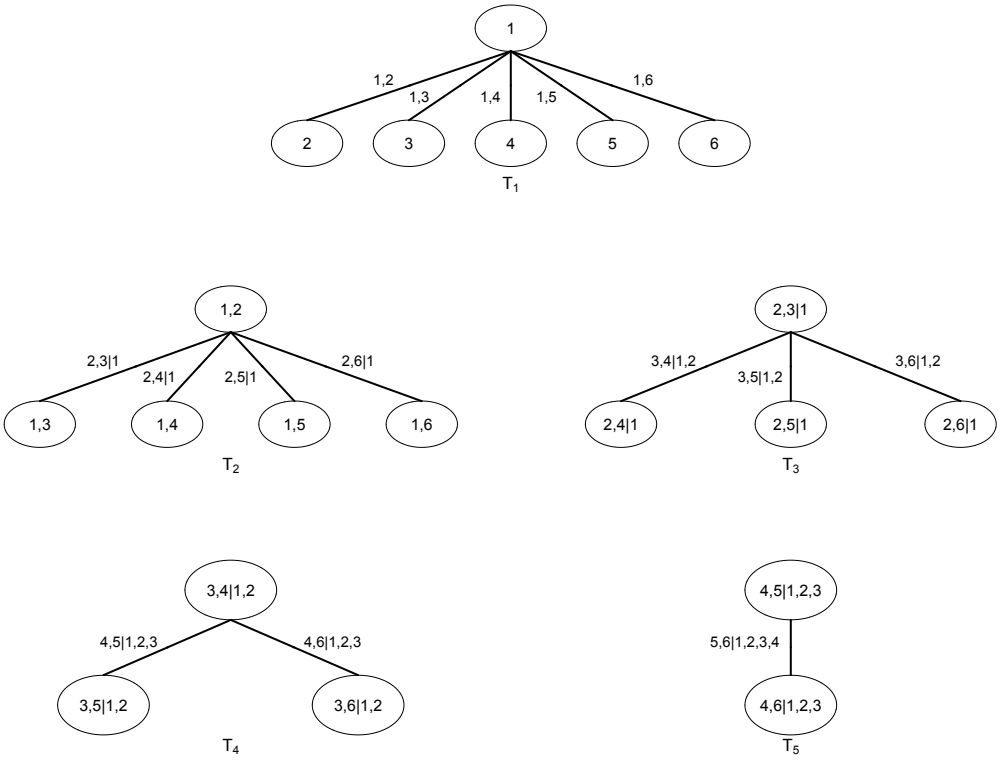

Figure 2.2. Six-dimensional C-vine trees

In this study, we consider the case when $n = 6$. The joint density function of a six-dimensional C-vine copula is given by:

(2.16) $f(x_1, x_2, \dots, x_6) = f_1 f_2 f_3 f_4 f_5 f_6 c_{1,2} c_{1,3} c_{1,4} c_{1,5} c_{1,6} c_{2,3|1} c_{2,4|1} c_{2,5|1} c_{2,6|1} c_{3,4|1,2}$

$$c_{3,5|1,2} c_{3,6|1,2} c_{4,5|1,2,3} c_{4,6|1,2,3} c_{5,6|1,2,3,4}$$

whereas the joint density function of a six-dimensional D-vine copula is given by:

(2.17) $f(x_1, x_2, \dots, x_6) = f_1 f_2 f_3 f_4 f_5 f_6 c_{1,2} c_{2,3} c_{3,4} c_{4,5} c_{5,6} c_{1,3|2} c_{2,4|3} c_{3,5|4} c_{4,6|5} c_{1,4|2,3}$

$$c_{2,5|3,4} c_{3,6|4,5} c_{1,5|2,3,4} c_{2,6|3,4,5} c_{1,6|2,3,4,5}$$

The structures of six-dimensional C- and D-vine copulas are depicted in Figure 2.2 and Figure 2.3, respectively.

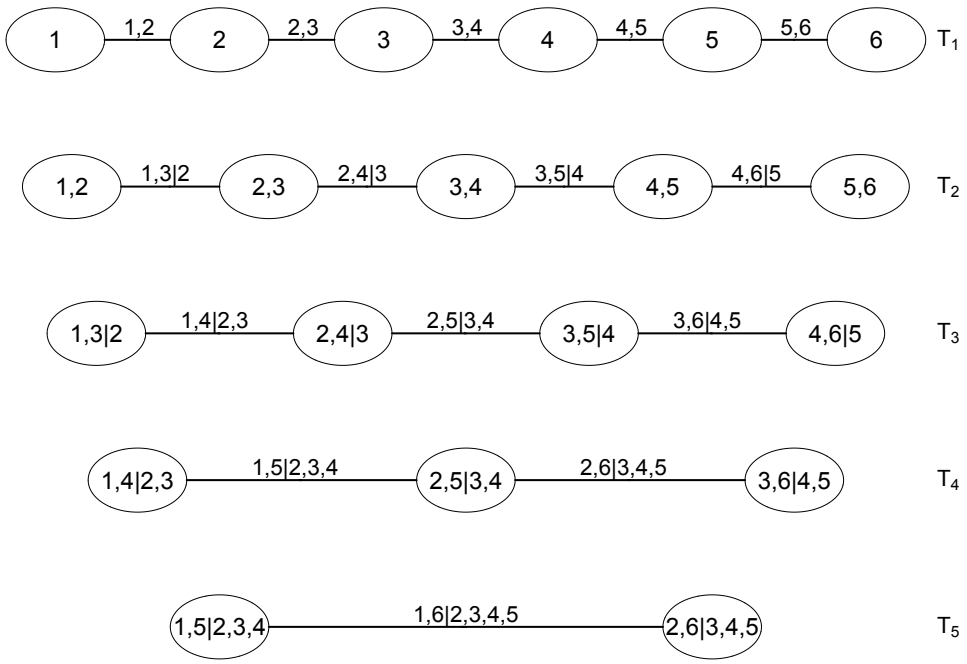

Figure 2.3. Six-dimensional D-vine trees

The procedure for fitting a joint distribution function using the C- or D-vine copula can be briefly summarized in four steps. The first step is to model the marginal distribution. For each price change series, we estimate its marginal distribution using an empirical distribution function and then transform the price change series into copula data (that is, a standard uniform variable)[11]. The second step is to select either the root nodes for each tree of the C-vine copula or the order of the variables in the first tree of the D-vine copula. Following Czado, Schepsmeier, and Min (2012), the root node of each C-vine tree is determined by first estimating all pairwise Kendall's tau coefficients, and then selecting the variable which maximizes the sum of the absolute values of its pairwise Kendall's tau coefficients. For the D-vine structure, we follow Dißmann et al. (2013) and order the variables in the first tree by identifying the shortest Hamiltonian path with one minus absolute value of pairwise Kendall's tau coefficient as a weight.

The third step is to choose a bivariate copula for each pair-copula. This study uses a sequential estimation approach proposed by Aas et al. (2009) with the Akaike Information Criterion (AIC) as a selection criterion (Nikoloulopoulos, Joe, and Li 2012; Dißmann et al. 2013; Weiß and Supper 2013). We consider 31 different parametric

[11] It should be noted that the marginal distribution could also be estimated using a parametric estimation method. In this study, each marginal distribution is estimated nonparametrically in order to avoid the possible misspecification of parametric distributions (Charpentier, Fermanian, and Scaillet 2007). Similar to Bouyè and Salmon (2009), Power and Vedenov (2010), and Barbi and Romagnoli (2014), the marginal distributions are estimated using the unfiltered data. Other studies first apply a GARCH filter to the original data and then model the dependence structure of the filtered series (see, for example, Hsu, Tseng, and Wang (2008), Lee (2009), and Sukcharoen, Choi, and Leatham (2015) for studies on copula-based hedge ratios). An advantage of using the unfiltered data is that it allows us to avoid the first-stage estimation errors – the errors in the estimation of conditional mean and variance models, which could lead to the copula approach being inferior to the nonparametric approach that constructs the distribution functions of random variables directly from the unfiltered data.

bivariate copulas[12]. Then, the final step is to estimate all copula parameters. In particular, the parameters are estimated sequentially starting from the first tree, where the maximum pseudo likelihood method described in Genest, Ghoudi, and Rivest (1995) is employed.

After obtaining the C- and D-vine copula structures and estimating all copula parameters, we compute the four downside risk measures using a Monte Carlo simulation method. More specifically, the estimated vine copula densities are used to generate 10,000 draws of the six standard uniform variables, $\{u_{1,s}, u_{2,s}, \dots, u_{6,s}\}_{s=1}^{10,000}$. For each variable i, these draws are converted to draws from the joint distribution of price changes using its inverse distribution function of the price change series. These simulated spot and futures price changes are then used to compute the refiner's hedged P&Ls in equation (2.3). For each hedging objective, the optimal hedge ratios are then derived by solving the minimization problems in equation (2.4) numerically using the Nelder-Mead direct search method (Nelder and Mead 1965).

This study examines the usefulness of the C- and D-vine copula models in dealing with the downside risk in the refining industry based on their hedging effectiveness. For each hedging objective, the hedging effectiveness is measured as a

[12] This is the maximal list of the R package: CDVine (Brechmann and Schepsmeier 2013). The 31 bivariate copulas include Gaussian, Student's t, Clayton, Gumbel, Frank, Joe, BB1 (Clayton-Gumbel), BB6 (Joe-Gumbel), BB7 (Joe-Clayton), BB8 (Joe-Frank) copulas and the rotated versions (90, 180 and 270 degrees) of Clayton, Gumbel, Joe, BB1, BB6, BB7, and BB8 copulas.

percentage reduction in the downside risk of the hedged P&Ls relative to that of the unhedged P&Ls[13]:

$$\text{(2.18)}\quad \text{HE} = \left(1 - \frac{Risk(y_t(\boldsymbol{b}^*))}{Risk(y_t(\mathbf{0}))}\right) \times 100$$

where $y_t(\boldsymbol{b}^*)$ is the hedged P&L, $y_t(\mathbf{0})$ is the unhedged P&L, and $Risk(\cdot)$ is SV, LPM, VaR, or ES, depending on the hedging objective. We also compare the hedging effectiveness of the vine copula models to that of the nonparametric method and three standard multivariate copula models: namely, the standard Gaussian, Student's t, and Clayton copula models[14].

2.3 Data and Preliminary Analysis

We use weekly Wednesday closing spot and futures prices for West Texas Intermediate (WTI) crude oil, unleaded gasoline, and number 2 heating oil. In the rare cases where Wednesday prices are missing, Tuesday prices are taken instead[15]. All prices are obtained from the Datastream database, and converted into dollars per barrel. The price data span from December 31, 1986 to December 30, 2015, from which a sample of weekly changes in spot and futures prices are constructed[16]. To calculate the

---

[13] This is a variant of the measure of hedging effectiveness proposed by Ederington (1979).

[14] The nonparametric method adopted here is similar to the nonparametric approach by Harlow (1991), Rockafellar and Uryasev (2002), and Lien and Tse (2000). This approach is also known as the historical simulation method or the empirical distribution method.

[15] In the extremely rare cases where both Wednesday and Tuesday prices are missing, Monday prices are taken instead.

[16] Similar to Alexander, Prokopczuk, and Sumawong (2013), prices during the period of abnormal market conditions caused by Hurricane Katrina – from August 29, 2005 to September 9, 2005 – are removed from the analysis. Excluding these data points when estimating optimal hedge ratios is justifiable because the probability of a Katrina-like event occurring in the near future is extremely low. Nevertheless, it is possible that the results regarding hedging effectiveness would change if these data points were included

changes in the futures prices, the closing prices for the nearest-to-expiration futures contracts are used with the rollover occurring on Wednesday a week before the expiry of the contract[17]. At the rollover date, care has been taken to ensure that the changes in futures prices are calculated using the same futures contract. Altogether, this results in a total of 1,511 weekly observations for the changes in spot and futures prices.

Figure 2.4 displays the time-series plots of the weekly changes in the spot and futures prices for the whole sample period. The spot and futures prices are fairly stable during the late 80s and 90s (apart from the 1990 oil price surge trigged by the Iraq's invasion of Kuwait). After the period of relative stability, the volatility of petroleum prices has changed significantly, rising from the year 2000 onwards up until the end of the global financial crisis in 2009 and declining slightly thereafter until the start of the 2014 oil price slump. Extreme fluctuations in crude oil, gasoline and heating oil prices during the last seven to ten years provide a good reason for the oil refineries to hedge adverse input and output price movements.

---

in the evaluation of the hedging models. We therefore perform another analysis where these data points are included in the calculation of out-of-sample hedging effectiveness. We find that the main findings remain valid.

[17] Carchano and Pardo (2009) show that the choice of rollover date to construct the changes in the futures price series is not relevant. Also, the problem of thin market trading is of limited importance because for the commodities under consideration trading continues in high volumes right up to the futures expiration dates.

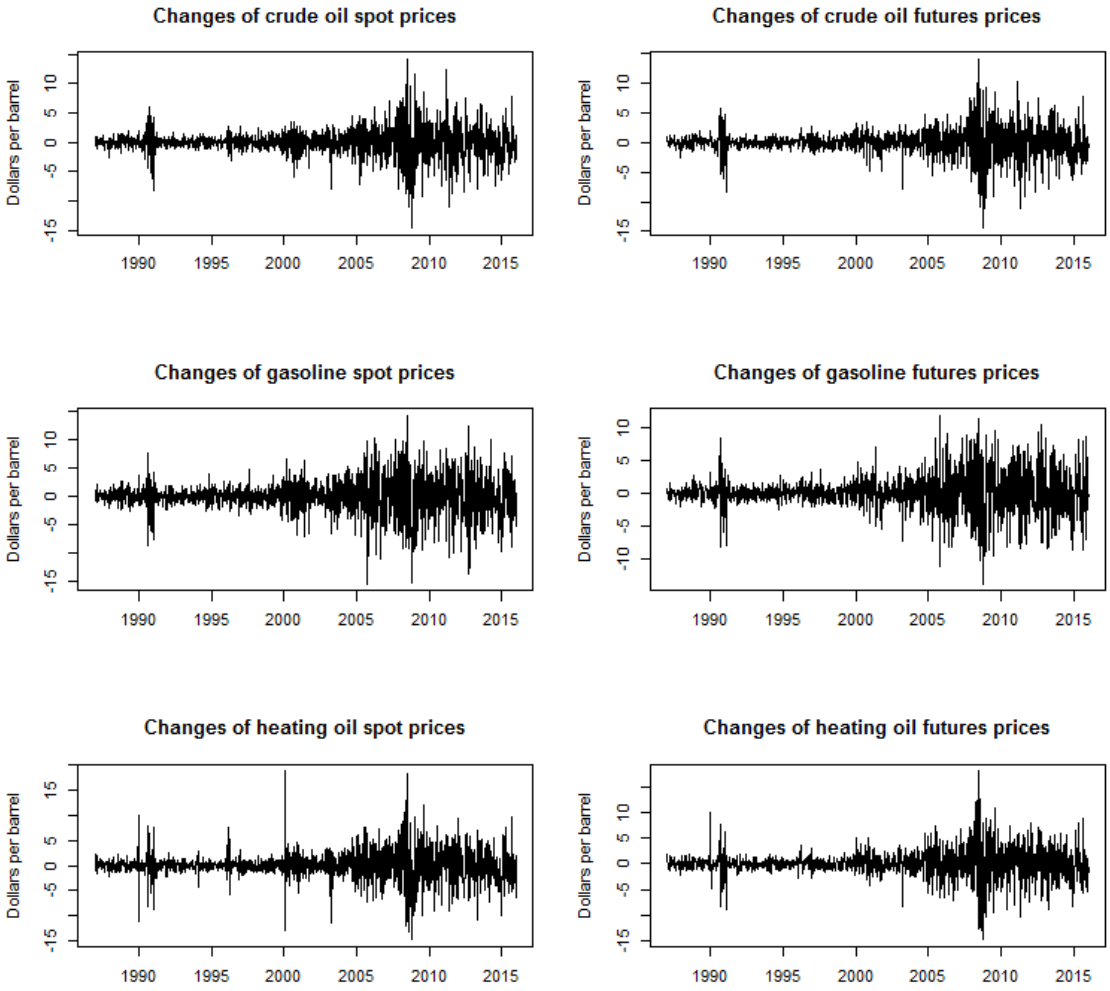

Figure 2.4. Weekly changes in petroleum spot and futures prices for the period January 7, 1987 to December 30, 2015

Table 2.1. Summary statistics and correlation analysis on weekly changes in spot and futures prices

	ΔS^C	ΔS^G	ΔS^H	ΔF^C	ΔF^G	ΔF^H
Panel A: Summary statistics						
Mean	0.0142	0.0134	0.0117	-0.0025	0.1159	0.0176
Min	-14.5600	-15.4812	-14.7756	-14.4100	-13.8600	-14.7840
Max	14.1300	14.3514	18.7320	14.0800	12.0120	18.0180
SD	2.3867	3.1020	2.8298	2.3041	2.8122	2.6611
Skew	-0.1871	-0.3420	0.0723	-0.3192	-0.1731	-0.0245
Ex. Kurt.	5.2186	2.9022	6.1381	5.4535	2.8083	5.6958
J-B	1730.60*	562.64*	2382.80*	1905.80*	506.79*	2050.90*
ADF	-27.1233*	-26.0688*	-27.8727*	-25.8060*	-25.9627*	-26.5328*
Panel B: Correlation matrix						
ΔS^C	1.0000	0.6588	0.7706	0.9774	0.7542	0.8325
ΔS^G		1.0000	0.6597	0.6733	0.9100	0.7015
ΔS^H			1.0000	0.7876	0.7278	0.9479
ΔF^C				1.0000	0.7700	0.8536
ΔF^G					1.0000	0.7907
ΔF^H						1.0000

Notes: Summary statistics (Panel A) and correlation matrix (Panel B) are presented for the weekly changes in the spot and futures prices for the period January 7, 1987 to December 30, 2015. Prices during the weeks of August 29, 2005 and September 9, 2005 are removed from the analysis due to abnormal market conditions caused by Hurricane Katrina. The total number of observations is 1,511 for each price change series. ΔS^C, ΔS^G, ΔS^H, ΔF^C, ΔF^G and ΔF^H denote the changes in crude oil spot, gasoline spot, heating oil spot, crude oil futures, gasoline futures, and heating oil futures prices, respectively. SD, Skew, and Ex. Kurt. represent sample standard deviation, skewness, and excess kurtosis, respectively. J-B is the Jarque-Bera test statistic, where * denotes the rejection of the null hypothesis of normality at the 1% significance level. ADF is the Augmented Dickey-Fuller test statistic, where * denotes the rejection of the null hypothesis that the respective price change series follows a unit root process at the 1% significance level.

Table 2.1 reports summary statistics (Panel A) and correlation matrix (Panel B) for the weekly changes in the spot and futures prices for the entire sample period. For each price change series, the mean is very small relative to its standard deviation. The changes in spot and futures prices of refined products (both gasoline and heating oil) are more volatile than those of raw material (crude oil), and for each commodity the price changes in the spot market is more volatile than the futures market. Each price change

series, except the heating oil spot series, is slightly negatively skewed and exhibit high excess kurtosis, suggesting that the price changes are not normally distributed. The significant Jarque-Bera test statistics for all the price change series confirm that the changes in spot and futures prices do not follow a normal distribution. The Augmented Dicky-Fuller (ADF) tests suggest that all the price change series are stationary. The correlation coefficients of at least 0.6 for all series pairs indicate that, more than half of the time, all the price series move in the same direction. The price changes in the spot and its corresponding futures markets are highly correlated (the correlation coefficients exceed 0.9) indicating that, on average, they have the same change trend. To visualize the evolution of the degree of dependence between spot and futures price changes, time series plots of rolling Kendall's Tau (Kendall's rank correlation) between the weekly price changes in the spot and its corresponding futures markets are presented in Figure 2.5[18]. The plots clearly show that the degree of dependence between the spot and futures price changes varies over time. This indicates that the distributions of price changes are time-varying.

[18] The rolling Kendall's rank correlations are computed using a rolling window of 261 weeks (i.e., 5 years).

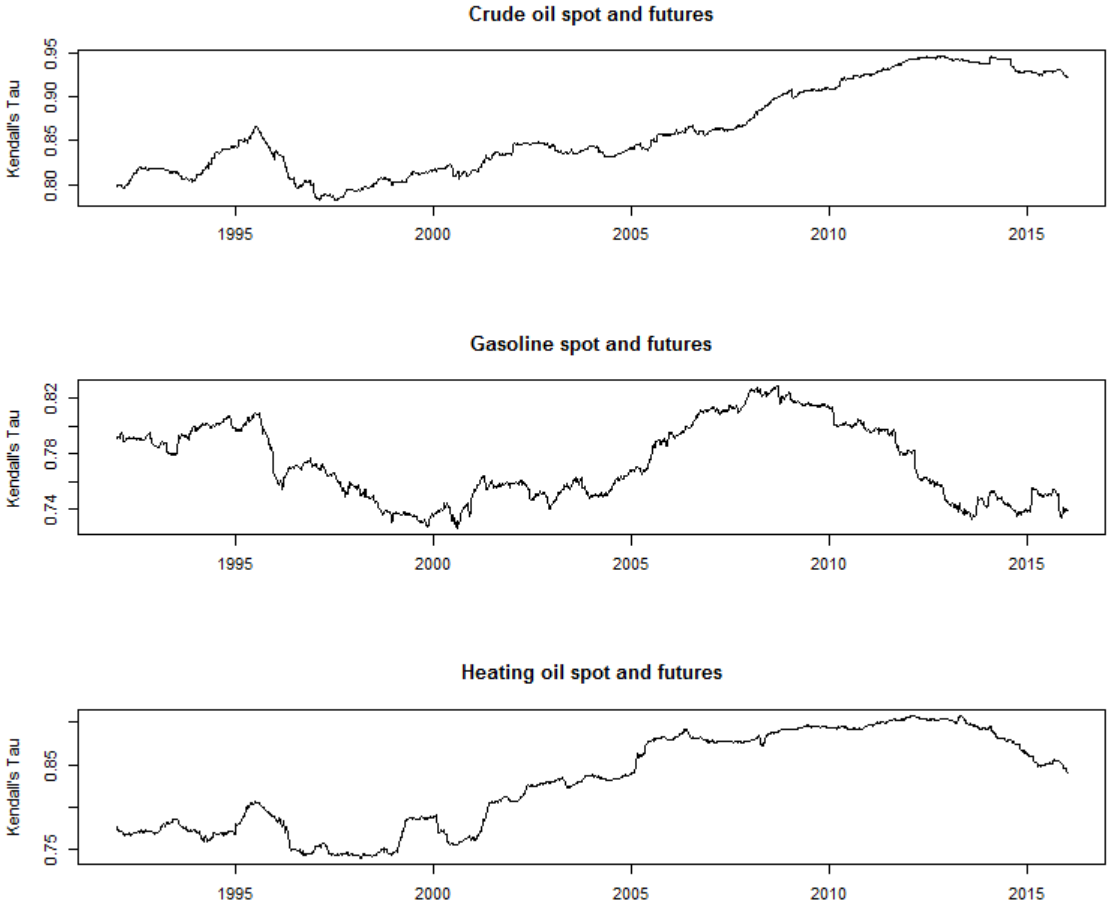

Figure 2.5. Time-varying Kendall's Tau (Kendall's rank correlation) between weekly price changes in spot and its corresponding futures markets (estimated with 261-week rolling window)

Turning to the core of the empirical analysis, we evaluate the different hedging models based on their out-of-sample hedging effectiveness. In the out-of-sample

analysis, the following rolling window approach is followed[19]. First, we estimate the minimum-SV, minimum-LPM, minimum-VaR, and minimum-ES hedge ratios using the first 261 weekly observations. That is, our estimation window is approximately 5 years[20]. Next, the estimated optimal hedge ratios are used to construct the hedged P&Ls for the following 130 weeks (i.e., 2.5 years) for each hedging objective[21]. Then, the estimation window is moved forward by 1 week, where the optimal hedge ratios and associated out-of-sample hedged P&Ls – the hedged P&Ls for the following 130 weeks – are recalculated[22]. This approach produces 1,121 out-of-sample test windows. Finally, within each test window, the out-of-sample hedging effectiveness for each hedging objective is computed for all the hedging models. The mean and median hedging effectiveness are then calculated across the 1,121 test windows[23].

2.4 Empirical Results

This section first presents evidence on the fit of the three standard multivariate copula models – the standard Gaussian copula (SGC), standard Student's t copula (SSC),

[19] Conlon and Cotter (2012, 2013) and Barbi and Romagnoli (2014) adopt a similar approach in their out-of-sample analyses. This rolling window approach allows us to account for the time variation in the distribution of price changes as well as to test the model's hedging effectiveness over a number of test windows.

[20] Alexander, Prokopczuk and Sumawong (2013) and Barbi and Romagnoli (2014) also use a 5-year rolling window approach. However, studies regarding the optimal length of the moving window for multiproduct hedging are still needed.

[21] We follow a recommendation of Chen, Lee, and Shrestha (2004) that the size of the out-of-sample period should be about half the size of the estimation period.

[22] Here, both the marginal distributions and dependence structure (i.e., the copula parameters) are re-estimated every week using the updated estimation window. Barbi and Romagnoli (2014) also re-estimate the marginal distributions each time the estimation window is moved forward. However, they assume that the dependence structure does not change frequently and only re-estimate the dependence structure periodically (every 5 years). We believe that our approach is more appropriate because the degree of dependence between the changes in spot and futures prices does vary over time (see Figure 2.5).

[23] All computations were performed using R (version 3.2.2).

and standard Clayton copula (SCC) models – and the two vine copula models – the C- and D-vine copula models. The section then proceeds to present our empirical findings for optimal crude oil, gasoline, and heating oil hedge ratios obtained using different hedging models (including the nonparametric (NP), SGC, SSC, SCC, C-vine copula and D-vine copula models). Then, comparisons of out-of-sample hedging effectiveness are made across different hedging models and hedging objectives.

2.4.1 Model Fit

Table 2.2 provides some evidence on the fit of the five multivariate copula models: the SGC, SSC, SCC, C-vine copula, and D-vine copula models[24]. On average, the D-vine copula model yields the highest log-likelihood and lowest values of the AIC and Bayesian Information Criterion (BIC), whereas the SCC model provides the worst fit to the data[25]. More specifically, the D-vine copula model provides a better fit (based on both AIC and BIC values) than the SGC, SSC, and SCC models for all the 1,121 estimation windows. Comparing to the C-vine copula model, the D-vine copula model produces lower AIC and BIC for about 90% of the cases[26].

The average number of parameters for each copula model is also listed in Table 2.2. The SCC model has only one parameter to characterize the overall dependence

---

[24] For each copula model, the empirical distribution is used in the estimation of the marginal distributions of price changes.

[25] It should be noted that the main purpose of this study is not to select the best-fit copula model, but to compare the alternative copula models in term of out-of-sample hedging effectiveness. For a model selection purpose, the Vuong's (1989) and/or Clarke's (2007) tests could be employed to compare two nested/non-nested copula models.

[26] Detailed results regarding model fit for each rolling window are provided in Appendix A (Figures A.1-A.3).

structure of the six random variables. It is very likely that this parameter restriction is a reason for the poor fit of the SCC model. The SGC model uses 15 pairwise correlation coefficients to capture the dependence structure of the random variables. However, it assumes no tail dependence, and could therefore underestimate the joint probability of extreme movements in all the petroleum prices. In addition to the 15 pairwise correlation coefficients, the SSC model adds one more parameter (a degree of freedom parameter) to characterize the tail dependence for all pairs of the random variables. However, using only one parameter to describe the overall tail dependence may be over-simplistic when dealing with more than two variables. These parameter restrictions are likely reasons for the superior fit of the vine copula models over the standard multivariate copula models.

Table 2.2. Average log-likelihood (LLH), Akaike Information Criterion (AIC), and Bayesian Information Criterion (BIC), and number of parameters for the multivariate copula models

	LLH	AIC	BIC	Number of parameters
SGC	1169.35	-2308.70	-2255.23	15
SSC	1316.73	-2601.45	-2544.42	16
SCC	591.43	-1180.85	-1177.29	1
C-vine	1356.27	-2667.15	-2586.27	23
D-vine	1373.50	-2701.54	-2620.52	23

Notes: Each model is estimated using a rolling window approach with a window of approximately 5 years or 261 weeks. The total number of estimation windows is 1,121 windows. SGC is the standard Gaussian copula model. SSC is the standard Student's t copula model. SCC is the standard Clayton copula model. C-vine is the canonical vine copula model. D-vine is the drawable vine copula model.

Comparing the two vine copula models, the superiority of the D-vine copula model may be explained by the difference in the way that the two models decompose the joint density function (more specifically, the difference in the structure of the first tree).

Referring to Figure 2.2 and equation (2.16), the first tree of the C-vine copula model uses only one variable to link with the other five variables through different unconditional bivariate copulas. As a result, the first tree of the C-vine copula model can capture the high dependence between the spot and its corresponding futures price changes in only one petroleum market. On the other hand, the first tree of the D-vine copula model permits a direct link between the spot and its corresponding futures price changes for all petroleum markets (see Figure 2.3 and equation (2.17)). In other words, the variables in the first tree of the D-vine copula model for each estimation window can be ordered such that the spot and its corresponding futures variables are next (or linked) to each other. For example, the structure $S_t^H - F_t^H - F_t^C - S_t^C - F_t^G - S_t^G$ is selected for the first tree of the D-vine copula for the first estimation window. This feature is not allowed by the C-vie copula model and may be a reason why the D-vine copula model fits the data better than the C-vine copula model.

2.4.2 Minimum-Downside Risk Hedge Ratios

Table 2.3 reports the average minimum-SV, minimum-LPM, minimum-VaR, and minimum-ES hedge ratios (as well as their respective standard deviations) generated using different hedging models. On average, most hedging models (except the SCC model) recommend the hedge ratios of fairly similar magnitude for all hedging objectives. Depending on the hedging models and objectives, the average crude oil, gasoline, and heating oil hedge ratios are between 0.8 and 1.3. On the other hand, the SCC model yields the optimal gasoline and heating oil hedge ratios fairly close to 0 (no

hedge), and the optimal crude oil hedge ratios slightly smaller than 0 (recommending a speculative position in the crude oil futures market – shorting crude oil futures instead of longing). The huge difference between the hedge ratios generated from the SCC model and the other copula models is due to the fact that the SCC model uses only one parameter to capture the dependence patterns across all the six markets. The parameter restriction of the SCC model could lead to rather disappointing hedging performance (as will be shown in the next section).

Examining the standard deviations of the optimal hedge ratios for the three petroleum commodities, the heating oil hedge ratios are found to be more volatile than the crude oil and gasoline hedge ratios (Table 2.3). This corresponds to the relatively high level of excess kurtosis in the heating oil price changes, which implies that the extreme price changes observed more often in the heating oil market than in the other two markets. This means that the optimal tail risk-minimizing hedge ratios are sensitive to the extreme price changes. In addition, we find that the NP method generates the most volatile hedge ratios for all the three petroleum commodities, except for the case of minimum-SV hedge ratio for gasoline (where the D-vine copula model produces slightly more volatile hedge ratios). This may be because the NP approach is very sensitive to new information from the data (especially when only 261 observations are used in the estimation of the nonparametric or empirical distribution). Further, the minimum-VaR and minimum-ES hedge ratios at the 99% confidence level are generally more dispersed than the other hedging objectives, which may be explained by the greater level of difficulty in estimating the extreme tails of the true distribution of the hedged P&Ls.

Table 2.3. Average optimal hedge ratios (with standard deviations in parentheses) of different hedging models and hedging objectives

Model	Hedging objective							
	Semivariance	Lower Partial	Value at Risk (VaR)			Expected Shortfall (ES)		
	(SV)	Moment (LPM)	90%	95%	99%	90%	95%	99%
Panel A: Crude oil hedge ratio								
NP	1.150 (0.225)	1.201 (0.251)	0.910 (0.253)	0.995 (0.300)	1.156 (0.433)	1.207 (0.219)	1.249 (0.300)	1.256 (0.407)
SGC	1.023 (0.133)	0.998 (0.159)	1.092 (0.118)	1.053 (0.127)	0.951 (0.186)	1.032 (0.131)	1.007 (0.152)	0.955 (0.223)
SSC	1.038 (0.093)	1.006 (0.115)	1.095 (0.112)	1.063 (0.112)	0.949 (0.187)	1.044 (0.092)	1.022 (0.101)	0.981 (0.141)
SCC	-0.090 (0.068)	-0.093 (0.079)	-0.064 (0.055)	-0.091 (0.067)	-0.053 (0.141)	-0.086 (0.055)	-0.089 (0.076)	-0.120 (0.126)
C-vine	1.078 (0.148)	1.047 (0.172)	1.106 (0.177)	1.094 (0.167)	1.012 (0.256)	1.086 (0.167)	1.069 (0.181)	1.006 (0.228)
D-vine	1.087 (0.113)	1.063 (0.128)	1.108 (0.157)	1.099 (0.145)	1.042 (0.219)	1.093 (0.134)	1.082 (0.138)	1.044 (0.185)
Panel B: Gasoline hedge ratio								
NP	1.155 (0.100)	1.189 (0.125)	0.970 (0.171)	1.112 (0.283)	1.054 (0.340)	1.171 (0.172)	1.196 (0.164)	1.232 (0.221)
SGC	1.077 (0.087)	1.078 (0.086)	1.063 (0.094)	1.055 (0.115)	1.054 (0.097)	1.052 (0.096)	1.048 (0.102)	1.067 (0.102)
SSC	1.106 (0.078)	1.091 (0.085)	1.088 (0.096)	1.090 (0.105)	1.083 (0.117)	1.081 (0.084)	1.081 (0.086)	1.061 (0.094)
SCC	0.048 (0.063)	0.048 (0.079)	0.020 (0.072)	0.049 (0.078)	-0.010 (0.180)	0.032 (0.074)	0.024 (0.104)	-0.015 (0.167)
C-vine	1.094 (0.100)	1.063 (0.105)	1.085 (0.130)	1.103 (0.117)	1.043 (0.128)	1.077 (0.108)	1.063 (0.110)	0.970 (0.150)
D-vine	1.138 (0.108)	1.131 (0.117)	1.116 (0.131)	1.140 (0.124)	1.136 (0.145)	1.126 (0.118)	1.124 (0.120)	1.085 (0.165)
Panel C: Heating oil hedge ratio								
NP	1.054 (0.585)	1.024 (0.737)	0.858 (0.600)	0.805 (0.649)	1.266 (0.816)	1.186 (0.548)	1.186 (0.651)	0.899 (1.021)
SGC	1.024 (0.300)	1.032 (0.340)	1.063 (0.264)	1.010 (0.331)	0.976 (0.405)	1.068 (0.300)	1.055 (0.326)	1.038 (0.430)
SSC	1.010 (0.249)	1.025 (0.293)	1.035 (0.247)	0.999 (0.275)	0.863 (0.418)	1.040 (0.239)	1.037 (0.253)	1.069 (0.336)
SCC	0.236 (0.145)	0.228 (0.158)	0.303 (0.191)	0.197 (0.165)	0.249 (0.261)	0.240 (0.147)	0.220 (0.146)	0.157 (0.174)
C-vine	1.156 (0.327)	1.216 (0.387)	1.082 (0.320)	1.096 (0.355)	1.153 (0.496)	1.188 (0.339)	1.225 (0.367)	1.340 (0.471)
D-vine	1.087 (0.244)	1.046 (0.298)	1.093 (0.302)	1.050 (0.295)	0.946 (0.439)	1.098 (0.265)	1.082 (0.286)	0.995 (0.393)

Notes: The optimal hedge ratios for different hedging objectives are estimated using a rolling window approach with a window of approximately 5 years or 261 weeks. The total number of estimation windows is 1,121 windows. NP is the nonparametric method. SGC is the standard Gaussian copula model. SSC is the standard Student's t copula model. SCC is the standard Clayton copula model. C-vine is the canonical vine copula model. D-vine is the drawable vine copula model.

Table 2.4. Out-of-sample hedging effectiveness of different hedging models and hedging objectives

Model	Hedging objective							
	SV	LPM	VaR reduction (%)			ES reduction (%)		
	reduction (%)	reduction (%))	90%	95%	99%	90%	95%	99%
NP	61.65 (64.89)	70.00 (75.26)	34.88 (35.31)	37.50 (37.73)	31.84 (33.23)	37.89 (39.93)	35.44 (37.06)	26.81 (28.39)
SGC	62.62 (64.17)	71.75 (77.60)	**41.61 (41.74)**	40.26 (40.91)	33.48 (38.47)	37.84 (37.83)	35.22 (36.13)	28.82 (32.40)
SSC	63.09 (64.82)	72.70 (77.20)	41.29 (41.38)	41.11 (41.88)	33.87 (38.70)	38.33 (38.52)	36.04 (37.22)	30.27 (**32.96**)
SCC	-3.75 (1.06)	-5.49 (0.45)	-3.58 (-1.75)	1.29 (0.81)	-2.20 (0.00)	-0.47 (0.00)	-0.60 (-0.33)	-4.47 (-2.07)
C-vine	63.04 (65.81)	72.92 (77.26)	40.00 (40.03)	41.06 (42.74)	34.49 (38.10)	38.32 (40.32)	36.29 (37.47)	30.03 (32.09)
D-vine	**63.61 (65.95)**	**73.80 (78.09)**	39.86 (39.84)	**42.33 (43.51)**	**36.36 (38.94)**	**39.15 (40.80)**	**37.41 (38.83)**	**32.43** (32.77)

Notes: The table reports the mean (median) out-of-sample hedging effectiveness for different hedging methods and hedging objectives. The mean and median hedging effectiveness are calculated across 1121 out-of-sample test windows. The best performing hedging method for each hedging objective is highlighted in bold type. NP is the nonparametric method. SGC is the standard Gaussian copula model. SSC is the standard Student's t copula model. SCC is the standard Clayton copula model. C-vine is the canonical vine copula model. D-vine is the drawable vine copula model. SV denotes Semivariance; LPM denotes Lower Partial Moment; VaR denotes Value at Risk; and ES denotes Expected Shortfall.

2.4.3 Out-of-Sample Hedging Effectiveness

Table 2.4 presents the out-of-sample hedging effectiveness of the minimum-SV, minimum-LPM, minimum-VaR, and minimum-ES objectives for the six hedging models – the NP, SGC, SSC, SCC, C-vine copula, and D-vine copula models. For each hedging objective and model, the table gives the mean and median percentage reductions in the respective downside risk of the hedged P&Ls relative to the unhedged P&Ls. The mean and median values are calculated across the 1,121 out-of-sample test windows. The best performing hedging model for each hedging objective is highlighted in bold type.

2.4.3.1 Minimum-SV Objective

Considering first the minimum-SV objective, all models (except the SCC model) produce, on average, at least 60% SV reductions. The D-vine copula model is the most effective model, with a mean (median) SV reduction of 63.61% (65.95%). Figure 2.6 shows that the hedging the hedging effectiveness of the D-vine copula model varies over time, ranging between 31.98% and 81.17%. The SCC model performs extremely poorly with the mean SV reduction of -3.75% (i.e., increasing risk) and median SV reduction of 1.06%. Recall from Table 2.3, the SCC model recommends the gasoline and heating oil hedge ratios fairly close to 0, and thus fails to protect against adverse price movements in the gasoline and heating oil markets. In addition, it supports a speculative position in the crude oil futures market (i.e., the crude oil hedge ratios being less than 0), which could end up adding more risk to the unhedged position. In particular, this disappointing performance may be explained by the very poor fit of the SCC model (see Table 2.2).

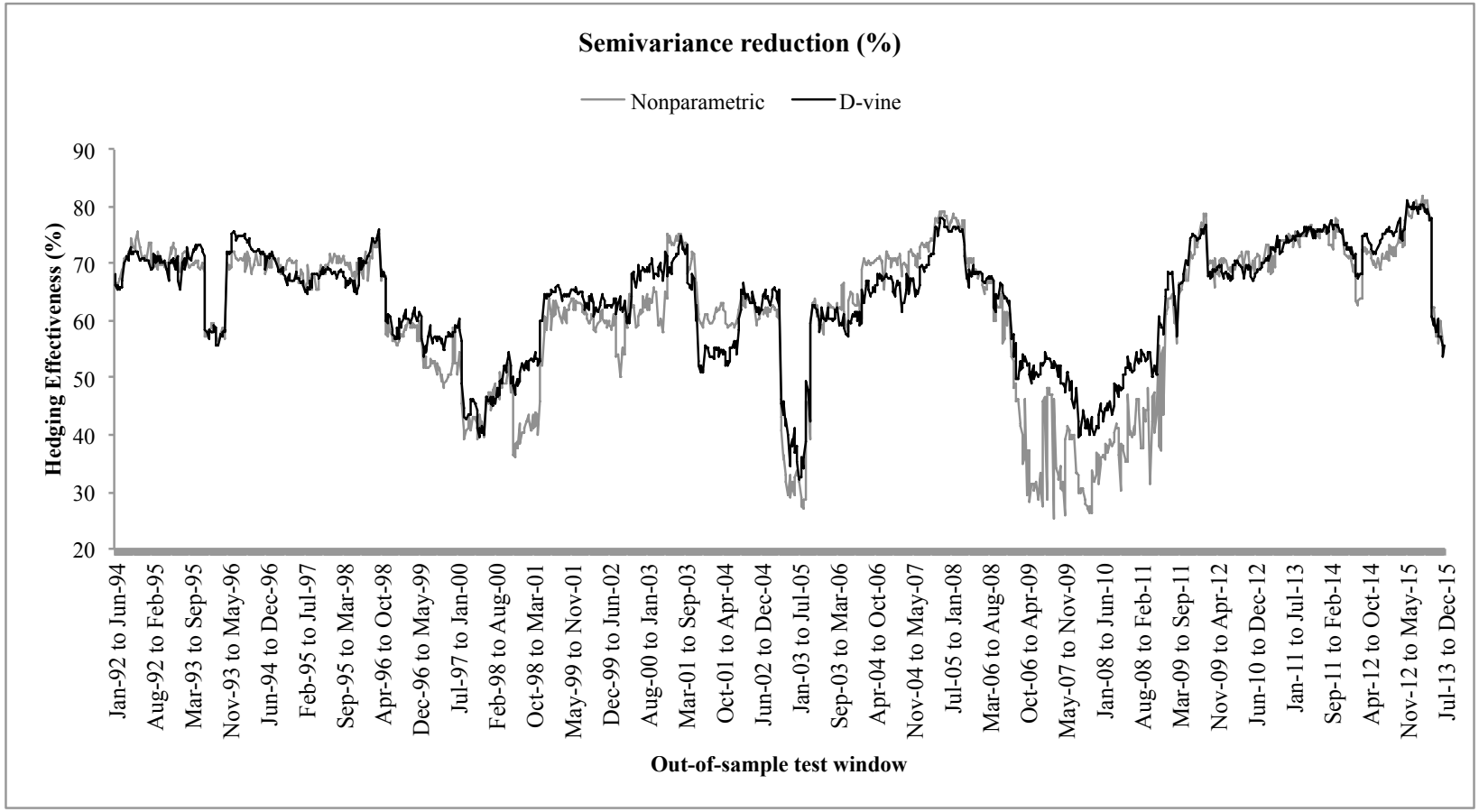

Figure 2.6. Out-of-sample hedging effectiveness: percentage reductions in Semivariance

Comparing with the widely used NP method, the D-vine copula model leads to a larger mean (median) SV reduction of about 1.96% (1.06%) points. It is evidence from Figure 2.6 that the D-vine copula model is superior to the NP method for most out-of-sample test windows (more specifically, about 61.11% of the cases). The maximum improvement of the D-vine copula model over the NP model is 26.48% points for the March-2007-to-September-2009 test window, which covers the period of extreme fluctuations in crude oil prices. In fact, the D-vine copula model performs much better than the NP method for most test windows covering the years 2007 to 2010. On the other hand, the greatest improvement of the NP method over the D-vine copula model is only 8.99% points for the October-2001-to-April-2004 test window. Nevertheless, this suggests that the NP method may outperform the D-vine copula model when prices are relatively stable.

The D-vine copula model also produces better outcomes than the other copula models both in mean and median terms. The D-vine copula model clearly outperforms the SCC model. The mean (median) improvement of the D-vine copula model over the SGC, SSC and C-vine copula models ranges between 0.52% (0.14%) point and 0.99% (1.78%) point. Overall, under the minimum-SV framework, the D-vine copula model is on average able to improve upon the NP method, the three standard copula models, and the C-vine copula model. However, except for the case of the SCC model, the mean and median improvement offered by the D-vine copula model is only moderate. This is not totally unexpected because these models recommend the hedge ratios of fairly similar magnitude (see Table 2.3).

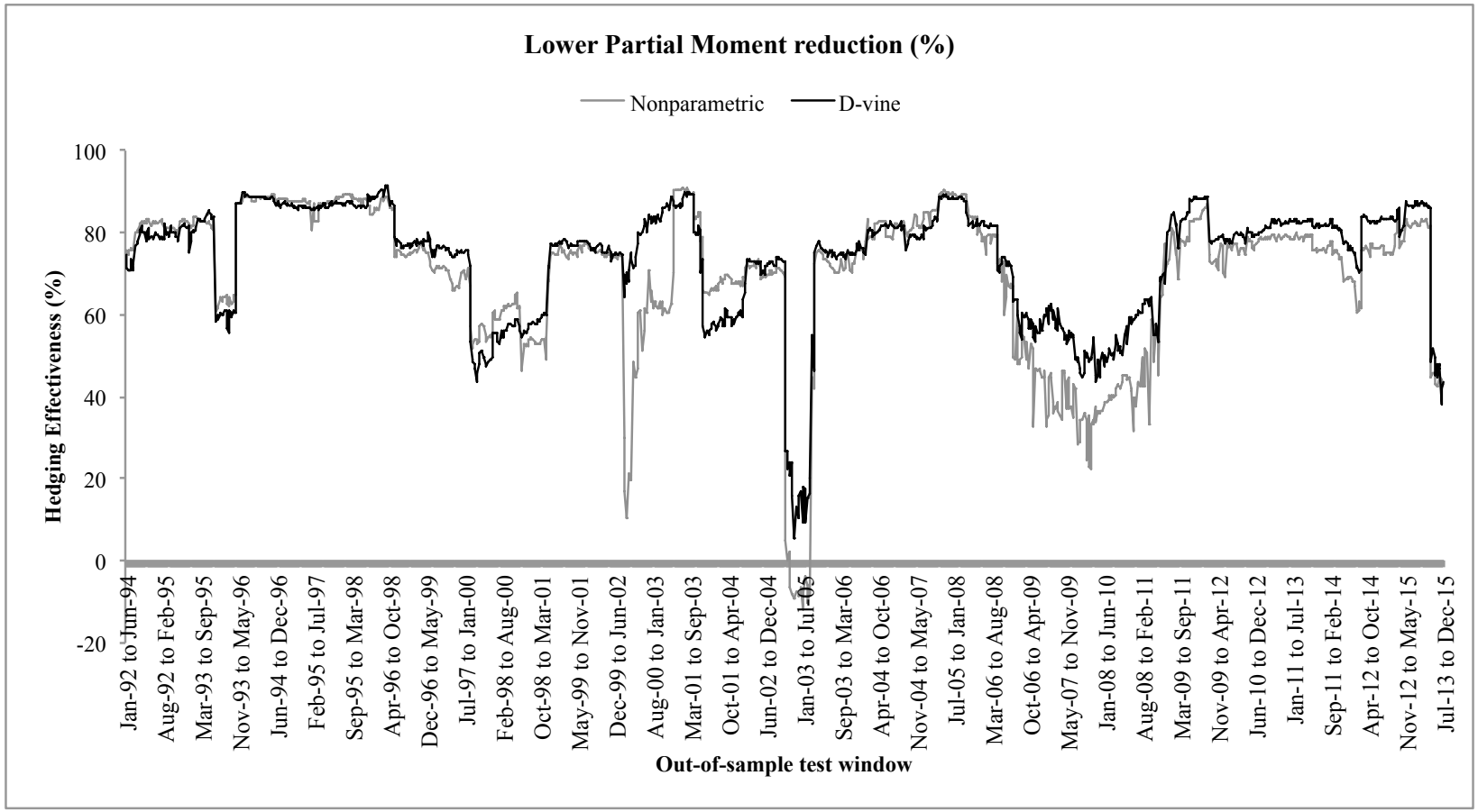

Figure 2.7. Out-of-sample hedging effectiveness: percentage reductions in Lower Partial Moment

2.4.3.2 Minimum-LPM Objective

We next consider the minimum-LPM objective. Similar to the minimum-SV objective, the D-vine copula model performs better than the other models both in mean and median terms (Table 2.4). In particular, it leads to a mean (median) LPM reduction of 73.80% (78.09%). As can be seen from Figure 2.7, the LPM reductions offered by the D-vine copula model vary across the out-of-sample test windows in a very similar pattern to the case of SV reductions (Figure 2.6). The LPM reductions of the D-vine copula model range from 5.47% (for the November-2002-to-May-2005 test window) to 91.62% (for the April-1996-to-September-1998 test window). Again, the SCC model performs the worst with the mean (median) hedging effectiveness of -5.49% (0.45%), confirming that using only one parameter is not enough to capture the dependence structure of the six-dimensional data.

Comparing with the NP method, the D-vine copula model leads to a 3.80% (2.83%) point increase in the mean (median) LPM reduction. Figure 2.7 shows that the D-vine copula model offers higher levels of LPM reductions for most out-of-sample test windows. More specifically, the D-vine copula model produces greater LPM reductions than the NP method about 67.62% of the cases, with the maximum improvement of 59.89% points for the March-2000-to-August-2002 test window. It is also worth mentioning that the greatest improvement of the NP method over the D-vine copula model is only about 11.58% points. Besides, the NP method yields negative LPM reductions (i.e., increases risk of the unhedged position) during the test windows November-2002-to-April-2005 to March-2003-to-August-2005 (a total of 18 out-of-

sample test windows). Again, the mean (median) LPM improvement of the D-vine copula model over the SGC, SSC, and C-vine copula models is quite modest, ranging between 0.88% (0.45%) and 2.05% (0.89%) points.

2.4.3.3 Minimum-VaR Objective

For the minimum-VaR objective, all hedging models (except the SCC model) provide a VaR reduction of at least 30% (35%) in mean (median) term (Table 2.4). The D-vine copula model performs the best at the 95% and 99% confidence levels, but not at the 90% confidence level. As expected, the SCC model performs the worst at all confidence levels. The hedging effectiveness of all hedging models is found to be lowest at the 99% confidence level, indicating that it is hard to hedge against a very extreme risk.

At the 90% confidence level, the mean and median reductions of VaR are greatest for the SGC model with a mean reduction of 41.61% and a median reduction of 41.74%. In particular, the SGC model leads to a higher mean (median) VaR reduction of 1.75% (1.90%) points relative to the D-vine copula model. At the 90% confidence level, the D-vine copula model also performs slightly worse than the SSC and C-vine copula models. However, the D-vine copula model is still able to improve upon the NP method with a larger mean (median) VaR reduction of about 4.98% (4.53%) points. It is evident from Figure 2.8 that the D-vine copula model results in positive VaR reductions across all test windows, and clearly outperforms the NP method for most test windows.

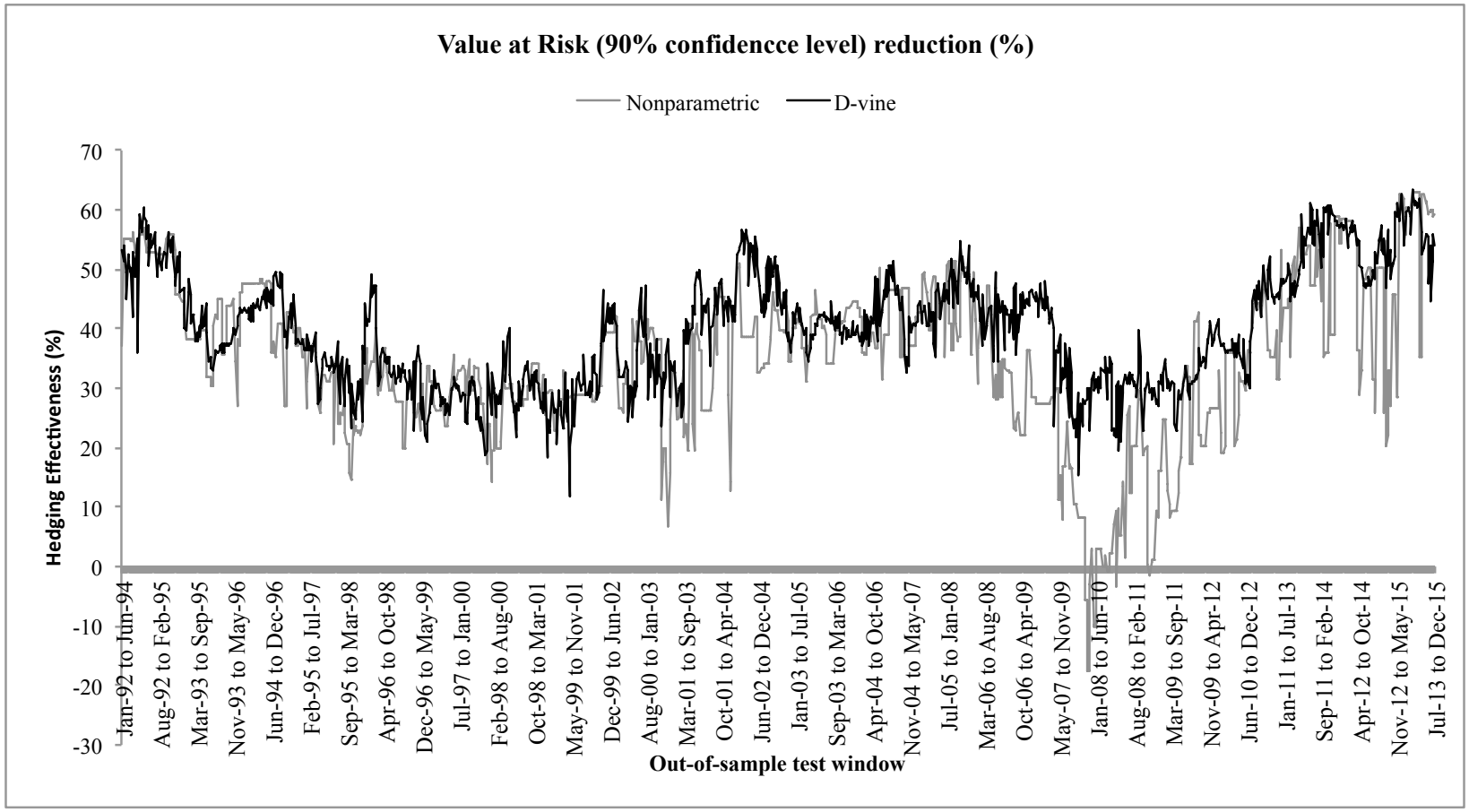

Figure 2.8. Out-of-sample hedging effectiveness: percentage reductions in Value at Risk at the 90% confidence level

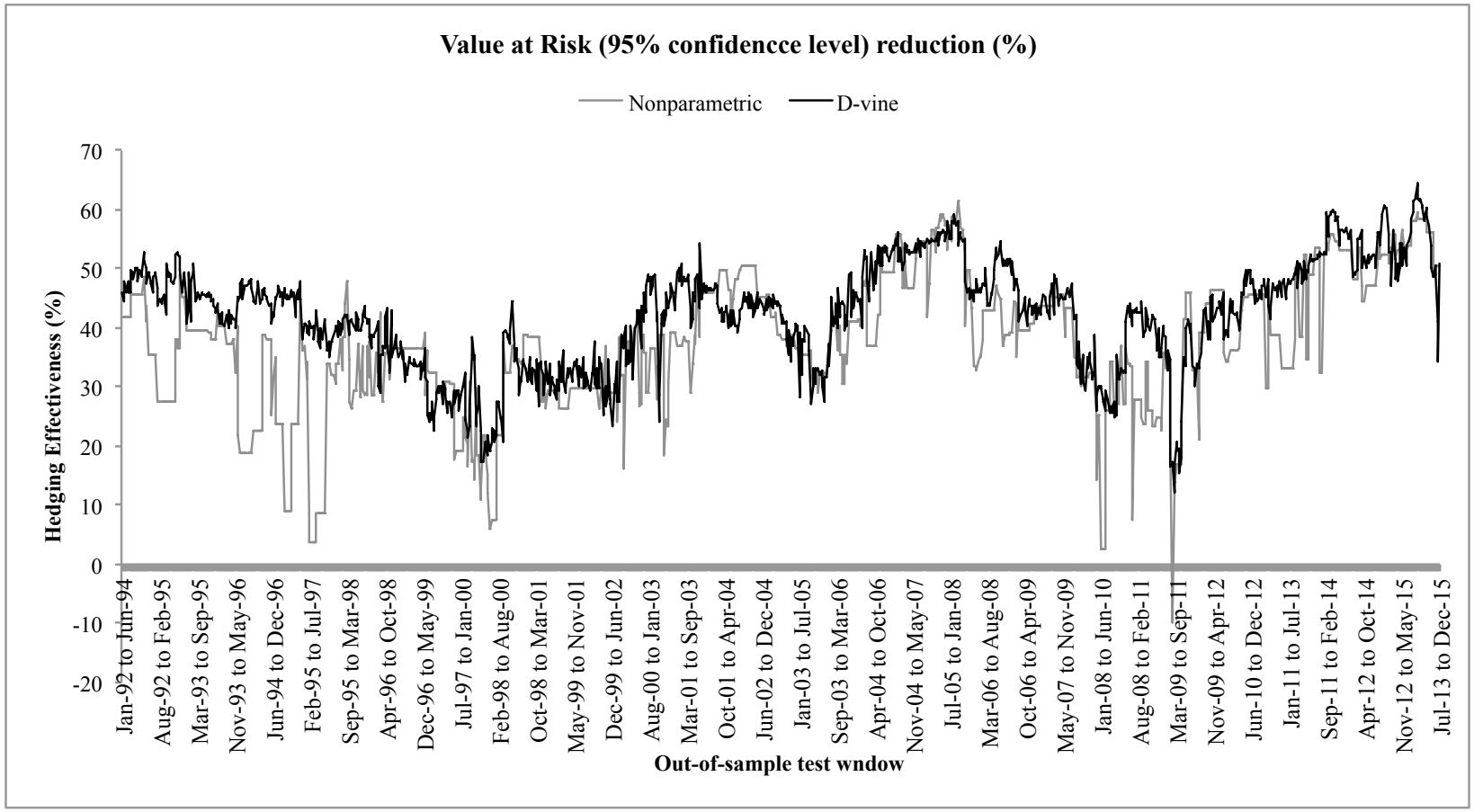

Figure 2.9. Out-of-sample hedging effectiveness: percentage reductions in Value at Risk at the 95% confidence level

At the 95% confidence level, the D-vine copula model yields a mean (median) VaR reduction of 42.33% (43.51%), which is about 4.83% (5.78%) points higher than the NP method. Figure 2.9 shows that the D-vine copula model always yields positive VaR reduction (ranging from 12.13% to 64.59%), and offers significant improvements over the NP method in many out-of-sample test windows. Comparing with the SGC, SSC and C-vine copula models, the D-vine copula model leads to a larger mean (median) VaR reduction of at least 1.22% (0.77%) points.

At the 99% confidence level, the best performing hedging model is also the D-vine copula model. If offers a mean (median) VaR reduction of 36.36% (38.94%). Figure 2.10 reveals that the hedging effectiveness of the D-vine copula model fluctuates greatly with the minimum VaR reduction of -4.41% and maximum VaR reduction of 64.37%. This means that the D-vine copula model yields negative VaR reductions for a few out-of-sample windows. Nevertheless, the D-vine copula model still performs better than the NP method with an increase in the mean (median) VaR reduction of 4.52% (5.71%) points. In addition, the negative VaR reductions are found in 34 test windows for the NP method but in only 6 test windows for the D-vine copula model. Again, the mean (median) VaR improvement of the D-vine copula model over the SGC, SSC and C-vine copula models is quite modest, ranging between 1.87% (0.24%) and 2.88% (0.84%) points. However, I find that the SGC, SSC and C-vine copula models produce negative VaR reductions (i.e., increase the VaR of the unhedged position) at least 6.5 times more often than the D-vine copula model. Thus, the D-vine copula model is a safer choice for hedging the VaR of the refinery than the other models.

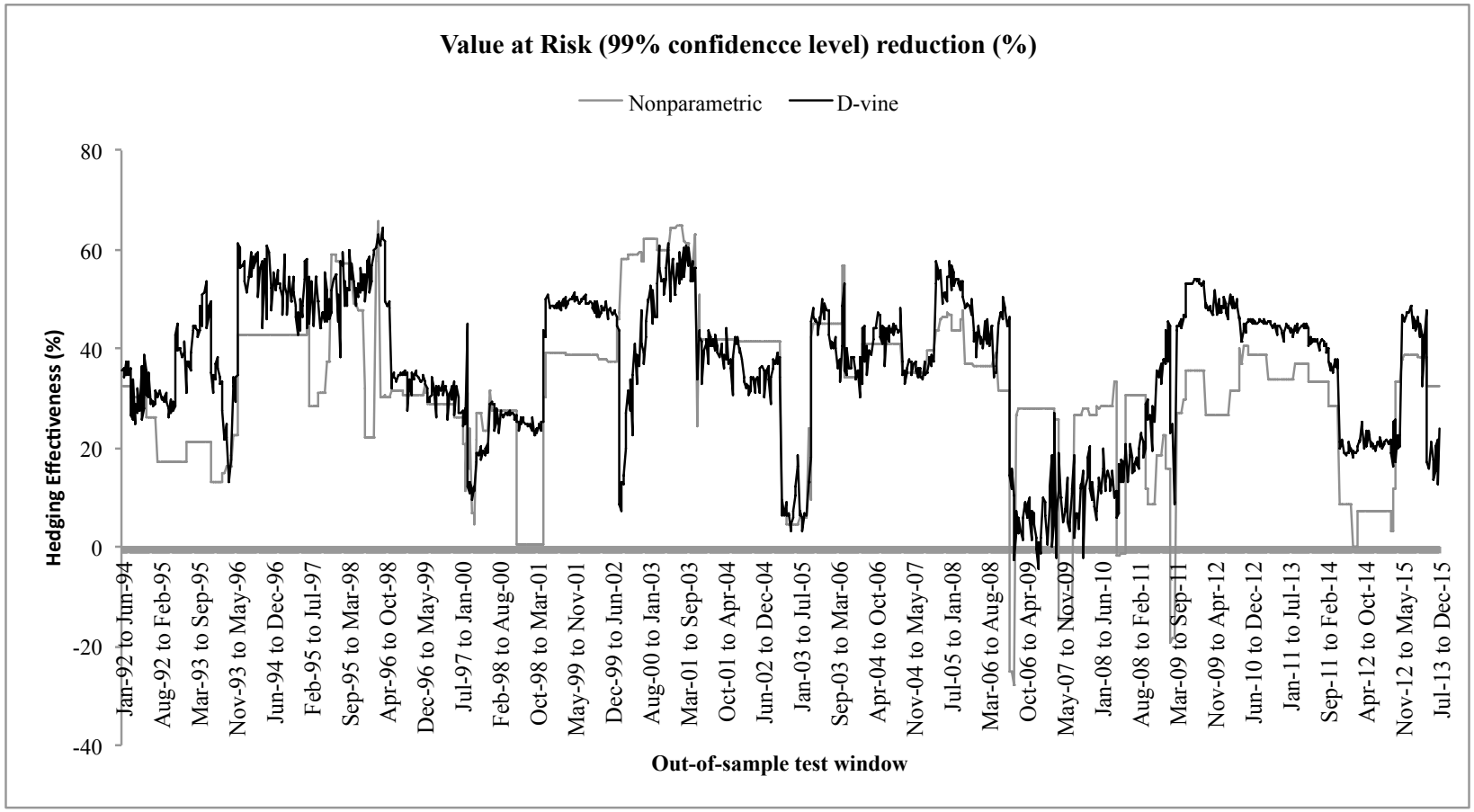

Figure 2.10. Out-of-sample hedging effectiveness: percentage reductions in Value at Risk at the 99% confidence level

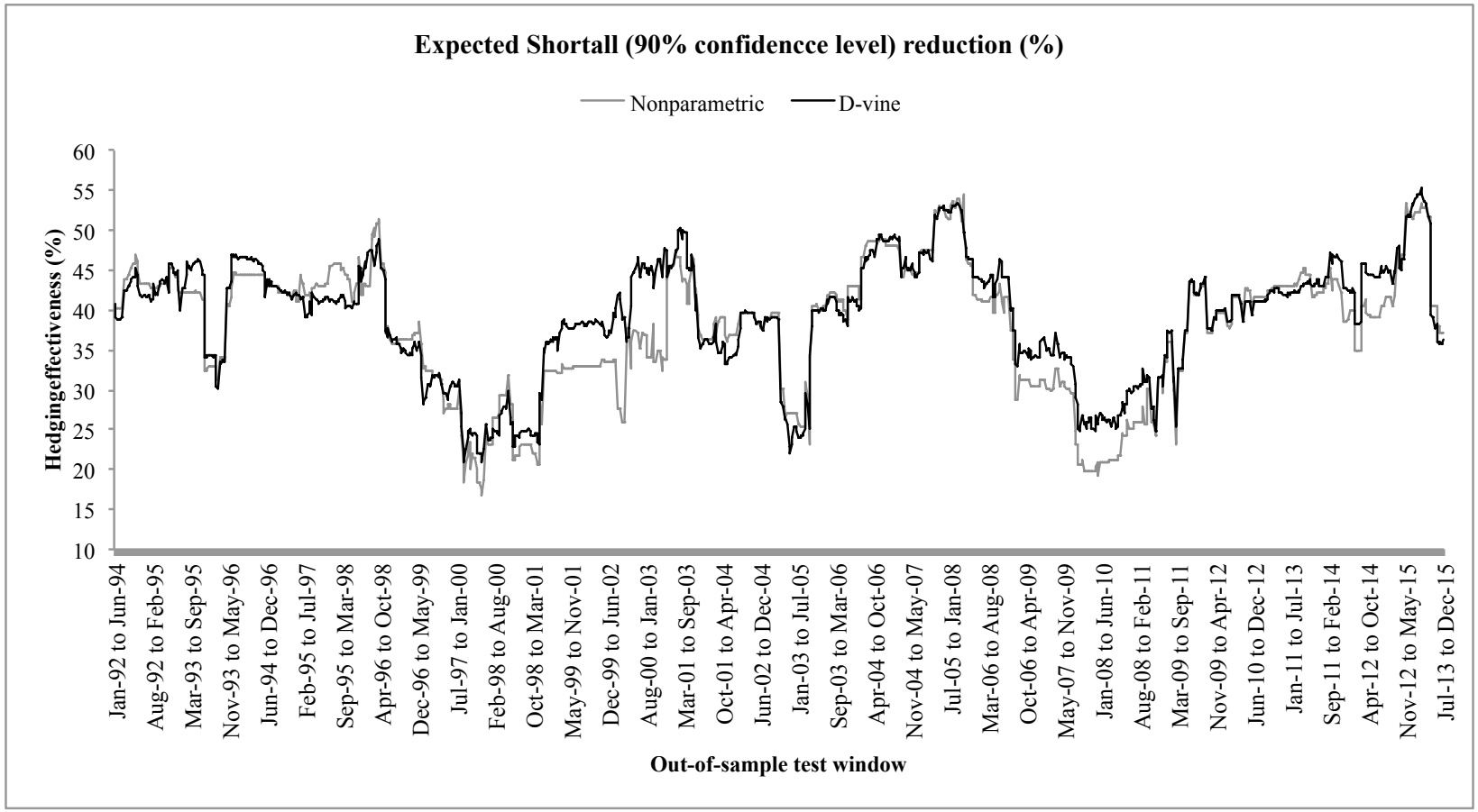

Figure 2.11. Out-of-sample hedging effectiveness: percentage reductions in Expected Shortfall at the 90% confidence level

2.4.3.4 Minimum-ES Objective

As can be seen from Table 2.4, in terms of ES reduction, the hedging effectiveness of all hedging models is found to be largest at the lowest confidence (90% confidence level) and smallest at the largest confidence level (99% confidence level). In other words, the hedging effectiveness decreases as the confidence level increases. This indicates a greater difficulty in hedging a more extreme (tail) risk. Focusing on the mean hedging effectiveness, the D-vine copula model leads to the greatest ES reductions at all confidence levels. When we consider the median hedging effectiveness, the D-vine copula model performs the best for the 90% and 95% confidence levels, but not the 99% confidence level for which the SSC model is preferred. As before, the SCC model performs extremely poorly at all confidence levels.

As can be seen from Figures 2.11-2.13, the D-vine copula model generally provides good hedging effectiveness at all the confidence levels. The mean (median) ES reductions offered by the D-vine copula model are 39.15% (40.80%), 37.41% (38.83%), and 32.43% (32.77%) for the 90%, 95%, and 99% confidence levels, respectively (Table 2.4). In particular, the ES reductions of the D-vine copula model range from 20.87% to 55.33% for the 90% confidence level, from 13.12% to 53.94% for the 95% confidence level, and from -30.77% to 66.80% for the 99% confidence level. Unlike at the 90% and 95% confidence levels, it is evidence from Figure 2.13 that the D-vine copula model produces negative reductions in ES at the 99% confidence level for several out-of-sample test windows (more specifically, for a total of 28 test windows).

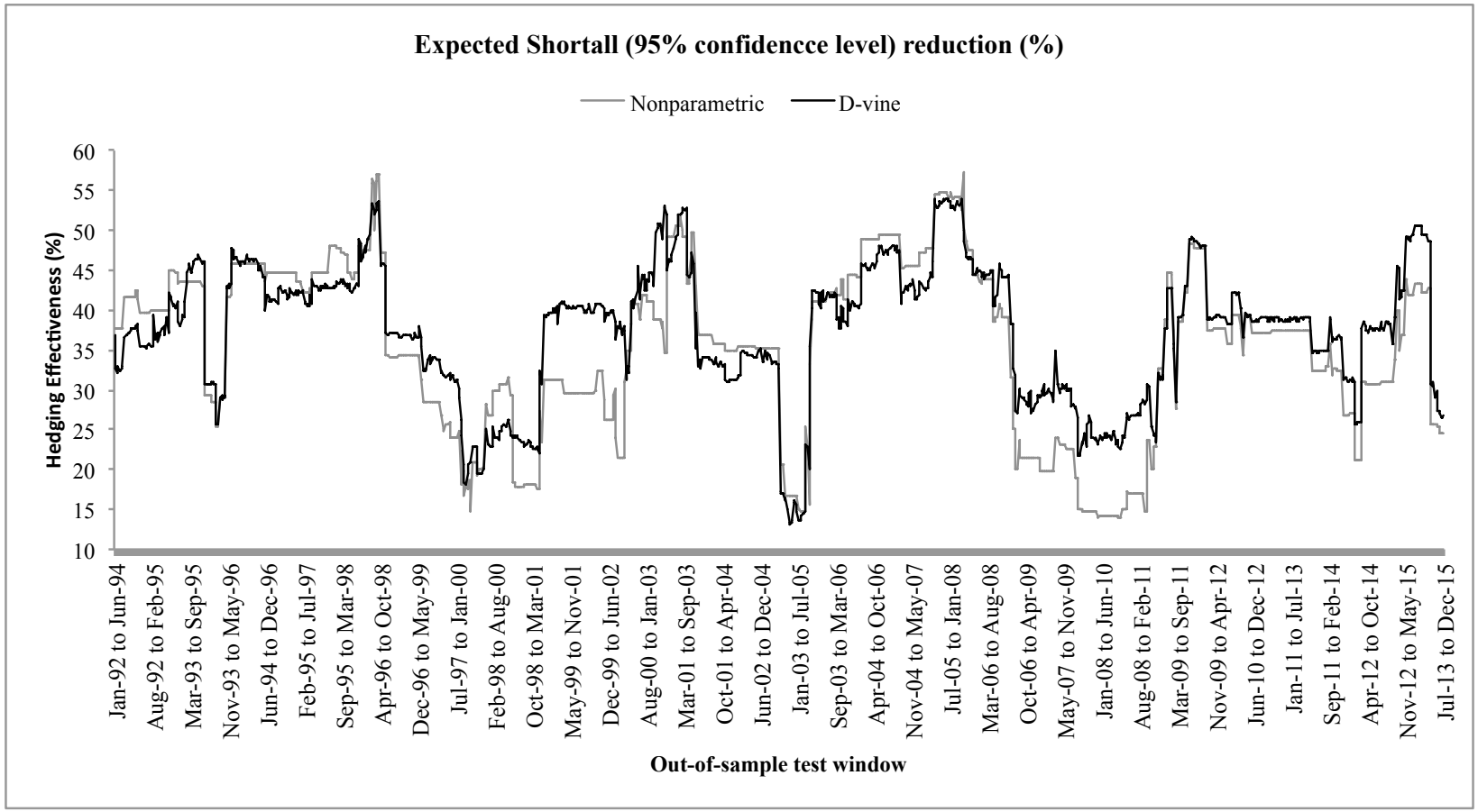

Figure 2.12. Out-of-sample hedging effectiveness: percentage reductions in Expected Shortfall at the 95% confidence level

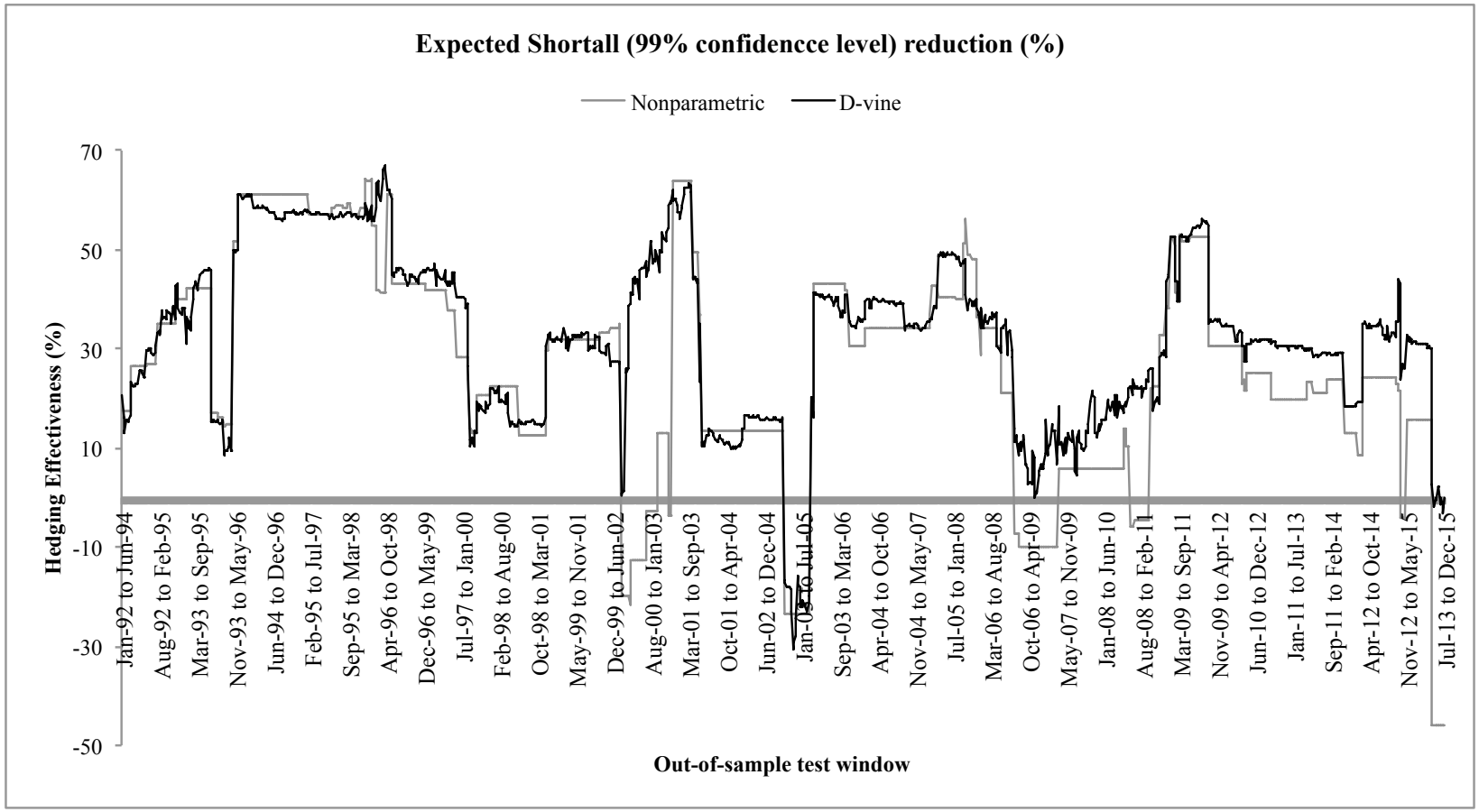

Figure 2.13. Out-of-sample hedging effectiveness: percentage reductions in Expected Shortfall at the 99% confidence level

To find a possible reason for the occasional poor performance of the D-vine copula model, we investigate these 28 out-of-sample test windows more closely. Given the rolling window approach, the 28 test windows correspond to two periods of bad performance: (1) during the test windows (October-2002-to-March-2005) to (March-2003-to-August-2005) and (2) during the test windows (May-2013-to-October-2015) to (July-2013-to-December-2015). For the first period, the negative reductions in ES at the 99% confidence level are due to an additional loss to the unhedged P&Ls on March 30, 2005 (when the unhedged P&L has already fallen by 4.26 dollars per barrel). The extra loss on March 30, 2005 is particularly as a result of (1) the gasoline futures price moving in the opposite directions from the gasoline spot price, and (2) the heating oil futures price advancing more than the heating oil spot price[27]. For the second period, the negative ES reductions (at the 99% confidence level) occurs particularly because of a large magnitude of basis risk in the gasoline market on October 21, 2015, when the gasoline spot and futures prices move in the opposite directions[28]. These two events

[27] This is known as basis risk – risk that the changes in the futures prices deviate from the changes in the spot prices. On March 30, 2005, the weekly changes in the spot (futures) prices of crude oil, gasoline, and heating oil are 4.53 (0.18), -0.71 (0.88), and 2.22 (3.07) dollars per barrel. This corresponds to the unhedged P&L of -4.26 dollars per barrel, and the hedged P&L of $-4.26 + b_C(0.18) - (2/3)b_G(0.88) - (1/3)b_H(3.07)$ (see equation (2.3)). Thus, any positive gasoline and heating oil hedge ratios would tighten the refining margin. In particular, depending on the estimation windows, the D-vine copula model results in an additional loss ranging from 1.05 to 1.81 dollars per barrel (with an average extra loss of 1.34 dollars per barrel). It is interesting to note that this sizable basis risk may be explained by fears of gasoline and heating oil supply disruptions caused by the BP Texas City Refinery Explosion (which occurred on the afternoon of March 23, 2005).

[28] On October 21, 2015, the weekly changes in the spot (futures) prices of crude oil, gasoline, and heating oil are -1.41 (-1.96), -1.64 (8.78), and -0.97 (-1.39) dollars per barrel. This corresponds to an unhedged P&L of about -0.01 dollar per barrel, and the hedge ratio (even a small number) would lead to a large decline in the refining margin. Depending on the estimation windows, the D-vine copula model results in an additional loss ranging from 6.32 to 6.90 dollars per barrel (with an average extra loss of 6.58 dollars per barrel). In this case, the adverse price movements in the gasoline futures market are likely caused by

suggest that the ability to hedge the extreme downside risk could decline considerably when the unhedged refining margin falls at the same time that the refining margin based on futures prices rises (presuming no speculation positions). In addition, it is worth noting that hedging may also increase the extreme risk if the refining margin based on futures prices rises (declines) more (less) than an increase (a decrease) in the unhedged refining margin. In other words, the occasional poor performance of the D-vine copula model is likely explained by a sizable basis risk.

Despite its occasional poor performance, comparing with the NP method, the D-vine copula model yields larger mean (median) ES reductions of about 1.26% (0.87%), 1.97% (1.77%), and 5.62% (4.38%) points for the 90%, 95%, and 99% confidence levels, respectively. As expected, the D-vine copula model offers a larger improvement over the NP method as the confidence level becomes larger. This is because the NP method is based on the empirical distribution of the price changes and is therefore likely to provide poor estimates of the very extreme quantiles of the distribution (Danielsson and De Vries 2000; Bekiros and Georgoutsos 2005; Pritsker 2006). It is also evident from Figures 2.11-2.13 that the D-vine copula model outperforms the NP method for most out-of-sample test windows at all confidence levels. In addition, the NP method produces negative ES reduction at the 99% confidence level much more often than the D-vine copula model (127 versus 28 test windows).

---

fears that Hurricane Patricia (which were predicted to devastate Mexico on October 23, 2015) would disrupt the gasoline supply.

The D-vine copula model is also preferred to the SGC, SSC, and C-vine copula models at all confidence levels, except at the 99% confidence level when the median hedging effectiveness is considered. In this case, the SSC model produces a slightly greater reduction in the ES of about 0.19% point. Overall, the mean (median) ES improvement of the D-vine copula model over these models is quite modest. Nevertheless, these models produce poor hedging performance much more often than the D-vine copula model. Specifically, at the 99% confidence level, the negative ES reductions are found in 190, 115, and 82 test windows for the SGC, SSC, and C-vine copula models, respectively. Given this result, the D-vine copula model seems to be a better and safer choice than the other hedging models in managing the ES of the refinery.

2.5 Conclusions

Oil refineries face the risk of profit margin erosion, which is associated with an increase in input prices (crude oil prices), a decrease in output prices (gasoline and/or heating oil prices), or a combination of both. In other words, they are exposed to price risks in multiple petroleum markets (including crude oil, gasoline and heating oil markets). To prevent the narrowing of their refining margin, the refineries may hedge against the risks of adverse input and output price movements using crude oil, gasoline, and heating oil futures. This chapter proposes a multiproduct futures hedging model that minimizes the downside risk of the oil refineries, measured by Semivariance (SV), Lower Partial Moment (LPM), Value at Risk (VaR), or Expected Shortfall (ES). This is

of special interest for the refineries that are particularly concerned about the negative impacts of shrinking refining margins (e.g., reduced company's liquidity and increased likelihood of bankruptcy).

The empirical analysis is based on a stylized problem of a typical U.S. oil refinery that converts 3 barrels of crude oil to 2 barrels of gasoline and 1 barrel of heating oil. The proposed hedging model constructs a joint distribution of six variables (spot and futures price changes in crude oil, gasoline, and heating oil markets) using a vine copula methodology, and determines the minimum-downside risk hedge ratios using a Monte Carlo optimization technique. The vine copula methodology, which is a relatively new class of multivariate copula approaches, is chosen because it allows to capture important characteristics of petroleum price changes such as an asymmetry (or skewness) in the distribution of each individual variable and heterogeneous (tail) dependence between different pairs of variables. In this chapter, two popular classes of vine copulas – the canonical (C-) and drawable (D-) vine copulas – are considered in the modeling of the dependence structure in petroleum markets. We evaluate the suitability of the C- and D-vine copula models by examining their hedging effectiveness over a number of (rolling) out-of-sample test windows. In addition, we compare the out-of-sample hedging effectiveness of the vine copula models to that of several common alternative approaches, including the nonparametric (NP), standard Gaussian copula (SGC), standard Student's t (SSC), and standard Clayton copula (SCC) models.

The main findings are as follows. First, on average we find that both C- and D-vine copula models are able to effectively reduce the risk of refining margin erosion, and

that the D-vine copula model provides better out-of-sample hedging effectiveness than the C-vine copula model. The results are consistent across all hedging objectives considered (namely, the minimum-SV, minimum-LPM, minimum-VaR, and minimum-ES objectives). The superiority of the D-vine copula model may be explained by its ability to directly capture the high dependence between the spot and its corresponding futures price changes in all petroleum markets, which is a feature that is not allowed by the C-vine copula model. Depending on the hedging objective, the mean (median) downside risk reductions offered by the D-vine copula model between 32.43% (32.77%) to 73.80% (78.09%). Second, the D-vine copula model yields negative hedging effectiveness (that is, increases risk of the unhedged position) in some out-of-sample test windows for the minimum-VaR and minimum-ES objectives (both at the 99% confidence level). We find that the occasional poor performance of the D-vine copula model is likely due to a sizable basis risk (or the risk that futures prices do not move in line with the underlying spot prices).

Third, the D-vine copula model is on average preferred to the widely used NP method regardless of which hedging objective is considered. While the superiority of the D-vine copula model over the NP method is generally seen across numerous out-of-sample test windows, it is strongest for most hedging objectives during the years of extreme petroleum price fluctuations (e.g., the years 2007 to 2010). This result signals the relevance of explicit modeling of the extreme price dependence. Finally, the D-vine copula model on average leads to greater downside-risk reductions than the SGC, SSC, SCC, and C-vine copula models. As expected, the improvement over the SCC model,

which uses only one parameter to capture the dependence structure of six variables, is enormous. However, the improvement over the SGC, SSC, and C-vine copula models is quite modest. Nevertheless, we find that these models (as well as the NP method) produce negative hedging effectiveness much more often than the D-vine copula model. Given these results, the D-vine copula model seems to be a good and safe hedging model for the refinery that wants to minimize the risk of refining margin contraction.

As indicated above, our analysis might be especially useful for petroleum (as well as non-petroleum) producers who seek to reduce the risks of adverse price movements in input and output markets. In addition, the findings reported in this chapter provide additional evidence that there is a benefit from modeling the joint distribution (more specifically, the dependence structure) more realistically. Nevertheless, this chapter leaves many interesting questions for future work. For example, we only consider the oil refinery business, and it would be interesting to compare the results obtained for other businesses (e.g. cattle feeders, soybean crushers, and international commodity traders). Further, it would be of great interest to investigate the impacts of estimation window sizes, of test window sizes, and of hedging horizons. Finally, it would also be interesting to compare the results of the models presented in this chapter with other classes of multivariate models such as a regime switching model of Ang and Bekaert (2002), a kernel copula model of Power and Vedenov (2010), and a regular vine copula model of Dißmann et al. (2013).

CHAPTER III

FORECASTING THE DISTRIBUTIONS OF ENERGY COMMODITY RETURNS: THE IMPORTANCE OF MODELING HETEROGENEOUS DEPENDENCE STRUCTURES

3.1 Introduction

Energy traders (including energy commodity producers, suppliers, consumers, and financial institutions) are typically exposed to price risks in multiple energy commodities. Obviously, prices of related energy commodities are not independent. Accurate risk assessment and effective risk management therefore require knowledge of joint distributions for the changes in spot energy commodity prices. During the last decades, copulas have been increasingly used by both practitioners and researchers to model and forecast the joint distributions of correlated random variables. This is due to their flexibility in separately modeling the marginal distributions of individual variables and the dependence structure that links all these marginal distributions. Accordingly, the copula-based density models can capture the empirically observed skewness and heavy tails of energy commodity returns, as well as the presence of non-linear dependence between commodity returns (see, for example, Grégoire, Genest, and Gendron 2008; Tong, Wu, and Zhou 2013; Aloui et al. 2014).

The main problem in practical applications of the copula technique is to identify the copula or the dependence structure. For the case of two random variables, a rich variety of copulas or types of dependence structure is available and well investigated.

However, the use of copulas is very challenging in higher dimensions because standard multivariate copulas (such as Gaussian, Student's t, Frank, Clayton, and Gumbel copulas) force all pairs of variables to have the same type of dependence. Accordingly, most of previous empirical studies on copula-based models have been limited to bivariate or trivariate settings (see, for example, Patton 2004, 2012; Diks, Panchenko, and van Dijk 2010; Chu, 2011). Vine copulas (or pair-copula constructions), introduced by Aas et al. (2009), overcome such limitations. More specifically, they permit heterogeneous dependence structures for different pairs of variables by building up a higher-dimension copula from bivariate copulas (or pair-copulas). This presents an important opportunity for extending literature on time series forecasting further.

Heretofore, vine copulas have been applied to forecast downside risk of financial portfolios (Weiß and Supper 2013; Brechmann, Czado, and Paterlini 2014; Zhang et al. 2014), to examine the dependence structures of financial and commodity markets (Chollete, Heinen, and Valdesogo 2009; Nikoloulopoulos, Joe, and Li 2012; Loaiza Maya, Gomez-Gonzalez, and Melo Velandia 2015), and to analyze portfolio management problems (Low et al. 2013; Harnandez 2014; Bekiros et al. 2015). However, to the best of our knowledge, there has been no study on the use of vine copulas in the context of out-of-sample multivariate density forecasting. The present study fills this gap by assessing and comparing quality of one-step-ahead density forecasts of returns produced by standard copula and more advanced vine copula models. In particular, we focus on analyzing the value of modeling heterogeneous

dependence structures with vine copulas in improving density forecasts for multivariate energy commodity returns.

The contribution of this chapter is twofold. First, we use both standard copulas and more advanced vine copulas to model the dependence structures of seven related energy commodities: crude oil, diesel fuel, gasoline, heating oil, jet fuel, natural gas, and propane. The importance of heterogeneous dependence structures for density forecasting is then measured by comparing the performance of density forecasts based on three types of vine copulas – canonical, drawable, and regular vine copulas – with density forecasts based on two standard copulas – Gaussian and Student's t copulas. To check whether the relative forecasting performance of different copula-based multivariate density models is robust to the choices of the marginal distributions, we model the marginal distribution of each return series using the four most popular choices for parametric marginal distributions (namely, the standard normal, skewed normal, Student's t, and skewed Student's t distributions). We assess the forecast accuracy of the competing density models using several calibration tests, and compare the predictive accuracy of competing models based on their out-of-sample likelihood (or Kullback-Leibler information criterion) scores.

Second, we contribute to the thin literature on density forecasting of energy commodity returns by estimating their joint density forecasts using various copula-based multivariate density models. Previous studies in this field have mainly focused on forecasting the distributions of oil prices (see, among several others, Morana 2001; Meade 2010; Høg and Tsiaras 2011). However, business and financial decision making

in the energy commodity markets involves more than one risky asset. Thus, knowledge of joint distributions of multiple energy commodity returns is especially crucial for energy risk management and portfolio allocation. Unfortunately, to our best knowledge, no study has examined forecasting accuracy of competing multivariate density models for related energy commodity returns. We address this here. Therefore, our findings would not only offer a richer understanding of applications of vine copulas in the context of forecasting multivariate time series, but also benefit energy risk managers as well as other energy market participants.

The remainder of this chapter is structured as follows. Section 3.2 presents the data on energy commodity price returns together with the preliminary statistical analysis of the data. Section 3.3 describes the copula-based multivariate density models, construction of forecast densities, and methods for evaluating density forecasts. Section 3.4 provides the empirical results, and Section 3.5 concludes the chapter.

3.2 Data

The empirical analysis is based on weekly spot prices for crude oil (West Texas Intermediate – Cushing Oklahoma), diesel fuel (Los Angeles, California), gasoline (New York Harbor), heating oil (New York Harbor), jet fuel (U.S. Gulf Coast), natural gas (Henry Hub), and propane (Mont Belvieu, Texas). The data are obtained from the Energy Information Administration (EIA). The price data span from January 10, 1997 to May 27, 2016, from which a sample of weekly percentage returns are constructed. This results in 1,010 weekly observations for each series of energy commodity returns. The

first two years of data (104 observations) are set aside for the initial estimation of one-step-ahead density forecasts for weekly energy commodity returns, while the out-of-sample period consists of 906 observations from January 15, 1999 to May 27, 2016.

Table 3.1. Summary statistics and correlation analysis on weekly spot returns for crude oil (CO), diesel fuel (DF), gasoline (GL), heating oil (HO), jet fuel (JF), natural gas (NG), and propane (PP)

	CO	DF	GL	HO	JF	NG	PP
Panel A: Summary Statistics							
Mean (%)	0.156	0.181	0.208	0.165	0.166	0.211	0.126
SD (%)	4.365	4.712	5.001	4.490	4.483	7.678	5.095
Skew	0.096	0.590	0.547	0.847	0.487	1.660	0.635
Ex. Kurt.	3.053	3.463	6.808	10.890	4.484	20.221	13.793
Min (%)	-17.497	-16.418	-20.141	-25.280	-20.402	-35.577	-29.315
Median	0.168	0.154	0.379	0.122	0.254	0.000	0.206
Max (%)	28.563	31.178	45.293	43.571	34.445	90.047	52.276
JB	396.94*	567.36*	2012.40*	5137.40*	891.58*	17751.0*	8112.6*
ADF	-22.37*	-21.26*	-20.40*	-22.75*	-22.22*	-22.02*	-21.77*
$Q(10)$	60.36*	111.61*	47.97*	93.64*	49.65*	28.12*	57.34*
$Q^2(10)$	262.94*	70.63*	39.73*	173.58*	161.82*	29.68*	107.54*
Panel B: Correlation Matrix							
CO	1.000	0.577	0.663	0.713	0.686	0.163	0.473
DF		1.000	0.554	0.662	0.674	0.166	0.417
GL			1.000	0.638	0.677	0.181	0.423
HO				1.000	0.809	0.275	0.558
JF					1.000	0.246	0.480
NG						1.000	0.417
PP							1.000

Notes: Summary statistics (Panel A) and correlation matrix (Panel B) are presented for the seven weekly energy commodity returns for the period January 10, 1997 to May 27, 2016. The total number of observations is 1,010 for each return series. SD, Skew, and Ex. Kurt. represent sample standard deviation, skewness, and excess kurtosis, respectively. JB is the Jarque-Bera test statistic, where * denotes the rejection of the null hypothesis of normality at the 1% significance level. ADF is the Augmented Dickey-Fuller test statistic, where * denotes the rejection of the null hypothesis that the respective return series follows a unit root process at the 1% significance level. $Q(10)$ is the Ljung-Box test statistic for the return series, where * denotes the rejection of the null hypothesis that there is no serial correlations in the return series up to order 10. $Q^2(10)$ is the Ljung-Box test statistic for the squared return series, where * denotes the rejection of the null hypothesis that there is no ARCH effect in the return series up to order 10.

Panel A of Table 3.1 reports summary statistics for the weekly energy commodity return series for the period January 10, 1997 to May 27, 2016 (the entire sample period). For all the return series, the means are rather small relative to the standard deviations. Based on weekly data, percentage changes in prices of natural gas are more volatile than those of crude oil and the five refined products. Also, natural gas returns exhibit the minimum (-35.58%) and maximum (90.05%) returns for our sample period. All return series are only slightly skewed to the right. However, they all have a high excess kurtosis, indicating that their distributions have thicker tails than a normal distribution. The significant Jarque-Bera test statistics confirm that all the return series are non-normally distributed. All the series reject the null hypothesis for the Augmented Dickey-Fuller (ADF) test of a unit root at 1% significance level, suggesting that all returns are stationary. In addition, the significant Ljung-Box statistics, $Q(10)$ and $Q^2(10)$, indicate that there are serial correlations and ARCH effects in the energy commodity returns.

Panel B of Table 3.1 presents sample correlations between weekly percentage returns for seven energy commodity markets over the full sample period. The highest correlation is found between heating oil and jet fuel returns (0.809) while the lowest correlation is found between crude oil and natural gas returns (0.163). To obtain more insights into the correlation and dependence structure of energy commodity markets, it is useful to visualize possible time-varying correlations between energy commodity returns. Figure 3.1 presents time series plots of rolling correlations between crude oil and

other energy commodity returns[29]. The plots clearly show that correlations are constantly changing. This indicates that it is important to update model parameters constantly to reflect current correlation and dependence structures.

3.3 Methodology

In this section, we first briefly introduce copula-based multivariate density models. Both standard and more advanced multivariate copula ("vine copula") models are discussed. We then proceed to describe the methods used to construct and evaluate the out-of-sample accuracy of competing density forecasts of energy commodity returns.

3.3.1 Copula-Based Multivariate Density Models

Let $\boldsymbol{X}_t = (X_{1,t}, X_{2,t}, \dots, X_{d,t})$ be a d-dimensional vector of stochastic variables. Sklar's theorem (Sklar 1959) states that the d-dimensional multivariate distribution, $F(\boldsymbol{x})$ of $\boldsymbol{X}_t$, can be expressed in terms of the marginal distributions $F_1, F_2, \dots, F_d$ and a copula function that describes their dependence structure. More formally,

(3.1) $F(\boldsymbol{x}) = C(F_1(x_1), F_2(x_2), \dots, F_d(x_d))$

where $F_i = F_i(x_i)$ for $i = 1,2, \dots, d$ and . $C: [0,1]^d \rightarrow [0,1]$. If F_i and C are differentiable, the joint density function, $f(\boldsymbol{x})$ of $\boldsymbol{X}_t$, can then be described as:

(3.2) $f(\boldsymbol{x}) = f_1(x_1) f_2(x_2) \cdots f_d(x_d)[c(F_1(x_1), F_2(x_2), \dots, F_d(x_d)]$

where $f_i = f_i(x_i)$ is the density of F_i and c is the density of the copula.

---

[29] The rolling correlations are computed using a rolling window of 104 weeks.

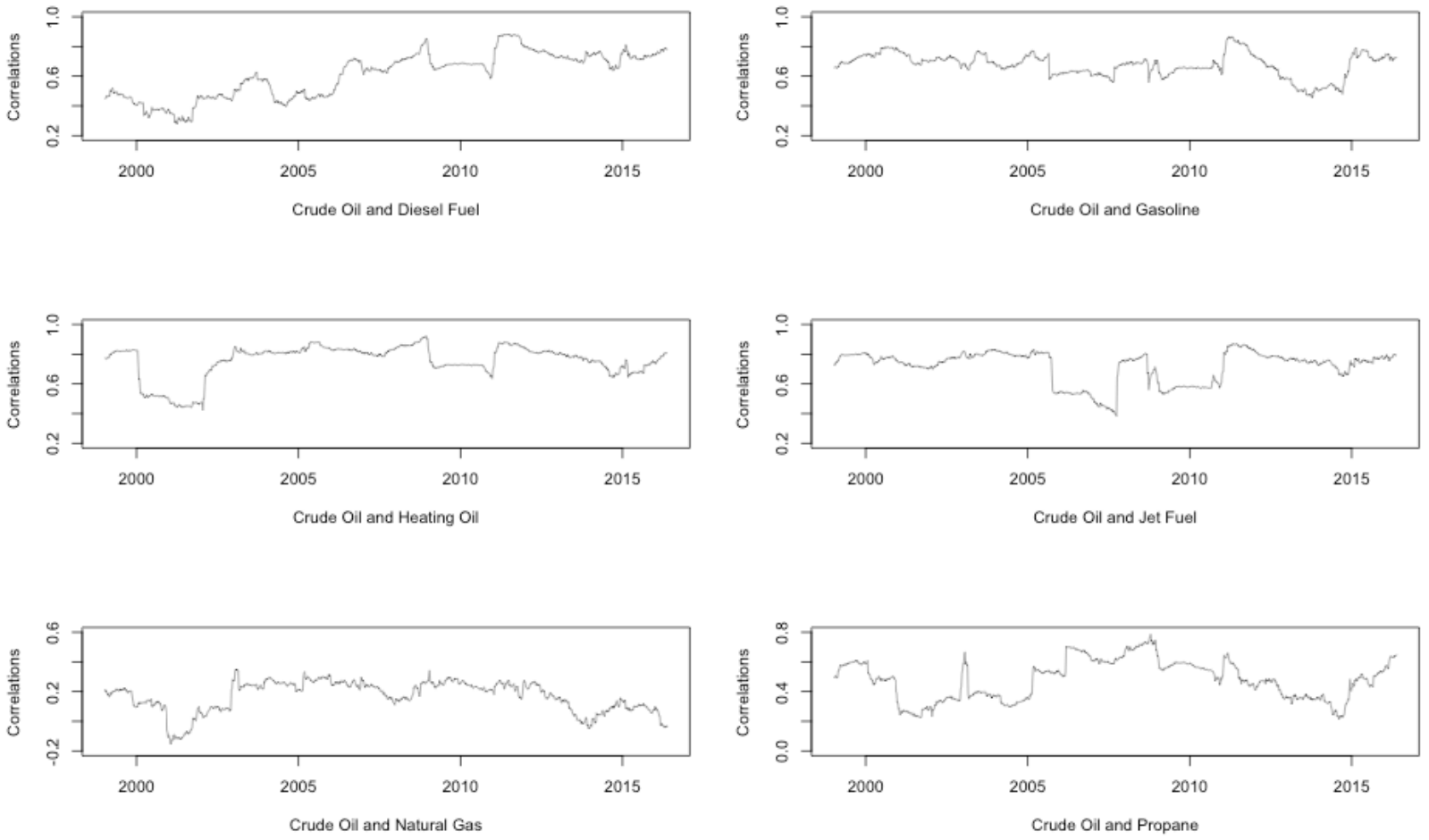

Figure 3.1. Time-varying linear correlation between weekly crude oil and other energy commodity returns (estimated with a 104-week rolling window)

The decompositions in equations (3.1) and (3.2) suggest that the marginal distributions and their dependence structure can be modeled separately. Thus, one can generate a broad range of joint distributions simply by combining different marginal distributions with different copula functions. This is clearly an attractive feature for modeling multivariate distributions. In terms of practical applications, there is a wide range of well-studied bivariate copula functions available (see, for example, Joe (1997) and Nelson (2006)). Nevertheless, the choice of multivariate copulas is rather limited and less known.

When modeling a joint distribution of more than two variables (i.e., when $d > 2$), a common approach is to rely on either a standard Gaussian copula (SGC thereafter) model or a standard Student's t copula (SSC thereafter) model. However, the SGC model assumes no tail dependence between each pair of $\left(F_i(x_i), F_j(x_j)\right)$. In other words, it assumes no extreme co-movements between random variables. While the SCC model allows for positive (symmetric) tail dependence, it forces every pair of $\left(F_i(x_i), F_j(x_j)\right)$ to have the same degree of tail dependence. Accordingly, the SGC and SSC models may be too restrictive for estimating the joint density of multiple random variables.

The vine copula or pair copula construction (PCC) model, first proposed by Joe (1996) and further extended by Bedford and Cooke (2001, 2002) and Kurowicka and Cooke (2006), has gained an increasing attention as an alternative and flexible way for building high-dimensional multivariate distributions. The modeling principle can be easily understood using a three-dimensional case (that is, $d = 3$). Without loss of

generality, a joint density function of x_1, x_2, and x_3, denoted as f_{123}, can be expressed as:

(3.3) $f_{123} = f_1 f_{2|1} f_{3|1,2} = f_1 \frac{f_{12}}{f_1} \frac{f_{23|1}}{f_{2|1}}$

where $f_{i|j,k} = f_{i|j,k}(x_i|x_j, x_k)$. The second expression in equation (3.3) is based on a definition of a conditional density function. Let $c_{ij|k} = c(F_{i|k}, F_{j|k})$ denote a conditional copula function of $F_{i|k}$ and $F_{j|k}$. From the Sklar's theorem, $f_{12} = f_1 f_2 c_{12}$ and $f_{23|1} = f_{2|1} f_{3|1} c_{23|1}$. We can also write $f_{3|1}$ as $f_{3|1} = c_{13} f_3$. Thus, the joint density function in equation (3.3) can be decomposed further as:

(3.4) $f_{123} = f_1 f_2 f_3 c_{12} c_{13} c_{23|1}$

where the conditional distribution function can be solved using:

(3.5) $F(x|\boldsymbol{v}) = \frac{\partial C_{x,v_j|\boldsymbol{v}_{-j}}(F(x|\boldsymbol{v}_{-j}), F(v_j|\boldsymbol{v}_{-j}))}{\partial F(v_j|\boldsymbol{v}_{-j})}$

That is, the vine copula model allows one to construct a joint distribution using (1) a cascade of conditional and unconditional bivariate copulas (called pair-copulas) and (2) a collection of conditional and unconditional marginal distributions.

Apparently, the decomposition in equation (3.4) is not unique. This implies that there are a large number of possible vine copula constructions from which to choose. Bedford and Cooke (2001, 2002) introduce a regular vine copula (RVC thereafter) model. A d-dimensional RVC is defined by a sequence of $d-1$ trees, $T_1, \ldots, T_{d-1}$. T_1 has d nodes and $d-1$ edges. Edges in T_1 then become nodes in T_2, and the two nodes in T_2 are joined by an edge in T_2 only if they share a common node in T_1 (proximity condition). In general, for $i = 2, \ldots, d-1$, the ith tree, T_i, has $d+1-j$ nodes that are

edges in T_{i-1}. The two nodes in T_i are joined by edge only if they share a common node in T_{i-1}. The joint density function of a d-dimensional RVC is given by[30]:

(3.6) $f_{1\cdots d} = \prod_{k=1}^{d} f_k \prod_{i=1}^{d-1} \prod_{e\in E_i} c_{j(e),k(e)|D(e)}(F_{j(e)|D(e)}, F_{k(e)|D(e)})$

where E_i is a set of edges in T_i, $j(e)$ and $k(e)$ are the two (conditional) nodes associated with each edge e, $D(e)$ is the conditioning set associated with edge e.

The number of different RVC decompositions is still very large. Morales-Nápoles, Cooke, and Kurowicka (2010) show that there are as many as $\binom{d}{2} \times (d-2)! \times 2^{\binom{d-2}{2}}$ different decompositions for the d-dimensions. Two special cases of RVC decompositions are canonical vine copula (CVC thereafter) and drawable vine copula (DVC thereafter) decompositions (Kurowicka and Cooke 2006). In d-dimensions, the joint density function of a CVC is given by:

(3.7) $f_{1\cdots d} = \prod_{k=1}^{d} f_k \prod_{i=1}^{d-1} \prod_{j=1}^{d-i} c_{i,i+j|1,\ldots,i-1}\left(F_{i|1,\ldots,i-1}, F_{i+j|1,\ldots,i-1}\right)$

whereas the joint density function of a DVC is given by:

(3.8) $f_{1\cdots d} = \prod_{k=1}^{d} f_k \prod_{i=1}^{d-1} \prod_{j=1}^{d-i} c_{i,i+j|1,\ldots,i-1}\left(F_{i|1,\ldots,i-1}, F_{i+j|1,\ldots,i-1}\right)$

For the d-dimensional case, there exist $d!/2$ different decompositions for both CVC and DVC models (Morales-Nápoles, Cooke, and Kurowicka 2010). Examples of four-dimensional CVC, DVC, and RVC trees are depicted respectively in Figures 3.2-3.4.

[30] The derivation of the joint density of RVC can be found in Kurowicka and Cooke (2006).

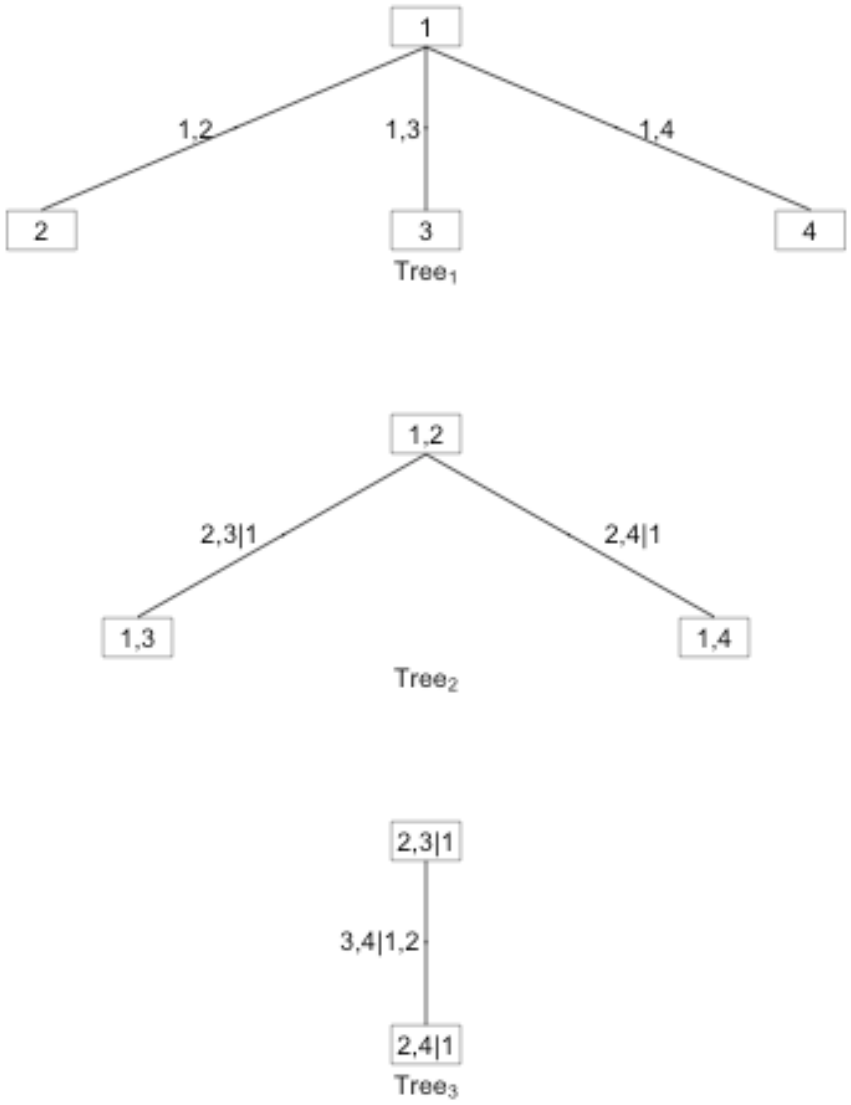

Figure 3.2. Four-dimensional canonical vine copula (CVC)

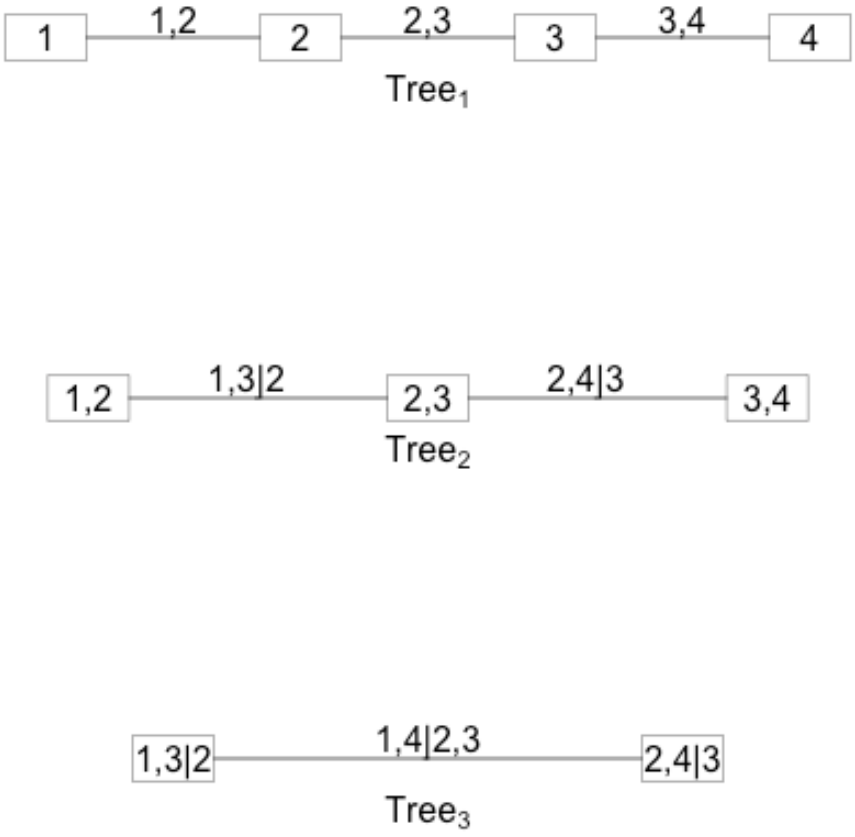

Figure 3.3. Four-dimensional drawable vine copula (DVC)

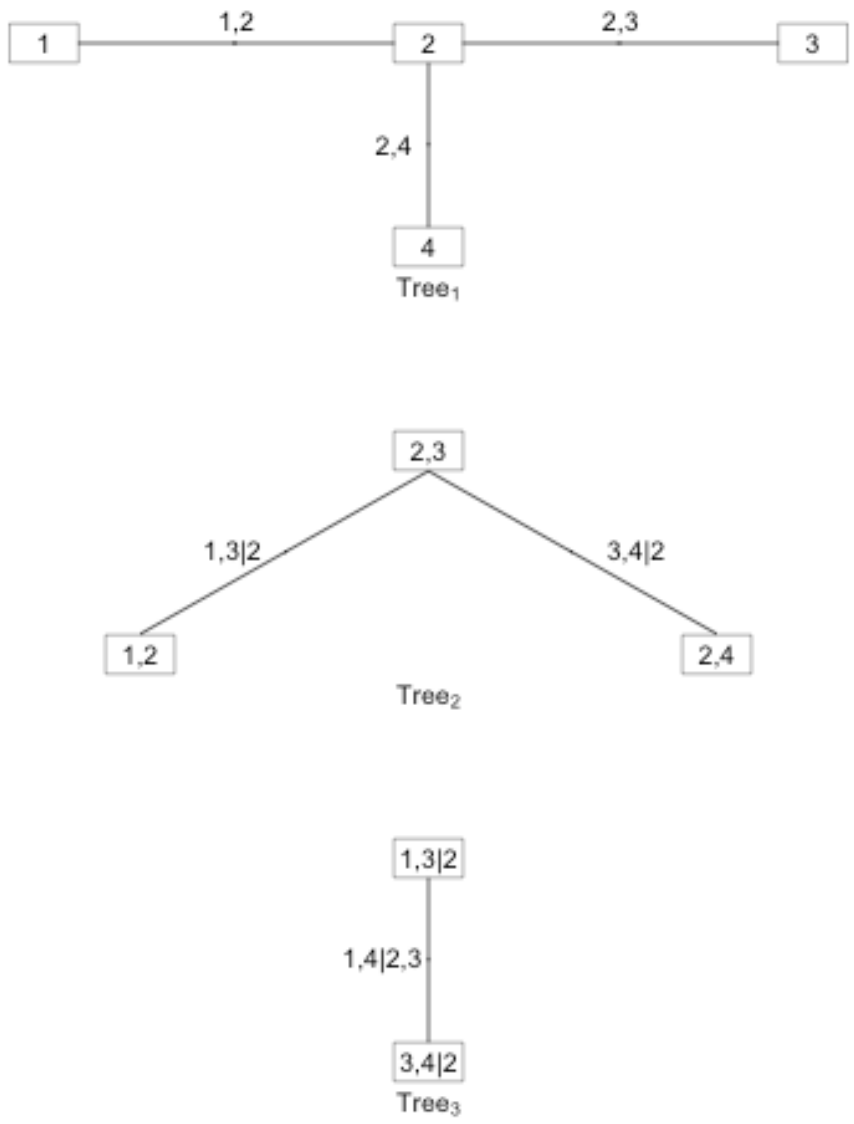

Figure 3.4. Four-dimensional regular vine copula (RVC)

3.3.2 Construction of Forecast Densities

In this chapter, we examine if the quality of one-step-ahead density forecast can be improved by modeling potentially heterogeneous dependence structures of energy

commodity returns using the more advanced vine copula models (namely, the CVC, DVC, and RVC models). The two standard multivariate copula models, the SGC and SSC models, are used as benchmark models. Our competing copula-based forecast densities are constructed using the following procedure.

For each week t, we use the data from week $t-103$ to t (estimation window = 104 weeks) to generate multivariate probability distributions at week $t+1$ from the competing multivariate copula models. Density forecasting based on multivariate copula models proceeds in three stages. In the first stage, we model a marginal distribution of each return series. Table 3.1 shows that all return series have a high excess kurtosis, but they are only slightly skewed (almost symmetric). Table 3.1 also indicates that there are serial correlations and ARCH effects in all energy commodity returns. To capture the heavy tails as well as the presence of heteroskedasticity, we model the marginal distribution of each return series using a GARCH model with Student's t innovations. In addition, to examine the impacts of the choice of the marginal distributions, we also consider a GARCH model with normal, skewed normal, and skewed Student's t innovations. More specifically, the conditional means and conditional variances for the seven return series are specified by an ARMA(1,1)-GARCH(1,1) model given by[31]:

(3.9) $$r_{i,t} = c_i + \phi_i r_{i,t-1} + \theta_i \varepsilon_{i,t-1} + \varepsilon_{i,t}$$

(3.10) $$\sigma_{i,t}^2 = \omega_i + \alpha_i \varepsilon_{i,t-1}^2 + \beta_i \sigma_{i,t-1}^2$$

[31] We also consider a GARCH(1,1) model with a constant mean, an AR(1)-GARCH(1,1) model, and an MA(1)-GARCH(1,1) model. These models are common univariate specifications for modeling the marginal distribution of asset returns. Nevertheless, we find that the ARMA(1,1)-GARCH(1,1) model does a better job than the other three models in removing autocorrelation in petroleum returns.

(3.11) $z_{i,t} = \frac{\varepsilon_{i,t}}{\sigma_{i,t}} \sim i.i.d.D(0,1)$

where $D(0,1)$ is a zero mean and unit variance probability distribution. We consider the four most popular choices for parametric marginal distributions in the literature: the standard normal, skewed normal, Student's t, and skewed Student's t distributions[32]. Although it is possible to use different univariate models for different return series, the same marginal processes are assumed for all return series. This allows us to investigate if the forecasting performance of each multivariate copula model is robust to possible misspecification of the marginal distributions. After fitting the ARMA(1,1)-GARCH(1,1), each series of standardized residuals (or innovations), $z_{i,t} = \varepsilon_{i,t}/\sigma_{i,t}$, are transformed into copula data (that is, a standard uniform variable) using either a normal, skewed normal, Student's t, or skewed Student's t distribution.

In the second stage, we fit the five multivariate copula models to the set of standard uniform variables, $\boldsymbol{u} = (u_{1,t}, u_{2,t}, \dots, u_{7,t})$, obtained from the previous stage. For the three vine copula models (CVC, DVC, and RVC models), the vine structures and bivariate copula parameters are estimated and selected using a sequential estimation procedure proposed by Aas et al. (2009) for the CVC and DVC models and by Dißmann et al. (2013) for the RVC model. In this study, the bivariate copula selection is based on the minimization of the Schwarz's Bayesian Information Criterion (BIC)[33]. In other

[32] The method proposed by Fernandez and Steel (1998) is used to incorporate skewness into the standard normal and Student's t distributions.

[33] A total of 31 different parametric bivariate copula functions – the maximal list of the R package: CDVine (Brechmann and Schepsmeier 2013) – are considered. These include Gaussian, Student's t, Clayton, Gumbel, Frank, Joe, BB1, BB6, BB7, BB8, Rotated Clayton (90, 180, and 270 degrees), Rotated Gumbel (90, 180, and 270 degrees), Rotated Joe (90, 180, and 270 degrees), Rotated BB1 (90, 180, and

words, we allow for each pair-copula to come from different parametric copula families. For the SGC and SSC models, copula parameters are estimated through a Maximum Likelihood Estimation (MLE) method.

In the third stage, one-step-ahead density forecasts of energy commodity returns from the competing multivariate copula models are computed using a Monte Carlo simulation method. This is done by first generating 10,000 draws of the seven standard uniform variables, $\{\tilde{u}_{1,s}, \tilde{u}_{2,s}, \dots, \tilde{u}_{7,s}\}_{s=1}^{10,000}$ from each estimated copula model. These simulated data are converted to a set of standardized residuals, $\{\tilde{z}_{1,s}, \tilde{z}_{2,s}, \dots, \tilde{z}_{7,s}\}_{s=1}^{10,000}$ using the inverse of the corresponding marginal distribution function of each return series. For each draw s, the forecast of energy commodity return for week $t+1$, $\tilde{r}_{i,s,t+1}$, is given by:

$$\tilde{r}_{i,s,t+1} = \hat{r}_{i,t+1} + \tilde{z}_{i,s}\hat{\sigma}_{i,t+1} \quad (3.12)$$

where $\hat{r}_{i,t+1}$ is the mean forecast based on the estimated conditional mean in equation (3.9) and $\hat{\sigma}^2_{i,t+1}$ is the variance forecast based on the estimated conditional variance in equation (3.10)[34]. As in Høg and Tsiaras (2010), a Gaussian kernel density is applied to

---

270 degrees), Rotated BB6 (90, 180, and 270 degrees), Rotated BB7 (90, 180, and 270 degrees) and Rotated BB8 (90, 180, and 270 degrees) copula functions.

[34] Following Diks, Panchenko, and van Dijk (2010), we ignore the presence of parameter estimation uncertainty and consider this as an integral part of each copula-based multivariate density model. Nonetheless, it would be useful to examine how the forecast results would change when the parameter estimation uncertainty is taken into account. See, for example, Kling and Bessler (1989), Garratt et al. (2003), and Reeves (2005) for how the uncertainty due to parameter estimation could be incorporate into the computation of density forecasts.

the 10,000 point forecasts of $r_{i,t+1}$ to generate a smooth estimate of the density of the forecast of energy commodity returns[35].

3.3.3 Evaluating Density Forecasts

We evaluate the out-of-sample performance of competing density forecasts of energy commodity returns using several evaluation methods. We begin by assessing whether a sequence of density forecasts produced by each multivariate copula model coincides with the true densities (that is, whether it is well calibrated). In doing so, we apply a nonparametric calibration method presented in Dawid (1984) and Kling and Bessler (1989). The method is briefly described below.

Let $f_{i,t}(r_i)$ be a forecast density of time series i produced by a particular multivariate copula model at time t, and $R_{i,t+1}$ be an actual realization of the random variable i at time $t+1$. The probability integral transform (PIT) value is defined as:

(3.13) $p_{i,t} = \int_{-\infty}^{R_{i,t+1}} f_{i,t}(r_i)\, dr_i$

If a sequence of density forecasts is well calibrated, then a sequence of $p_{i,t}$ is independently and uniformly distributed over [0,1] (Dawid 1984). Following Kling and Bessler (1989), uniformity is assessed by inspection of calibration plots and performing a chi-square test of good calibration. To obtain a nonparametric calibration function, the sequence of $p_{i,t}$ is first sorted in ascending order, $p_i(1), p_i(2), \ldots, p_i(K)$, where K is the

[35] This study relies on the Silverman's rule of thumb (Silverman 1986) to select a bandwidth for the kernel density estimation. In particular, the bandwidth is given by $bw = 0.9An^{-1/5}$, where A is the minimum of the sample standard deviation and the sample interquartile range divided by 1.34, and n is a sample size. We also consider an empirical distribution function for generating the density of the forecast of petroleum returns, and find that the main results still hold.

number of out-of-sample data points. The nonparametric calibration function, $\hat{C}(p_i)$ for p_i, is then calculated as:

(3.14) $\hat{C}\big(p_i(k)\big) = k/K, \quad k = 1,2,\dots,K$

This is simply an empirical (stepwise) cumulative distribution function (CDF). For a sequence of density forecasts to be well calibrated, the calibration function should be sufficiently close to a cumulative uniform distribution (or the 45° line). Nevertheless, expert judgment is needed in deciding whether the calibration function (or calibration plot) deviates sufficiently from the 45° line to reject a hypothesis of good calibration.

A more formal test of good calibration – a Pearson's chi-square test – can be used to further verify the uniformity. The idea of the test is to divide the unit interval (that is, the exhaustive range of observed fractiles or PITs) into J non-overlapping subintervals of equal length (that is, of length $1/J$), and compare the fraction of observed fractiles in each subinterval to the expected (or theoretical) fraction. For a uniform distribution, the expected fraction of outcome in any subinterval is equal to $1/J$. Therefore, under the null hypothesis of good calibration or uniformity of PITs, the fraction of observed fractiles in each subinterval should be close to $1/J$. To assess the closeness of the observed fractions to the expected fractions, a Pearson's chi-square test statistic is computed as:

(3.15) $\chi^2 = \sum_{j=1}^{J} \frac{\left(O_j - K/J\right)^2}{K/J}$

where O_j is the number of observed fractiles in the subinterval j, and K is a number of density forecasts. Under very weak conditions (not requiring independence), the χ^2 test

statistic follows, asymptotically, a chi-square distribution with $J-1$ degrees of freedom under the null hypothesis of good calibration (Seillier and Dawid 1993).

We further evaluate the goodness of the density forecasts using an inverse standard cumulative normal transform of the PIT sequence defined as:

(3.16) $q_{i,t} = \Phi^{-1}(p_{i,t})$

where $\Phi^{-1}(\cdot)$ is an inverse cumulative normal distribution function. As discussed in Diebold, Gunther, and Tay (1998) and Berkowitz (2001), a series of $q_{i,t}$ should be independently, identically and normally distributed with zero mean and unit variance (or i.i.d. $N(0,1)$) if the density forecasts are correctly specified. Following Diebold, Gunther, and Tay (1998), we use separate tests for examining the normality and independence of $q_{i,t}$. In particular, we test the hypothesis of normality using the Anderson-Darling (AD) test (Stephens 1974). The AD test statistic is computed as:

(3.17) $AD = -K - \frac{1}{K}\sum_{k=1}^{K}[2k-1][\ln(\Phi[q_i(k)]) + \ln(1-\Phi[q_i(K-k+1)])]$

where $\Phi[\cdot]$ is the cumulative distribution function of the standard normal distribution; $q_i(k)$ is the kth smallest value of $q_{i,t}$; K is the number of out-of-sample data points; and $\ln(\cdot)$ is the natural logarithm. As recommended by D'Agostino and Stephens (1986), the p-value for the AD test statistic is calculated from the modified statistic $AD^* = AD(1.0 + 0.75/K + 2.25/K^2)$[36].

As mentioned previously, a correctly specified density forecast model should produce a $p_{i,t}$ series (or, equivalently, a $q_{i,t}$ series) that is independently distributed. In

[36] The formulas for computing the p-value of the AD^* statistic are given in Table 4.9 in D'Agostino and Stephens (1986).

testing the independence hypothesis, we follow Mitchell and Wallis (2011), and examine the independence hypothesis based on both the $p_{i,t}$ and $q_{i,t}$ series. For the $p_{i,t}$ series, we apply the Ljung-Box test for autocorrelation in the $p_{i,t}$ series up to lag four. For the $q_{i,t}$ series, we apply a likelihood ratio (LR_1) test of Berkowitz (2001). In particular, Berkowitz (2001) suggests testing the null hypothesis of independence against an alternative hypothesis that the $q_{i,t}$ series follows a first-order autoregressive structure. In doing so, the following model is estimated via the MLE method:

(3.18) $q_{i,t} - \mu_i = \rho_i\left(q_{i,t-1} - \mu_i\right) + \varepsilon_{ti,}$

where $\varepsilon_{ti,}$ is i.i.d. $N(0, \sigma_i^2)$. The LR_1 test statistic is then computed as:

(3.19) $LR_1 = -2(L(\hat{\mu}_i, \hat{\sigma}_i^2, 0) - L(\hat{\mu}_i, \hat{\sigma}_i^2, \hat{\rho}_i))$

where $L(\mu_i, \sigma_i^2, \rho_i)$ denotes a log likelihood function. The LR_1 statistic approximately follows a chi-square distribution with one degree of freedom under the null hypothesis of independence.

While the aforementioned statistical tests of calibration are useful for evaluating the overall forecasting performance of each density model, they do not allow us to directly compare the predictive accuracy of competing multivariate copula specifications. Toward this purpose, we employ a statistical test for equal predictive accuracy suggested by Diks, Panchenko, and van Dijk (2010). The proposed test compares the predictive accuracy of two candidate copula specifications, $\hat{c}_t^{(a)}$ and $\hat{c}_t^{(b)}$,

using their out-of-sample log-likelihood scores[37]. Let $R_{i,t+1}$ denote an ex-post realization of the return series i, $\hat{r}_{i,t+1}$ denote its conditional mean forecast from equation (3.9), and $\hat{\sigma}^2_{i,t+1}$ denote its conditional variance forecast from equation (3.10). The standardized prediction error of the one-step-ahead forecast for each series i can be calculated as:

(3.20) $\hat{z}_{i,t+1} = \frac{R_{i,t+1} - \hat{r}_{i,t+1}}{\hat{\sigma}_{i,t+1}}$

Its corresponding PIT, denoted as $\hat{u}_{i,t+1}$, is given by $\hat{u}_{i,t+1} = \widehat{D}_{i,t}(\hat{z}_{i,t+1})$, where $\widehat{D}_{i,t}(\cdot)$ is its associated conditional marginal density (either a normal, skewed normal, Student's t or Skewed Student's t distribution).

Let $\widehat{\boldsymbol{u}}_{t+1} = (\hat{u}_{1,t+1}, \hat{u}_{2,t+1}, \dots, \hat{u}_{7,t+1})'$ denote a vector of PITs, and $\hat{c}_t$ denote a multivariate copula density associated with the one-step-ahead density forecasts. The out-of-sample log-likelihood score is defined as:

(3.21) $S_{t+1} = \sum_{i=1}^{7} \log \widehat{D}_{i,t}(\hat{z}_{i,t+1}) + \log \hat{c}_t(\widehat{\boldsymbol{u}}_{t+1})$

The expression in equation (3.21) is derived from the fact that any joint log-likelihood can be decomposed into the log-likelihood of each marginal distribution, $\log \widehat{D}_{i,t}(\hat{z}_{i,t+1})$, and log-likelihood of a multivariate copula $\log \hat{c}_t(\widehat{\boldsymbol{u}}_{t+1})$. Because the two competing copula-based multivariate density models are constructed using the same marginal distributions, the difference in their out-of-sample likelihood scores, $d_{t+1} = S^A_{t+1} - S^B_{t+1}$, is given by:

(3.22) $d_{t+1} = \log \hat{c}^{(a)}_t(\widehat{\boldsymbol{u}}_{t+1}) - \log \hat{c}^{(b)}_t(\widehat{\boldsymbol{u}}_{t+1})$

---

[37] This is an extension of the in-sample pseudo-likelihood ratio testing approach of Chen and Fan (2006) and Patton (2006).

To test the null hypothesis of equal out-of-sample likelihood scores (i.e., $\mathbb{E}(d_{t+1}) = 0$), the following test statistic is calculated[38]:

$$t = \frac{\bar{d}}{\sqrt{\hat{\sigma}_d^2/K}} \tag{3.23}$$

where K is the total number of out-of-sample forecasts, $\bar{d} = (1/K)\sum_{k=1}^{K} d_k$ is the sample average of the score differences, $\hat{\sigma}_d^2$ is a standard estimate of the heteroskedasticity and autocorrelation consistent (HAC) variance of $\sqrt{K}\bar{d}$. More specifically, $\hat{\sigma}_d^2$ is calculated as: $\hat{\sigma}_d^2 = \hat{\gamma}_0 + 2\sum_{j=1}^{J-1} a_j \hat{\gamma}_j$, where $\hat{\gamma}_j = cov(d_k, d_{k-j})$ is the lag-j sample autocovariance of the sequence $\{d_k\}_{k=1}^{K}$ and $a_j = 1 - (j/J)$ is the Bartlett weights (Bartlett 1950) with $J = \lfloor K^{1/4} \rfloor$.

Giacomini and White (2006) show that t has an asymptotic standard normal distribution under the null of equal predictive accuracy. A significantly positive (negative) average score difference suggests that the copula specification $\hat{c}_t^{(a)}$ performs significantly better (worse) than the copula specification $\hat{c}_t^{(b)}$. In addition, as discussed in Diks, Panchenko, and van Dijk (2010), the average of S_{t+1} across the out-of-sample period can be interpreted as measuring the Kullback-Leibler divergence (Kullback and Leibler 1951) or the divergence between the true density and the candidate density. Therefore, the sign of $\bar{d}$ also indicates which of the two copula specifications produces forecasts that are closer to the true density.

[38] This is a Diebold-Mariano type statistic (Diebold and Mariano 1995).

Table 3.2. Average log-likelihood (LLH), Akaike Information Criterion (AIC), Schwarz's Bayesian Information Criterion (BIC), and number of parameters for the five multivariate copula models

Model	LLH	AIC	BIC
Panel A: Normal marginal distributions			
CVC	307.26	-570.08	-511.3
DVC	306.95	-569.33	-510.39
RVC	307.93	-571.21	-512.17
SGC	275.29	-508.59	-453.05
SSC	287.60	-531.19	-473.02
Panel B: Skewed normal marginal distributions			
CVC	304.03	-563.78	-505.25
DVC	303.75	-563.19	-504.61
RVC	304.52	-564.71	-506.09
SGC	272.30	-502.61	-447.07
SSC	283.05	-522.10	-463.93
Panel C: Student's t marginal distributions			
CVC	311.12	-577.38	-518.05
DVC	310.40	-575.85	-516.44
RVC	311.06	-577.17	-517.73
SGC	278.46	-514.92	-459.39
SSC	292.91	-541.82	-483.64
Panel D: Skewed Student's t marginal distributions			
CVC	306.16	-567.77	-508.85
DVC	305.89	-567.16	-508.17
RVC	306.49	-568.38	-509.41
SGC	274.68	-507.36	-451.83
SSC	287.18	-530.37	-472.19

Notes: Each multivariate copula model is estimated using a rolling window approach with an estimation window of 104 weeks. The total number of estimation windows is 906 windows. Panels A, B, C, and D report the in-sample fit results for the five copula models with normal, skewed normal, Student's t, and skewed Student's t marginal distributions, respectively. CVC, DVC, RVC, SGC, and SSC denote the canonical vine copula, drawable vine copula, regular vine copula, standard Gaussian copula, and standard Student's t copula models.

3.4 Empirical Results

This section first reports the in-sample fit of the five multivariate copula models: the canonical vine copula (CVC), drawable vine copula (DVC), regular vine copula (RVC), standard Gaussian copula (SGC), and standard Student's t copula (SSC) models. The marginal distributions are either modeled as a normal, skewed normal, Student's t, or skewed Student's t distribution. The section then proceeds to present our calibration test results. Then, comparisons of predictive accuracy are made across competing multivariate copula specifications.

3.4.1 In-Sample Fit

Table 3.2 presents the average log-likelihood (LLH), Akaike Information Criterion (AIC), and BIC values of the three vine copula models – CVC, DVC, and RVC models – and the two standard multivariate copula models – SGC and SSC models. The average values of LLH, AIC, and BIC are calculated across the 906 estimation windows. Panels A, B, C, and D reports the results for the five multivariate copula models with normal, skewed normal, Student's t, and skewed Student's t marginal distributions, respectively. On average, the three vine copula models provide a better fit (based on LLH, AIC, and BIC values) than the two standard copula models regardless of the choices of marginal distributions. Thus, from an in-sample perspective, the vine copula models give a superior fit over the more restrictive standard copula models. Comparing across the four types of marginal distributions, both AIC and BIC favor the copula models with Student's t marginal distributions. Among all considered models, the CVC

model with Student's t marginal distributions has the highest average LLH value, and smallest average AIC and BIC values. Nevertheless, The CVC, DVC, and RVC models have roughly the same average AIC and BIC values. Therefore, we could not discriminate among the CVC, DVC, and RVC models based on their in-sample fit.

3.4.2 Calibration Test Results

We next consider the calibration tests discussed in Section 3.3.3. We start by inspecting the closeness of the calibration plots of the five copula-based density forecast models to the 45° line. Figures 3.5-3.11 display the calibration plots for the density forecasts of the seven energy commodity returns based on CVC, DVC, RVC, SGC, and SCC models with Student's t marginal distributions[39]. As can be observed from Figures 3.5-3.11, the calibrations plots from the five copula models do not show any significant departure from the 45° line. This indicates that the density forecasts from these models seem to be well calibrated. More importantly, the density forecasts from the three vine copula models are very close in accuracy to the density forecasts from the two standard copula models. That is, based on the visual inspection of the calibration plots, the more advanced multivariate copula models do not help produce better one-step-ahead density forecasts of energy commodity returns than the standard multivariate copula models. Nevertheless, it is still too early to draw any solid conclusions on the importance of

[39] Calibration plots of the five copula-based models with normal, skewed normal, and skewed Student's t marginal distributions are provided in Appendix B (Figures B.1-B.21).

modeling heterogeneous dependence structures in the context of forecasting the distributions of energy commodity returns.

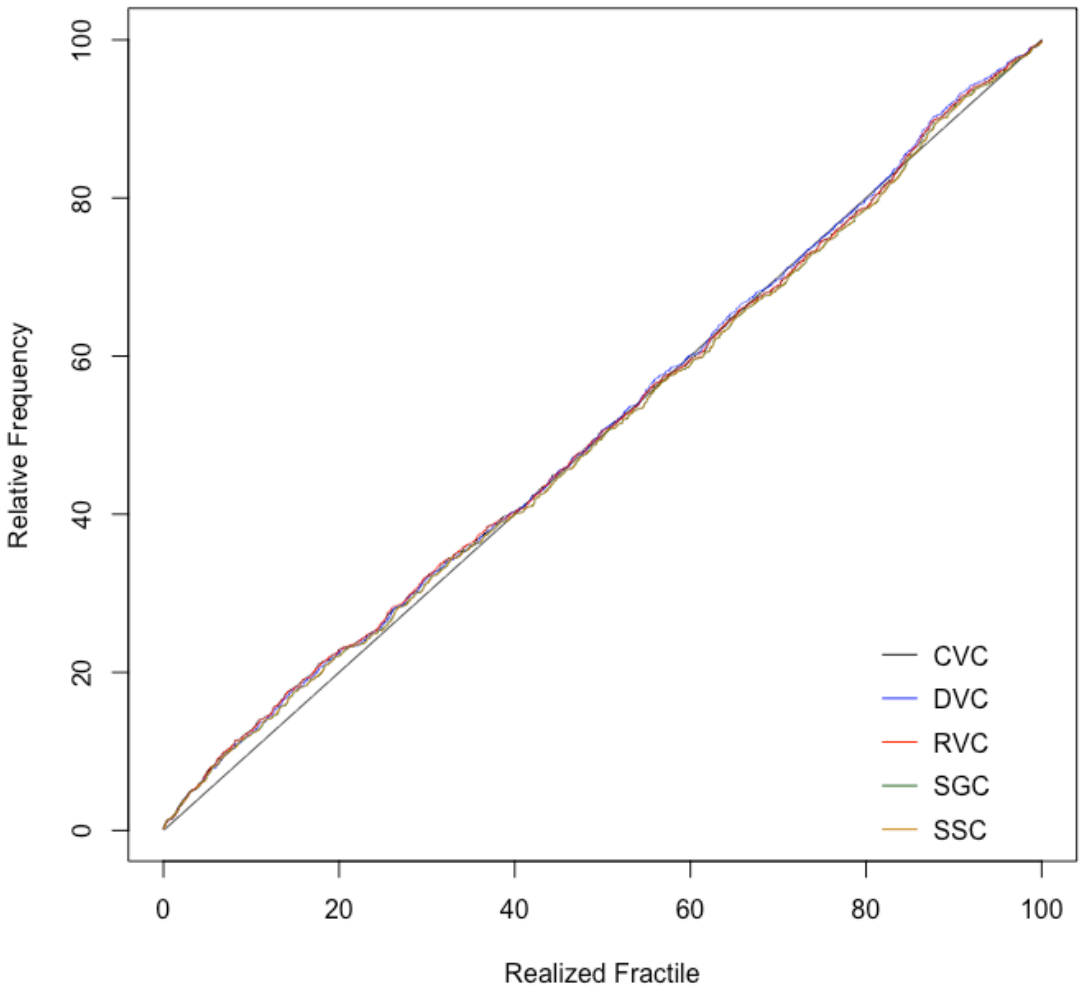

Figure 3.5. Calibration plots for the density forecasts of crude oil returns based on the canonical vine copula (CVC), drawable vine copula (DVC), regular vine copula (RVC), standard Gaussian copula (SGC), and standard Student's t copula (SSC) models with Student's t marginal distributions

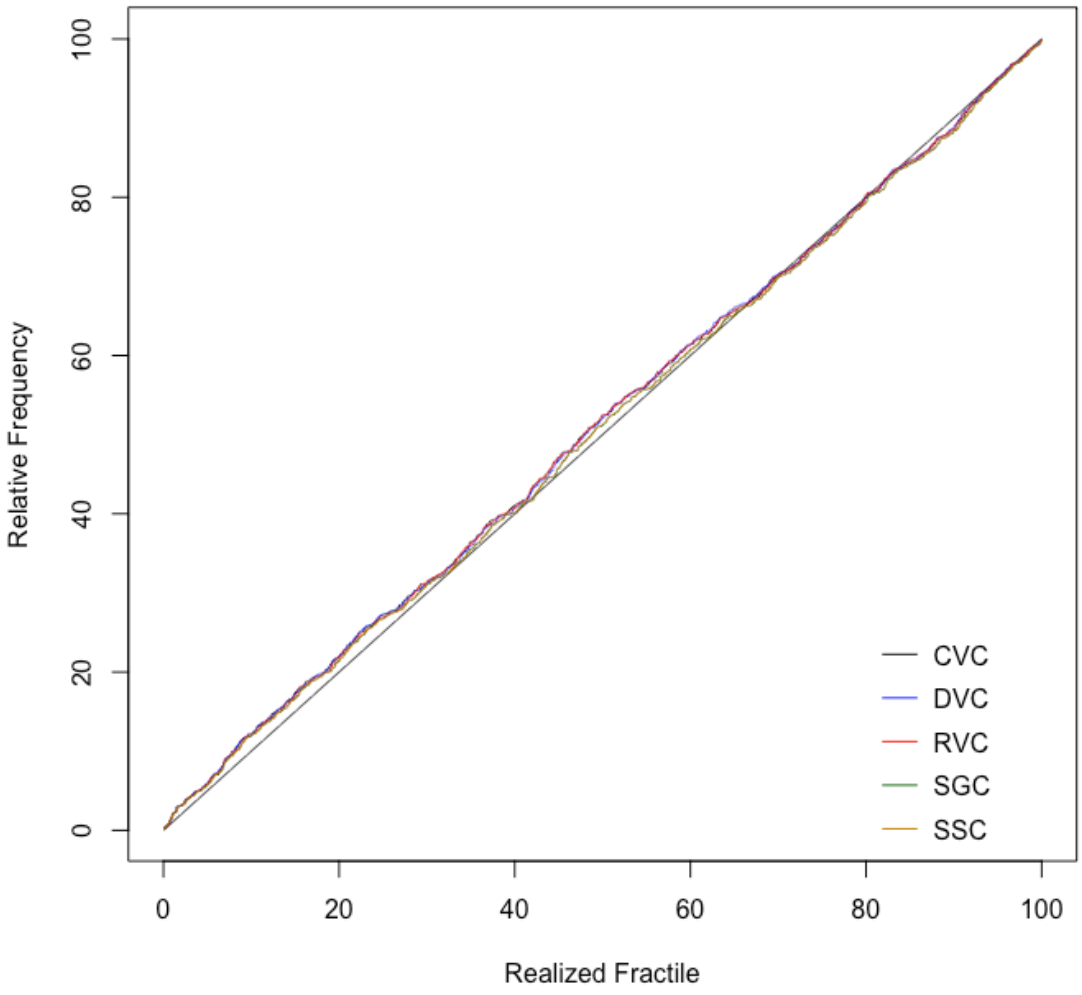

Figure 3.6. Calibration plots for the density forecasts of diesel fuel returns based on the canonical vine copula (CVC), drawable vine copula (DVC), regular vine copula (RVC), standard Gaussian copula (SGC), and standard Student's t copula (SSC) models with Student's t marginal distributions

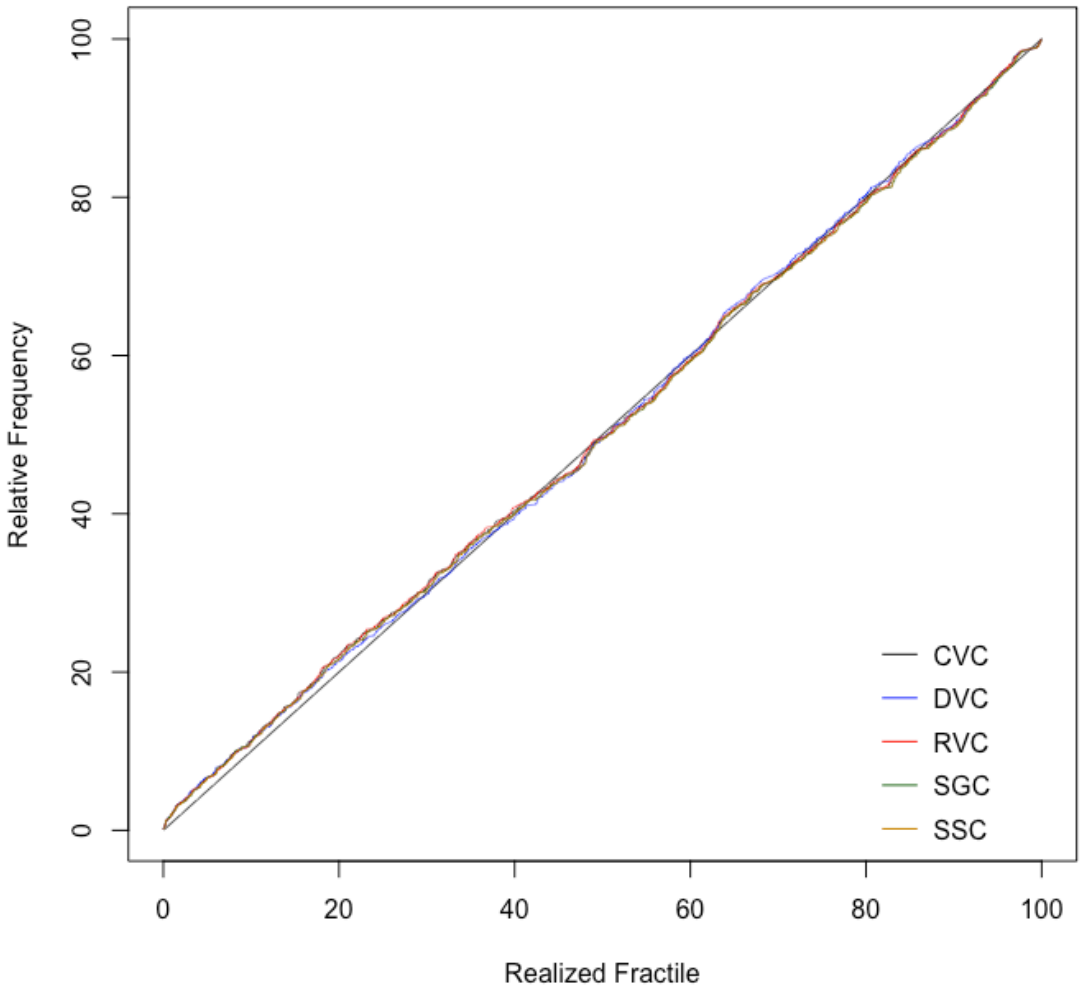

Figure 3.7. Calibration plots for the density forecasts of gasoline returns based on the canonical vine copula (CVC), drawable vine copula (DVC), regular vine copula (RVC), standard Gaussian copula (SGC), and standard Student's t copula (SSC) models with Student's t marginal distributions

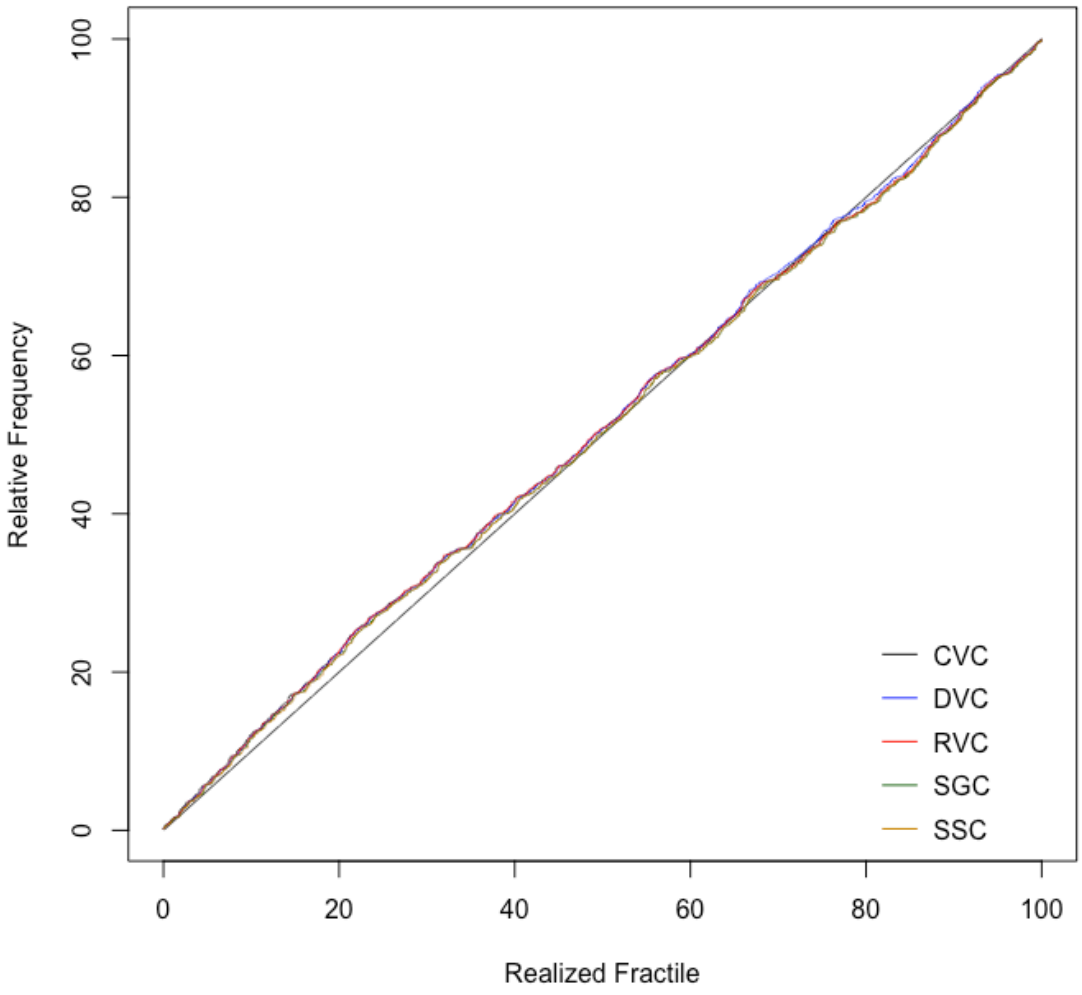

Figure 3.8. Calibration plots for the density forecasts of heating oil returns based on the canonical vine copula (CVC), drawable vine copula (DVC), regular vine copula (RVC), standard Gaussian copula (SGC), and standard Student's t copula (SSC) models with Student's t marginal distributions

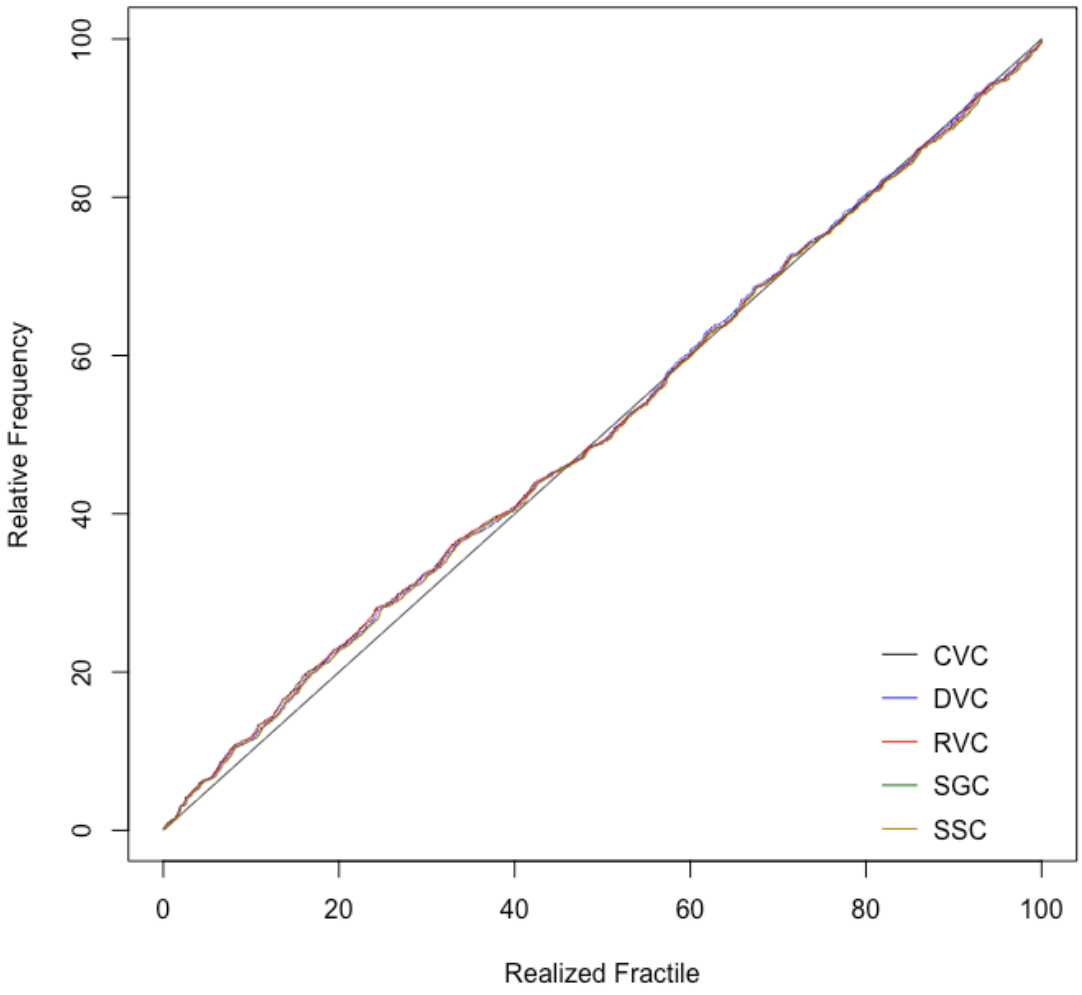

Figure 3.9. Calibration plots for the density forecasts of jet fuel returns based on the canonical vine copula (CVC), drawable vine copula (DVC), regular vine copula (RVC), standard Gaussian copula (SGC), and standard Student's t copula (SSC) models with Student's t marginal distributions

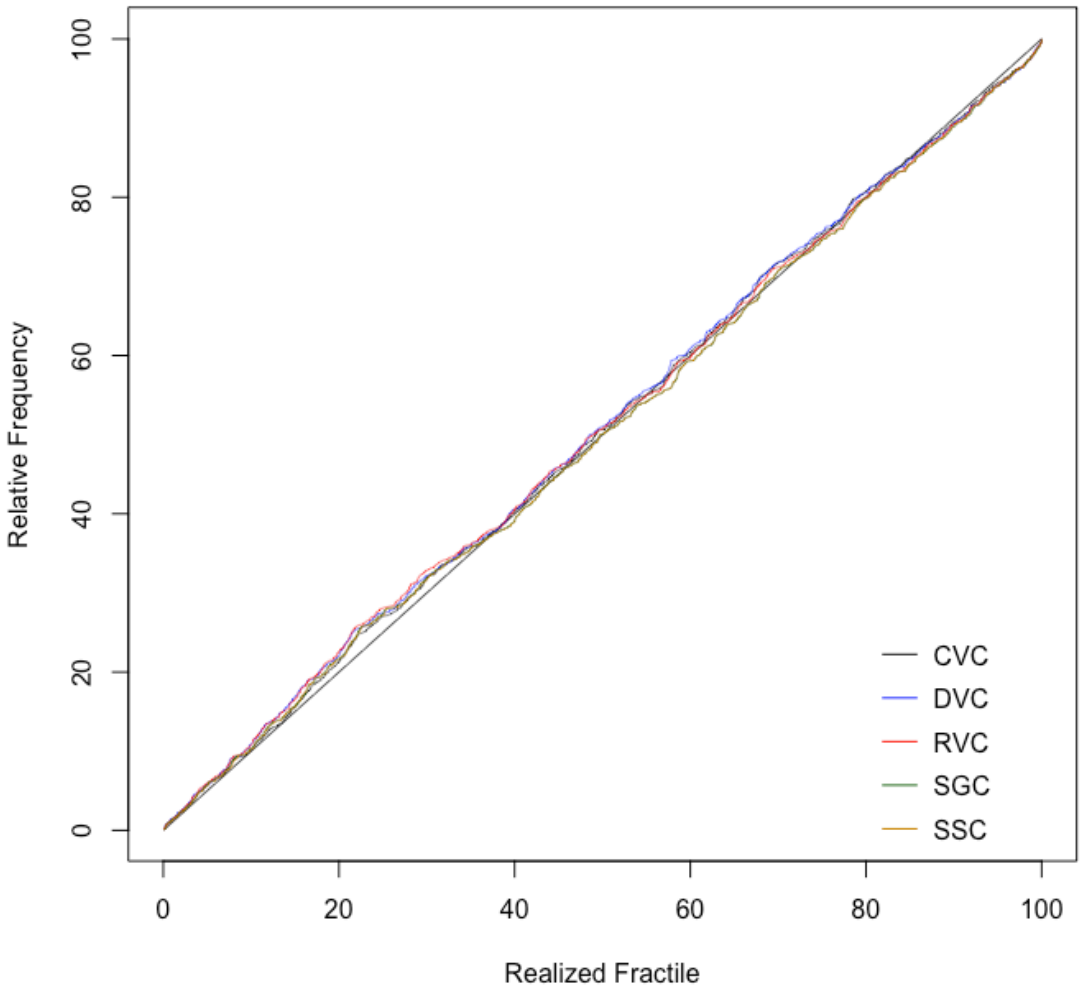

Figure 3.10. Calibration plots for the density forecasts of natural gas returns based on the canonical vine copula (CVC), drawable vine copula (DVC), regular vine copula (RVC), standard Gaussian copula (SGC), and standard Student's t copula (SSC) models with Student's t marginal distributions

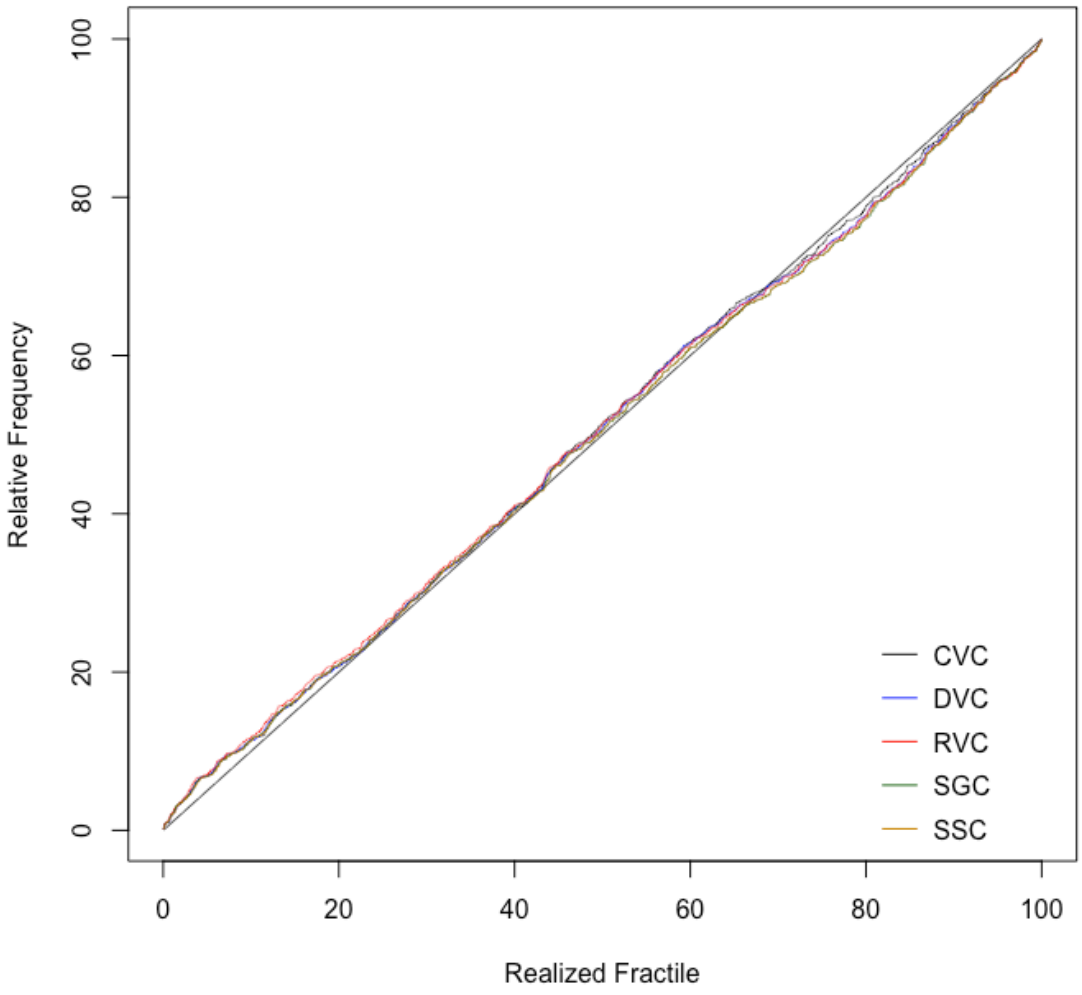

Figure 3.11. Calibration plots for the density forecasts of propane returns based on the canonical vine copula (CVC), drawable vine copula (DVC), regular vine copula (RVC), standard Gaussian copula (SGC), and standard Student's t copula (SSC) models with Student's t marginal distributions

Table 3.3. Pearson's chi-square test statistic

Model	Crude Oil	Diesel Fuel	Gasoline	Heating Oil	Jet Fuel	Natural Gas	Propane
Panel A: Normal marginal distributions							
CVC	27.687	14.442	15.678	14.530	15.060	23.757	22.698
DVC	30.291*	13.912	18.680	12.057	14.265	20.490	20.490
RVC	31.616*	14.795	18.106	15.104	14.618	24.861	22.698
SGC	27.201	7.996	16.826	11.660	13.868	24.905	26.274
SSC	27.863	8.658	17.311	12.587	12.411	25.876	26.141
Panel B: Skewed normal marginal distributions							
CVC	18.724	10.336	26.715	17.091	27.068	46.904**	42.653**
DVC	21.461	12.543	31.400*	17.576	27.157	55.810**	48.702**
RVC	20.534	10.159	28.834	16.826	24.155	57.179**	41.196**
SGC	15.898	10.777	26.406	14.353	24.905	45.258**	47.731**
SSC	14.883	9.673	25.126	14.971	24.508	45.700**	44.066**
Panel C: Student's t marginal distributions							
CVC	35.634*	19.872	19.475	17.267	21.859	16.649	14.221
DVC	27.951	16.737	22.698	15.854	20.446	14.486	20.137
RVC	31.748*	22.653	25.611	16.252	20.358	20.976	19.960
SGC	31.042*	14.132	24.331	15.854	24.287	22.124	20.402
SSC	25.832	14.927	22.477	15.722	21.461	22.918	20.269
Panel D: Skewed Student's t marginal distributions							
CVC	22.962	21.152	22.389	19.431	19.960	26.494	33.559*
DVC	20.137	16.561	23.536	15.545	21.064	29.232	34.088*
RVC	20.490	16.384	23.757	16.737	23.713	28.613	33.249*
SGC	12.278	16.201	24.817	18.768	20.799	24.155	36.737**
SSC	12.057	16.958	27.863	17.841	21.638	23.448	28.525

Notes: The number of subintervals for the Pearson's chi-square test is 20. * and ** denote the rejection of the null hypothesis of good calibration (or uniformity) at the 5% and 1% significance levels. Panels A, B, C, and D report the Person's chi-square test results for the five copula models with normal, skewed normal, Student's t, and skewed Student's t marginal distributions, respectively. CVC, DVC, RVC, SGC, and SSC denote the canonical vine copula, drawable vine copula, regular vine copula, standard Gaussian copula, and standard Student's t copula models.

As discussed in Section 3.3.3, a correctly specified density forecast model should produce a PIT series (that is, a $p_{i,t}$ series) that is independently and uniformly distributed over the support of $[0,1]$. This also implies that a series of the inverse normal cumulative distribution function of the PITs (i.e., a $q_{i,t}$ series) generated by any correctly specified density forecast model should be i.i.d. $N(0,1)$. In particular, a necessary condition for any multivariate density forecast model to be ideal requires that the seven $p_{i,t}$ series are

each uniformly distributed or, equivalently, the seven $q_{i,t}$ series are each normally distributed (Diebold, Hahn, and Tay 1999). The test statistics from the Pearson's chi-square test of uniformity of the $p_{i,t}$ series are given in Table 3.3, whereas the test statistics from the Anderson-Darling (AD) test of normality of the $q_{i,t}$ series are reported in Table 3.4[40].

Both Pearson's chi-square and AD tests reveal that the forecast accuracy largely based on the choices of marginal distributions. For copula models with normal marginal distributions, the CVC, SGC and SSC models pass the Pearson's chi-square test of good calibration at the 5% significance level (Table 3.3, Panel A). Nevertheless, none of these models pass the AD test of normality at any conventional significance level (Table 3.4, Panel A). In addition, incorporating skewness within the normal marginal distributions seems to be unproductive. As can be seen from Table 3.3 (Panel B) and Table 3.4 (Panel B), all the five copula models deliver unsatisfactory results. More specifically, the null hypothesis of uniformity is rejected at the 1% significance level for natural gas and propane return series, and the null of normality is rejected at the 5% significance level for all energy commodity return series. This is not totally surprising because each return series is only slightly skewed (see Table 3.1, Panel A).

[40]D'Agostino and Stephens (1986) suggest the number of subintervals to be around $1.88K^{2/5}$, where K is the number of data points. In this study, the number of subintervals used for calculating the Pearson's chi-square test statistics is 20.

Table 3.4. Anderson-Darling (AD) test of normality

Model	Crude Oil	Diesel Fuel	Gasoline	Heating Oil	Jet Fuel	Natural Gas	Propane
Panel A: Normal marginal distributions							
CVC	1.709**	0.892*	1.329**	0.556	1.324**	3.391**	2.846**
DVC	1.727**	0.937*	1.540**	0.539	1.278**	3.514**	3.061**
RVC	1.664**	0.871*	1.417**	0.513	1.283**	3.309**	3.139**
SGC	1.790**	1.121**	1.409**	0.572	1.498**	3.438**	3.124**
SSC	1.707**	1.031*	1.394**	0.559	1.477**	3.394**	3.026**
Panel B: Skewed normal marginal distributions							
CVC	2.015**	1.077**	1.416**	0.844*	1.961**	2.600**	4.076**
DVC	2.010**	1.103**	1.609**	0.805*	1.773**	2.808**	4.364**
RVC	1.898**	1.089**	1.545**	0.765*	1.810**	2.703**	4.473**
SGC	2.082**	1.277**	1.554**	0.767*	2.102**	2.803**	4.502**
SSC	2.160**	1.191**	1.611**	0.760*	2.037**	2.755**	4.227**
Panel C: Student's t marginal distributions							
CVC	1.042*	0.170	0.505	0.191	0.356	0.639	0.503
DVC	1.060**	0.190	0.765	0.208	0.370	0.619	0.498
RVC	1.022*	0.178	0.531	0.216	0.376	0.510	0.419
SGC	0.857*	0.205	0.472	0.228	0.412	0.521	0.404
SSC	0.851*	0.167	0.478	0.208	0.382	0.530	0.384
Panel D: Skewed Student's t marginal distributions							
CVC	0.605	0.211	0.459	0.324	0.713	1.002*	0.794*
DVC	0.818*	0.191	0.574	0.283	0.710	1.478**	0.943*
RVC	0.662	0.170	0.519	0.296	0.721	1.057**	0.776*
SGC	0.712	0.240	0.518	0.303	0.812*	1.083**	0.703
SSC	0.735	0.182	0.534	0.300	0.787*	1.174**	0.662

Notes: This table presents the test statistics from the Anderson-Darling (AD) tests of normality of the inverse normal cumulative distribution function of probability integral transforms (PITs) for the seven weekly energy commodity returns. * and ** denote the rejection of the null hypothesis of normality at the 5% and 1% significance levels. Panels A, B, C, and D report the test results for the five copula models with normal, skewed normal, Student's t, and skewed Student's t marginal distributions, respectively. CVC, DVC, RVC, SGC, and SSC denote the canonical vine copula, drawable vine copula, regular vine copula, standard Gaussian copula, and standard Student's t copula models.

For copula models with Student's t marginal distributions, only the DVC and SSC models pass the Pearson's chi-square test at the 5% significance level (Table 3.3, Panel C). Similar to the case of normal marginal distributions, none of these models pass the AD test of normality at the 5% significance level (Table 3.4, Panel C). Nevertheless, for the case of Student's t marginal distributions, the null hypothesis of normality is rejected only for crude oil return series. In addition, all models, but the DVC model,

marginally pass the AD test at the 1% significance level. Therefore, allowing for heavy tails in the marginal distributions seems to help improve forecast accuracy. For copula models with skewed Student's t marginal distributions, the Pearson's chi-square test suggests that only the SSC model delivers satisfactory density forecasts, and the AD test reveals that none of the models produce correct multivariate density forecasts (Tables 3.3 and 3.4, Panel D). This confirms the previous result that incorporating asymmetric marginal distributions (when unnecessary) can lead to less reliable density forecasts. Overall, based on the Pearson's chi-square and AD tests, the SSC model with Student's t marginal distributions performs relatively better than all other models under consideration. Moreover, it seems that forecast quality of each copula model depends largely upon the choices of marginal specifications.

We then turn to the tests of independence. Table 3.5 presents the results of the Ljung-Box test for autocorrelation in the $p_{i,t}$ series up to lag four. Except for copula models with skewed normal distributions, all copula models pass the Ljung-Box test of independence at the 5% significance level. Table 3.6 displays the results of the Berkowitz (2001) test of independence of the $q_{i,t}$ series. The likelihood ratio statistics indicate that the copula models with normal and Student's t marginal distributions produce satisfactory multivariate density forecasts because the null hypothesis of independence cannot be rejected at any conventional significance level. Putting this together with our previous results on uniformity of $p_{i,t}$ series (or normality of $q_{i,t}$ series), the SSC model with Student's t marginal distributions is superior to the other copula models under consideration.

Table 3.5. Test of independence of the probability integral transform (PIT) series

Model	Crude Oil	Diesel Fuel	Gasoline	Heating Oil	Jet Fuel	Natural Gas	Propane
Panel A: Normal marginal distributions							
CVC	3.022	3.438	1.488	0.711	0.281	6.880	7.262
DVC	3.069	3.379	1.531	0.719	0.273	6.918	7.381
RVC	2.953	3.388	1.463	0.702	0.269	6.903	7.335
SGC	3.134	3.434	1.511	0.711	0.285	6.838	7.433
SSC	3.131	3.418	1.517	0.704	0.278	6.853	7.419
Panel B: Skewed normal marginal distributions							
CVC	2.008	3.206	2.694	0.521	0.710	14.315**	7.724
DVC	2.043	3.174	2.684	0.512	0.699	14.232**	7.737
RVC	2.045	3.241	2.607	0.517	0.704	14.282**	7.789
SGC	2.106	3.257	2.706	0.528	0.733	14.988**	7.849
SSC	2.099	3.255	2.730	0.531	0.741	15.083**	7.845
Panel C: Student's t marginal distributions							
CVC	2.201	2.510	1.867	0.310	0.144	4.557	5.323
DVC	1.075	2.759	2.072	0.349	0.207	5.388	6.088
RVC	2.013	2.409	1.871	0.332	0.143	5.596	6.525
SGC	2.096	2.519	1.840	0.323	0.151	5.534	6.581
SSC	2.077	2.538	1.829	0.338	0.149	5.579	6.611
Panel D: Skewed Student's t marginal distributions							
CVC	2.761	3.167	2.074	0.448	0.261	5.261	6.641
DVC	1.918	2.506	2.447	0.510	0.468	5.222	6.920
RVC	2.640	2.720	2.080	0.450	0.246	5.934	6.764
SGC	2.795	2.732	2.069	0.465	0.263	6.024	6.821
SSC	2.778	2.722	2.078	0.461	0.259	6.042	6.772

Notes: This table presents the test statistics from the Ljung-Box test for autocorrelation in the PIT series up to lag four. ** denotes the rejection of the null hypothesis of no autocorrelation at the 1% significance level. Panels A, B, C, and D report the test results for the five copula models with normal, skewed normal, Student's t, and skewed Student's t marginal distributions, respectively. CVC, DVC, RVC, SGC, and SSC denote the canonical vine copula, drawable vine copula, regular vine copula, standard Gaussian copula, and standard Student's t copula models.

Table 3.6. Berkowitz (2001) likelihood ratio (LR_1) test of independence

Model	Crude Oil	Diesel Fuel	Gasoline	Heating Oil	Jet Fuel	Natural Gas	Propane
Panel A: Normal marginal distributions							
CVC	0.539	0.034	0.109	0.565	0.117	0.366	0.430
DVC	0.536	0.019	0.093	0.515	0.132	0.386	0.386
RVC	0.524	0.026	0.060	0.529	0.100	0.418	0.399
SGC	0.524	0.040	0.088	0.509	0.106	0.374	0.422
SSC	0.560	0.037	0.081	0.541	0.100	0.383	0.457
Panel B: Skewed normal marginal distributions							
CVC	0.103	0.410	0.000	0.854	0.342	5.693*	1.624
DVC	0.082	0.310	0.000	0.811	0.318	5.858*	1.772
RVC	0.080	0.312	0.002	0.810	0.343	6.067*	1.775
SGC	0.103	0.361	0.000	0.772	0.336	6.000*	1.631
SSC	0.088	0.364	0.001	0.786	0.365	6.165*	1.685
Panel C: Student's t marginal distributions							
CVC	0.355	0.339	0.205	0.982	0.139	0.373	0.858
DVC	0.204	0.355	0.369	0.834	0.274	0.456	1.246
RVC	0.380	0.274	0.190	0.949	0.078	0.560	1.205
SGC	0.367	0.258	0.187	0.897	0.062	0.560	1.244
SSC	0.301	0.277	0.169	0.884	0.050	0.538	1.214
Panel D: Skewed Student's t marginal distributions							
CVC	0.099	0.170	0.584	0.958	0.142	2.904	1.122
DVC	0.074	0.126	0.578	0.972	0.408	5.300*	1.590
RVC	0.063	0.116	0.474	0.906	0.089	5.348*	1.367
SGC	0.089	0.110	0.492	0.914	0.083	5.431*	1.361
SSC	0.068	0.129	0.492	0.985	0.111	5.575*	1.393

Notes: This table presents the likelihood ratio (LR_1) statistics from the Berkowitz (2001) test of independence against a first-order autoregression structure for the seven weekly energy commodity returns. * denotes the rejection of the null hypothesis of independence at the 5% and 1% significance levels. Panels A, B, C, and D report the test results for the five copula models with normal, skewed normal, Student's t, and skewed Student's t marginal distributions, respectively. CVC, DVC, RVC, SGC, and SSC denote the canonical vine copula, drawable vine copula, regular vine copula, standard Gaussian copula, and standard Student's t copula models.

Table 3.7. Tests of equal predictive accuracy between two copula models

Model	DVC	RVC	SGC	SSC
Panel A: Normal marginal distributions				
CVC	0.193	-1.396	0.368	-3.393**
DVC		-1.405	0.374	-3.592**
RVC			0.854	-3.211**
SGC				-3.407**
Panel B: Skewed normal marginal distributions				
CVC	1.058	-1.366	1.211	-2.977**
DVC		-2.180*	0.670	-3.324**
RVC			1.702	-2.726**
SGC				-3.301**
Panel C: Student's t marginal distributions				
CVC	0.032	0.183	0.223	-3.256**
DVC		0.107	0.271	-3.398**
RVC			0.163	-3.555**
SGC				-3.260**
Panel D: Skewed Student's t marginal distributions				
CVC	0.840	-0.667	1.024	-2.776**
DVC		-1.142	0.673	-3.114**
RVC			1.130	-2.639**
SGC				-3.134**

Notes: This table presents the test statistics from the test of equal predictive accuracy between two competing copula models. A positive (negative) value indicates that the model to the left (above) is better than the model above (to the left). * and ** denote the rejection of the null hypothesis of equal predictive accuracy at the 5% and 1% significance levels. Panels A, B, C, and D report the test results for the five copula models with normal, skewed normal, Student's t, and skewed Student's t marginal distributions, respectively. CVC, DVC, RVC, SGC, and SSC denote the canonical vine copula, drawable vine copula, regular vine copula, standard Gaussian copula, and standard Student's t copula models.

3.4.3 Equal Predictive Accuracy Test Results

We now consider out-of-sample comparisons of the five multivariate copula models. Table 3.7 presents the test statistics from the test of equal predictive accuracy between two competing copula models with the same marginal distributions. Based on the sign of the test statistics, the three vine copula models produce forecasts that are

closer to the true density than the standard Gaussian copula or SGC model. However, there is insufficient evidence to reject the null hypothesis of equal predictive accuracy between the SGC model and any vine copula model. Consistent with the calibration test results, the standard Student's t copula or SSC model performs significantly better than all other copula specifications since the null hypothesis of equal predictive accuracy is rejected at the 1% significance level. It is also worth noting that these results are quite robust to marginal distribution assumptions.

Table 3.8. Tests of equal predictive accuracy between two copula models for two sub-periods

Model	DVC	RVC	SGC	SSC
Panel A: First sub-period (January 15, 1999 to September 21, 2007)				
CVC	-1.456	-0.431	-1.606	-2.338*
DVC		1.011	-0.007	-2.026*
RVC			-0.951	-2.389*
SGC				-2.113*
Panel B: Second sub-period (September 28, 2007 to May 27, 2016)				
CVC	1.358	0.778	0.725	-2.928**
DVC		-0.916	0.295	-3.785**
RVC			0.566	-3.251**
SGC				-2.729**

Notes: This table presents the test statistics from the test of equal predictive accuracy between two competing copula models. A positive (negative) value indicates that the model to the left (above) is better than the model above (to the left). * and ** denote the rejection of the null hypothesis of equal predictive accuracy at the 5% and 1% significance levels. Panels A and B report the results from the first sub-period and second sub-period, respectively. CVC, DVC, RVC, SGC, and SSC denote the canonical vine copula, drawable vine copula, regular vine copula, standard Gaussian copula, and standard Student's t copula models with Student's t marginal distributions.

To examine the robustness of the results, we partition our evaluation period into two equal parts and perform sub-period analysis. The first sub-period covers a sample

ranging from January 15, 1999 to September 21, 2007, and the second sub-period covers a sample ranging from September 28, 2007 to May 27, 2016. The equal predictive accuracy test results for the two sub-periods are reported in Table 3.8. For the sub-period analysis, we only consider the copula models with Student's t marginal distributions. Similar to case of full sample, the test cannot discriminate the differences of overall forecasting accuracy between any vine copula model and the SGC model. Moreover, the results in Table 3.8 indicate that the SSC model significantly outperforms the SGC as well as the three vine copula models both during the first and second sub-periods. Therefore, overall we can conclude that the SSC model produces forecasts that are significantly closer to the true density than the other copula models.

Indeed, the superior forecasting performance of the SSC model over the SGC model suggests that there is a statistically significant gain from allowing for the presence of lower and upper tail dependence among energy commodity returns. In addition, we find that modeling heterogeneous dependence structures between different pairs of energy commodity returns using vine copula models (with mixed pair-copulas) does not help improve quality of multivariate density forecasts of energy commodity returns. Nevertheless, it would be too premature to conclude that modeling heterogeneous dependence structures using vine copulas is not worth it when forecasting the multivariate density of energy commodity returns. In this study, we consider the vine copula models with mixed pair-copulas, and select a bivariate copula family for each pair of energy commodity returns according to the BIC values. Based on our pair-copula selection results, it turns out that one-parameter bivariate copula families are chosen for

almost all pair-copulas. Therefore, it is possible that the restrictive nature of the one-parameter bivariate copulas (which impose zero dependence in either lower or upper tails) is indeed a reason for inferior forecasting performance of the vine copula models relative to the SSC copula model (which allows for non-zero, though homogeneous, dependence in the lower and upper tails of all pairs of returns). Thus, it would be interesting to also consider mixing only two-parameter bivariate copula families in the vine copula structure, and we leave this for future research.

3.5 Conclusions

In this chapter, we consider the value of modeling heterogeneous dependence structures with vine copulas in improving one-step-ahead density forecasts for multivariate energy commodity returns. Specifically, we compare the forecasting accuracy of three vine copula models – the canonical vine copula (CVC), drawable vine copula (DVC), and regular vine copula (RVC) models – with the forecasting performance of two standard multivariate copula models – the standard Gaussian copula (SGC) and standard Student's t copula (SSC) models. For all copula models, the marginal distribution of each return series is modeled using either a normal, skewed normal, Student's t, or skewed Student's t distribution. Our empirical analysis is based on weekly spot prices for seven energy commodities from January 10, 1997 to May 27, 2016. The seven energy commodities include crude oil, diesel fuel, gasoline, heating oil, jet fuel, natural gas, and propane. We set aside the first 104 weeks of the data for the initial estimation of density forecasts, and use the last 906 weeks (the data from January

15, 1999 to May 27, 2016) for an out-of-sample evaluation of the competing multivariate copula models.

Our calibration test results reveal that forecast densities constructed from the SSC model with Student's t marginal distributions provide a good description of the multivariate energy commodity returns. Moreover, this particular model is the only model that passes all the calibration tests (though only marginally pass the Anderson Darling test of normality at the 1% significance level). It is therefore superior to the other copula models under consideration. In addition, regardless of the marginal distribution assumptions, the SSC model delivers significantly higher out-of-sample likelihood scores than the other four multivariate copula models. In other words, the SSC model produces forecast densities that are significantly closer to the true density than the other copula models.

We also conduct a sub-period analysis by splitting the out-of-sample period into two equal sub-periods. The sub-sample results confirm that the SSC model significantly outperforms the SGC and the three vine copula models for both sub-periods. Based on these results, we can conclude that there is a statistically significant gain from allowing for the presence of lower and upper tail dependence among energy commodity returns. However, modeling heterogeneous dependence structures between different pairs of energy commodity returns using vine copula models (with mixed pair-copulas) does not help improve quality of multivariate density forecasts of energy commodity returns. It should be noted that the inferior performance of the vine copula models might be explained by the fact that the one-parameter bivariate copulas are chosen by the

Bayesian Information Criterion for almost all pair-copulas. Therefore, it would be of great interest to investigate the impact of pair-copula choices in the vine copula structure on the forecasting performance, and we leave this for future research.

CHAPTER IV

MEASURING TAIL DEPENDENCE BETWEEN AGRICULTURAL AND ENERGY COMMODITY MARKETS: A REGULAR VINE COPULA METHOD

4.1 Introduction

It is widely believed that the expansion of the ethanol production in the United States has reshaped the linkages between agricultural and energy commodity markets. Traditionally, agricultural and energy commodity markets have been linked through the input channel (in terms of production and transportation costs). Now, due primarily to the very rapid expansion of crop-based ethanol production in the United States, the agricultural and energy commodity markets are increasingly connected through the demand channel – mainly through the policy-driven demand for corn as an ethanol feedstock – rather than the input channel[41]. In particular, various studies have reported a tighter linkages between agricultural and energy commodity markets since the boom of the U.S. ethanol industry took off in 2006.

For instance, Muhammad and Kebede (2009) found that from 2005 to 2008 oil price movements could explain more than 60 percent of the change in corn prices, whereas from 1990 to 2004 only about 2 percent of the change in corn prices could be

[41] Specifically, the Renewable Fuel Standard (RFS) program, created under the Energy Policy Act of 2005 and later expanded under the Energy Independence and Security Act of 2007, is the root of cause of the rapid growth in corn-based ethanol production in the United States. Compared to 3.9 billion gallons of biofuel produced in 2005, the act requires that 36 billion gallons be produced in 2022. Of the 36 billion gallons of biofuels, at least 21 billion gallons must come from advanced biofuels and the remainder, at most 15 billion gallons, can come from conventional biofuels such as corn-based ethanol (Schnepf and Yacobucci 2013).

explained by oil prices. In addition, Tyner (2010) showed that, for the 1988-2005 period, the correlation between oil and corn prices was low and negative (-0.26). However, since 2006 there appears to be a strong and positive correlation between the prices of oil and corn. Indeed, Tyner (2010) reported a 0.80 (0.95) correlation between oil and corn prices for the period 2006 to 2008 (2008 to 2009). Hertel and Beckman (2012) also documented a similar change in the correlation pattern between oil and corn prices.

Increased connection between agricultural and energy commodity markets raises the need for deeper understanding of the links and comovements between agricultural and energy commodity price returns. Over the last decade, a number of empirical studies have examined the interrelationship between agricultural and energy commodity markets[42]. Motivated by concurrent swings in agricultural and energy commodity prices experienced after the change in U.S. biofuel policies in 2006, some of these studies focus on the question of whether the ethanol/biofuel boom has caused a stronger dependence between agricultural and energy commodity prices. However, the results from these studies are rather mixed.

For example, Campiche et al. (2007) showed that the prices of corn and soybean – the key agricultural commodities used for ethanol/biofuel production – were cointegrated with crude oil prices over the period of 2006-2007 but not during the period 2003-2005. Similarly, Du and McPhail (2012), Kristoufek, Janda, and Zilberman (2012), and Lucotte (2016) examined the connections among the prices of agricultural and

[42] See Serra and Zilberman (2013) and Zilberman et al. (2013) for a literature review on price linkages and transmission patterns in biofuel-related markets.

energy commodities before and after the food crisis of 2007/2008, and found that their prices were much more closely linked after the crisis. On the contrary, Gilbert (2010) reported that the 2007-2008 agricultural price spikes could mostly be explained by macroeconomic and monetary factors, and that the biofuel demand growth was not the main cause of the agricultural price booms. Consistent with Gilbert (2010), Reboredo (2012a) investigated extreme market dependence between oil and agricultural commodity prices using copulas, and found that price spikes in the corn and soybean markets during the period 2007 to 2011 were not caused by extreme upward oil price movements. In addition, Baumeister and Kilian (2014) showed that there was no compelling evidence that the change in U.S. biofuel policies in May 2006 had created a tight link between oil and agricultural commodity markets.

Despite a number of empirical studies on the agriculture-energy nexus, relatively little attention has been paid to the dependence structure between agricultural and energy commodity prices and their extreme comovements. Reboredo (2012a) and Han, Zhou, and Yin (2015) are among the few recent authors who analyzed tail dependence patterns (or extreme comovements) between the prices of agricultural and energy commodities during the last decade. Considering weekly data from January 1998 to April 2011, Reboredo (2012a) employed several bivariate copulas to study the extreme market dependence between oil prices and agricultural commodity prices (namely, corn, soybean and wheat prices). The results from his study indicate that agricultural commodity prices were independent of extreme upward price movements in the oil market even in the last three years of the sampling period. Han, Zhou, and Yin (2015)

investigated tail dependence between the returns on agricultural and energy commodity indices using a time varying symmetrized Joe-Clayton copula. Using daily data from January 2000 to January 2014, their results suggest that both lower and upper tail dependence were strongest during the financial crisis of 2008. Similar to Reboredo (2012a), they found that lower tail dependence is in general stronger than upper tail dependence. While these studies provide useful information on the dependence structure as well as tail dependence between two commodity markets, little is still known on the multivariate dependence structure of agricultural and energy commodity markets.

Accordingly, this chapter attempts to fill the gap in the literature by analyzing the dependence structure among daily prices of three agricultural commodities – corn, soybean, and wheat – and two energy commodities – ethanol and crude oil – using a regular vine (or R-vine) copula methodology. The major advantage of the R-vine copula approach is that it allows us to capture potentially complex dependence structure and tail dependence patterns in a multivariate framework. Therefore, it allows us to uncover not only information regarding the upper and lower tail dependence between any two commodity markets but also information regarding the overall connections among multiple commodity markets. Furthermore, we add to the literature by examining whether and how the dependence structure and the degree of tail dependence change between the two periods of ethanol production: rapid growth (June 2006 to June 2011) and slowing growth (June 2011 to June 2016). Our findings should provide valuable information for practitioners, academics and policy makers regarding the linkages between the agricultural and energy commodity markets. In addition, as agricultural

commodity markets are often thought of as an alternative market for risk diversification purposes, the results from this study should also provide useful information for investors about portfolio diversification and risk management.

The remainder of this chapter is organized as follows. Section 4.2 describes the data used in our analysis. Section 4.3 is devoted to explaining the regular vine copula methodology. Section 4.4 presents the results of the empirical analysis, and Section 4.5 concludes the chapter.

4.2 Data

Our empirical analysis is based on daily prices for three agricultural commodity futures: corn, soybean and wheat futures; and two energy commodity futures: ethanol and crude oil futures. All prices are obtained from the Datastream database. The price data span from June 1, 2006 to June 30, 2016, from which a sample of daily log return series are constructed using the nearest futures contracts. At the rollover date, care has been taken to ensure that the same futures contract is used to calculate the daily log returns. This yields a total of 2,536 observations for each return series. Apart from examining the dependence structure of the five commodity markets for the whole sample period, we also investigate how the dependence structure and the degree of tail dependence change over the two sub-periods: June 2, 2006 to June 16, 2011 and June 17, 2011 to June 30, 2016. The first sub-period corresponds to the period of rapid expansion of ethanol production in the United States, whereas the second sub-period

corresponds to the period of slowing growth in ethanol production (U.S. Energy Information Administration 2011). Each sub-period has a total of 1,268 observations.

Table 4.1. Summary statistics and correlation analysis on daily log returns on the futures contracts of corn, soybean, wheat, ethanol, and oil

	Corn	Soybean	Wheat	Ethanol	Oil
Panel A: Summary Statistics					
Mean (%)	-0.003	0.062	-0.035	0.094	-0.051
Standard Deviation (%)	1.974	1.654	2.191	1.874	2.390
Skewness	-0.102	0.385	-0.012	-0.561	0.082
Excess Kurtosis	1.813	10.684	1.503	5.786	3.904
Minimum (%)	-10.409	-8.141	-9.973	-16.990	-13.065
Maximum (%)	8.6618	20.3209	8.7943	9.7525	14.5464
JB	353.30*	12149.00*	239.93*	3678.90*	1618.20*
ADF	-36.05*	-36.11*	-36.23*	-33.283*	-36.90*
$\rho(1)$	0.019	0.010	0.000	0.129*	-0.061*
$Q(5)$	4.98	3.65	3.22	49.66*	16.35*
$Q^2(5)$	167.50*	50.79*	219.80*	285.40*	699.50*
Panel B: Correlation Matrix					
Corn	1.000				
Soybean	0.610	1.000			
Wheat	0.647	0.469	1.000		
Ethanol	0.546	0.406	0.413	1.000	
Oil	0.291	0.342	0.247	0.308	1.000

Notes: Summary statistics (Panel A) and correlation matrix (Panel B) are presented for daily log returns on the futures contracts of corn, soybean, wheat, ethanol, and oil for the period June 2, 2006 to June 30, 2016. The total number of observations is 2,536 for each return series. JB is the Jarque-Bera test statistic, where * denotes the rejection of the null hypothesis of normality at the 1% significance level. ADF is the Augmented Dickey-Fuller test statistic, where * denotes the rejection of the null hypothesis that the respective return series follows a unit root process at the 1% significance level. $\rho(1)$ is the first-order autocorrelation, where * denotes the rejection of the null hypothesis that the first-autocorrelation of the respective return series is equal to zero at the 1% significance level. $Q(5)$ is the Ljung-Box test statistic for the return series, where * denotes the rejection of the null hypothesis that there is no serial correlations in the return series up to order 5. $Q^2(5)$ is the Ljung-Box test statistic for the squared return series, where * denotes the rejection of the null hypothesis that there is no ARCH effect in the return series up to order 5.

Table 4.1 reports summary statistics (Panel A) and correlation matrix (Panel B) for the daily log returns on the futures contracts of corn, soybean, wheat, ethanol, and oil for the entire sample period. For each return series, the mean is very small relative to its

standard deviation. As expected, oil returns are the most volatile series among the five commodity returns. All returns series are only slightly skewed, but have a high excess kurtosis (especially for the soybean, ethanol, and oil return series). The significant Jarque-Bera (JB) test statistics indicate that all daily log returns are not normally distributed. The Augmented Dickey-Fuller tests show that all commodity returns are stationary.

Both first-order autocorrelation ($\rho(1)$) and Ljung-Box ($Q(5)$) tests indicate that there are serial correlations in the two energy commodity returns but not in the three agricultural commodity returns. In addition, the Ljung-Box test statistics for the squared return series ($Q^2(5)$) suggest that ARCH effects (or volatility clustering) are present in all return series. Unconditional correlations provide evidence of weak dependence between oil and other commodities. More specifically, the linear correlation coefficients between oil and other commodities range between 0.247 (for the pair of oil and wheat returns) and 0.342 (for the pair of oil and soybean returns). The highest linear correlation is found between corn and wheat returns (0.647).

4.3 Methodology

In this chapter, we apply the R-vine copula approach to study the dependence structure and tail dependence (or extreme comovements) among prices of three agricultural commodity futures (corn, soybean, and wheat futures), and two energy commodity futures (ethanol and crude oil futures). The approach consists of three stages. The first stage involves modeling the marginal distributions for the individual

commodity returns. In the second stage, the R-vine copula is estimated using the standardized residuals obtained from the first stage. The third stage involves calculating the upper and lower tail dependence coefficients.

4.3.1 Modeling Marginal Distributions

In the first stage, the marginal distributions for all commodity returns are modeled. To account for possible serial correlation and volatility clustering in commodity returns, we consider four alternative GARCH models: a GARCH(1,1) model with a constant unconditional mean, an AR(1)-GARCH(1,1) model, an MA(1)-GARCH(1,1) model, and ARMA(1,1)-GARCH(1,1) model. Let $y_{i,t}$ denote the daily log return for commodity i. The ARMA(1,1)-GARCH(1,1) model is specified as follows:

(4.1) $y_{i,t} = \mu_i + \phi_i y_{i,t-1} + \theta_i \varepsilon_{i,t-1} + \varepsilon_{i,t}$

(4.2) $\sigma_{i,t}^2 = \omega_i + \alpha_i \varepsilon_{i,t-1}^2 + \beta_i \sigma_{i,t-1}^2$

(4.3) $z_{i,t} = \frac{\varepsilon_{i,t}}{\sigma_{i,t}} \sim i.i.d.D(0,1)$

where $D(0,1)$ is a zero mean and unit variance probability distribution[43]. For each return series, the mean model with the lowest Bayesian Information Criterion (BIC) is chosen. The series of standardized residuals, $z_{i,t}$, is then transformed into a standard uniform variable or copula data (denoted as $u_{i,t}$) using an empirical distribution function (EDF). The series $z_{i,t}$ is also referred to as filtered returns. Several goodness-of-fit tests are performed to ensure that the marginal distributions are appropriately specified.

[43] For the GARCH(1,1) model with a constant unconditional mean, both ϕ_i and θ_i are set to zero. θ_i is set to zero for the AR(1)-GARCH(1,1) model, whereas ϕ_i is set to zero for the MA(1)-GARCH(1,1) model.

4.3.2 Selecting and Estimating Regular Vine Copula

The second stage involves estimating the R-vine copula using the standard uniform variables obtained from the first stage. Simply put, an R-vine copula is a multivariate distribution for which the marginal distribution of each variable is standard uniform. Let $\boldsymbol{z} = (z_1, z_2, z_3, z_4, z_5)$ be a five-dimensional random vector of filtered commodity returns (or standardized residuals in equation (4.3)) with a joint distribution function $F(\boldsymbol{z})$ and a joint density function $f(\boldsymbol{z})$. According to the Sklar's theorem (Sklar 1959), the joint distribution of $\boldsymbol{z}$ can be expressed as:

(4.4) $F(\boldsymbol{z}) = C(u_1, u_2, u_3, u_4, u_5)$

where $C: [0,1]^5 \rightarrow [0,1]$ is a copula function, and $u_i = F_i(z_i)$ is the marginal distribution function of z_i for $i = 1,2, \dots,5$. Suppose that C and F_i are differentiable. Then, the joint distribution function of $\boldsymbol{z}$ can be written as:

(4.5) $f(\boldsymbol{z}) = f_1(z_1)f_2(z_2) \cdots f_5(z_5)[c(F_1(z_1), F_2(z_2), \dots, F_5(z_5)]$

where c is the density of the copula and $f_i = f_i(z_i)$ is the density of $F_i = F_i(z_i)$.

In particular, the copula function represents the dependence structure of a multivariate random vector of filtered commodity returns. Thus, we can use multivariate copulas to analyze tail dependence among multiple commodity returns. Two most obvious choices of multivariate copulas are the Gaussian and Student's t copulas. However, the Gaussian copula cannot capture non-linear dependence between random variables. In other words, it assumes that the dependence pattern between each pair of variables does not change with market conditions. In addition, it unrealistically imposes independence in the tails or during extreme market movements. On the other hand, the

Student's t copula allows us to capture tail dependence. However, it requires all pairs of random variables to have exactly the same degree of tail dependence, which seem to be unrealistic. Therefore, both Gaussian and Student's t copulas are too restrictive, especially when modeling the dependence structure of more than two random variables.

This chapter exploits the more flexible multivariate copula construction method ("pair-copula construction (PCC) method"). The PCC method was first proposed by Joe (1996) and further extended by Bedford and Cooke (2001, 2002) and Kurowicka and Cooke (2006). The idea of the PPC method begins by factorizing a joint density function into marginal and conditional density functions. For example, a five-dimensional density function can be factorized as:

(4.6) $$f(\boldsymbol{z}) = f_1(z_1) f_{2|1}(z_2|z_1) f_{3|1,2}(z_3|z_1,z_2) f_{4|1,2,3}(z_4|z_1,z_2,z_3) f_{5|1,2,3,4}(z_5|z_1,z_2,z_3,z_4)$$

Using the Sklar's theorem, any conditional marginal distributions in the right hand of equation (4.6) can be expressed as:

(4.7) $$f(z_i|\boldsymbol{\nu}) = c_{z_i,\nu_j|\boldsymbol{\nu}_{-j}}\left(F\left(z_i\middle|\boldsymbol{\nu}_{-j}\right), F\left(\nu_j\middle|\boldsymbol{\nu}_{-j}\right)\right) f(z_i|\boldsymbol{\nu}_{-j})$$

with

(4.8) $$F(z_i|\boldsymbol{\nu}) = \frac{\partial C_{z_i,\nu_j|\boldsymbol{\nu}_{-j}}(F(z_i|\boldsymbol{\nu}_{-j}),F(\nu_j|\boldsymbol{\nu}_{-j}))}{\partial F(\nu_j|\boldsymbol{\nu}_{-j})}$$

where $\boldsymbol{\nu}$ is the conditioning set of marginal distribution of z_i, ν_i is a variable in the set $\boldsymbol{\nu}$, and $\boldsymbol{\nu}_{-j}$ is the set of variables in $\boldsymbol{\nu}$ excluding ν_i. For example, $f_{2|1}(z_2|z_1)$ can be written as $c_{1,2}(F_1,F_2)f_2$, and $f_{3|1,2}(z_3|z_1,z_2)$ can be expressed as $c_{2,3|1}\left(F_{2|1},F_{3|1}\right)f_{3|1}$.

Accordingly, the joint density function, $f(\boldsymbol{z})$, can be decomposed as products of bivariate copula densities and marginal density function of z_i.

Obviously, the factorization in equation (4.6) is not unique. This suggests that there are a large number of possible PCCs from which to choose. Bedford and Cooke (2001) introduce a graphical structure called regular vine (or R-vine) structure to help organize different decompositions. In particular, a five-dimensional R-vine structure is defined by a sequence of four trees: T_1, T_2, T_3, T_4. T_1 has five nodes and four edges. Edges in T_1 then become nodes in T_2. The two nodes in T_2 are connected by an edge only if they share a common node in T_1 (proximity condition). Edges in T_2 then become nodes in T_3. Again, the two nodes in T_3 are connected by an edge only if they share a common node in T_2 (proximity condition). Then, edges in T_3 become nodes in T_4, and the two nodes in T_4 are connected by an edge only if they share a common node in T_3.

The joint density function of a five-dimensional R-vine copula is given by[44]:

$$f(\boldsymbol{z}) = \prod_{k=1}^{5} f_k \prod_{i=1}^{4} \prod_{e \in E_i} c_{j(e),k(e)|D(e)}(F_{j(e)|D(e)}, F_{k(e)|D(e)}) \tag{4.9}$$

where E_i is a set of edges in T_i, $j(e)$ and $k(e)$ are the two (conditional) nodes associated with each edge e, $D(e)$ is the conditioning set associated with edge e. An example of a five-dimensional R-vine structure is illustrated in Figure 4.1, and its corresponding joint density function is:

$$f(\boldsymbol{z}) = f_1 f_2 f_3 f_4 f_5 c_{1,2} c_{1,4} c_{2,3} c_{2,5} c_{1,3|2} c_{2,4|1} c_{3,5|2} c_{1,5|2,3} c_{3,4|1,2} c_{4,5|1,2,3} \tag{4.10}$$

[44] Kurowicka and Cooke (2006) provide the derivation of the joint density of a general R-vine copula.

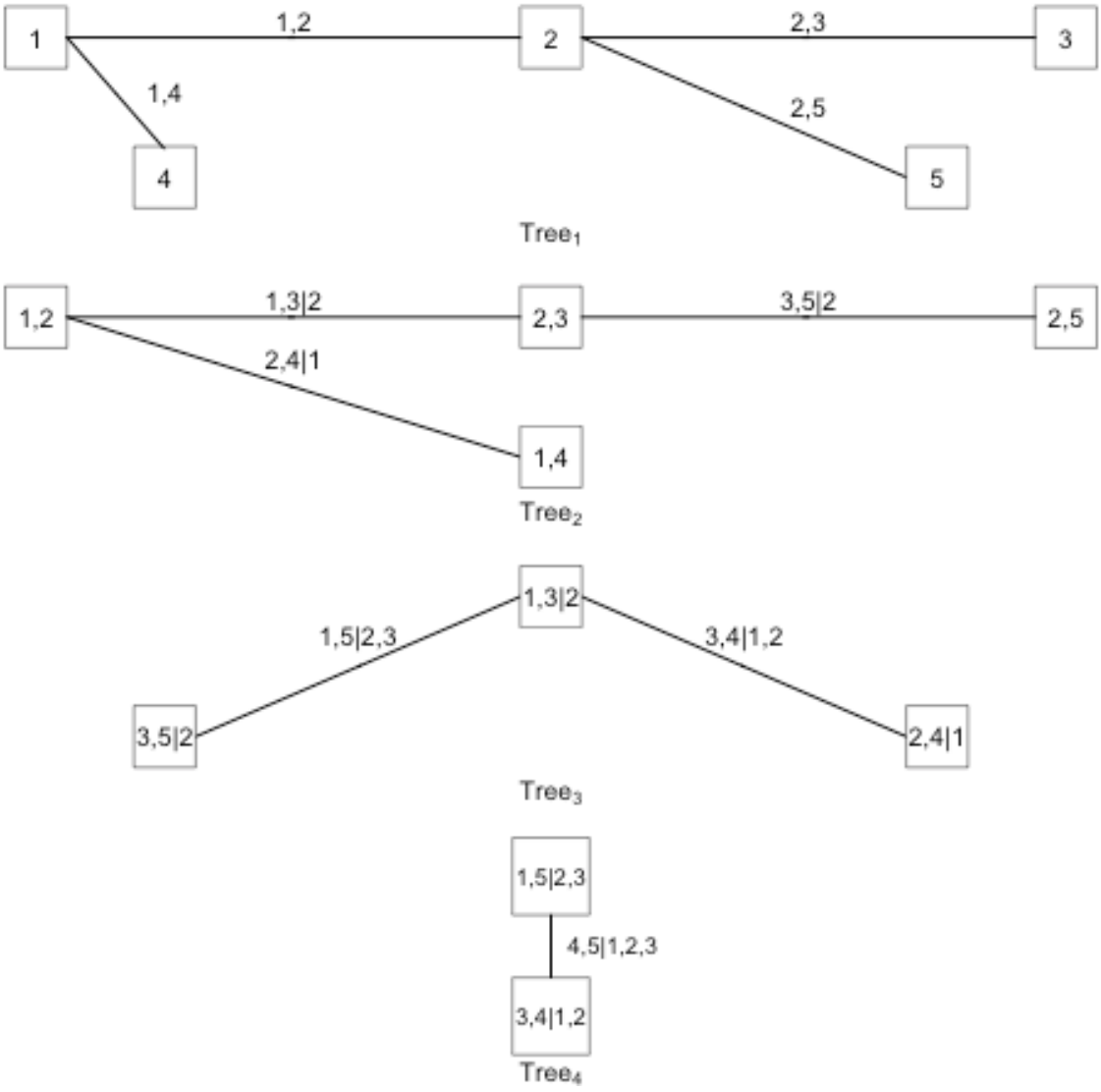

Figure 4.1. Estimated R-vine copula structure with 1 = Ethanol, 2 = Corn, 3 = Soybean, 4 = Oil, and 5 = Wheat

According to Morales-Nápoles, Cooke, and Kurowicka (2010), there exist $(d!/2)\times 2^{\binom{d-2}{2}}$ different R-vine decompositions for the d-dimensions. Thus, there are 480 possible R-vine structures for a five-variate density. In this study, we employ a

sequential estimation procedure proposed by Dißmann et al. (2013) to select and estimate an R-vine structure as well as its corresponding bivariate copulas. This procedure begins in the first tree of the R-vine structure. The structure of the first tree is formed by maximizing the sum of the absolute values of pairwise Kendall's tau coefficients. For the first tree, this is done using the standard uniform variables obtained from the first stage. Given the selected structure, the pair copulas are chosen from a range of 39 different parametric bivariate copula families by minimizing the BIC[45]. Copula parameters are estimated using the maximum likelihood estimation (MLE) method. Once the first tree is specified and the pair-copula families are chosen, the same is done for the second, the third, and forth trees using the transformed observations, $F(z_i|\boldsymbol{\nu})$, calculated from equation (4.8).

4.3.3 Measuring Tail Dependence Coefficients

In the third stage, the upper and lower tail dependence coefficients are calculated to measure the degree of comovements between two commodity markets at the extreme events. The upper and lower tail dependence coefficients for commodities i and j are defined, respectively, as:

(4.11) $\lambda_U = \lim_{u\to 1^-} \Pr\left[Z_i > F_i^{-1}(u) \middle| Z_j > F_j^{-1}(u)\right] = \lim_{u\to 1^-} \frac{1-2u+C(u,u)}{1-u}$

(4.12) $\lambda_L = \lim_{u\to 0^+} \Pr\left[Z_i < F_i^{-1}(u) \middle| Z_j < F_j^{-1}(u)\right] = \lim_{u\to 0^+} \frac{C(u,u)}{u}$

[45] The 39 bivariate copula families include Gaussian, Student's t, Clayton, Gumbel, Frank, Joe, BB1 (Clayton-Gumbel), BB6 (Joe-Gumbel), BB7 (Joe-Clayton), BB8 (Joe-Frank), Tawn type 1, Tawn type 2, and the rotated versions (90, 180 and 270 degrees) of Clayton, Gumbel, Joe, BB1, BB6, BB7, BB8, Tawn type 1, and Tawn type 2 copulas.

In this study, we follow Loaiza Maya, Gomez-Gonzalez, and Velandia (2015) and calculate the non-parametric tail dependence coefficients for all pairs of commodities through a simulation exercise. Specifically, the estimated R-vine copula density obtained from the second stage is used to generate $S = 10{,}000$ draws of the five standard uniform variables, $\{u_{1,s}, u_{2,s}, u_{3,s}, u_{4,s}, u_{5,s}\}_{s=1}^{s=10,000}$. This simulation exercise is replicated $R = 1{,}000$ times. For each replication r, the upper and lower tail dependence coefficients are respectively estimated using the following non-parametric estimators:

(4.13) $\hat{\lambda}_U^r = \lim_{k_U \to S^-} \frac{1 - 2\frac{k_U}{S} + \hat{C}(\frac{k_U}{S}, \frac{k_U}{S})}{1 - \frac{k_U}{S}}$

(4.14) $\hat{\lambda}_L^r = \lim_{k_L \to 0^+} \frac{\hat{C}(\frac{k_L}{S}, \frac{k_L}{S})}{\frac{k_L}{S}}$

where k_U/S and k_L/S are the thresholds used in the estimation of tail dependence coefficients.

Similar to Loaiza Maya, Gomez-Gonzalez, and Velandia (2015), we set $k_U/S = 0.99$ and $k_L/S = 0.01$. $\hat{C}(k_1/S, k_2/S)$ is the empirical copula, which can be estimated using:

(4.15) $\hat{C}\left(\frac{k_1}{S}, \frac{k_2}{S}\right) = \frac{1}{S}\sum_{s=1}^{S} \mathbf{1}\left(F_i(z_{i,s}) \leq \frac{k_1}{S}, F_j(z_{j,s}) \leq \frac{k_2}{S}\right)$

The upper and lower tail dependence coefficients for each pair of commodities are calculated as $\hat{\lambda}_U = (1/R)\sum_{r=1}^{R} \hat{\lambda}_U^r$ and $\hat{\lambda}_L = (1/R)\sum_{r=1}^{R} \hat{\lambda}_L^r$, respectively. Confidence intervals for $\hat{\lambda}_U$ and $\hat{\lambda}_L$ are then constructed by computing the associated percentiles of their empirical distributions.

Table 4.2. Results for the marginal distributions

	Corn	Soybean	Wheat	Ethanol	Oil
Panel A: June 2, 2006 to June 30, 2016					
μ_i	-0.000081	0.000673	-0.000700	0.000899	0.000061
	(0.000346)	(0.000268)	(0.000472)	(0.000354)	(0.000346)
ϕ_i				0.122495	
				(0.021330)	
ω_i	0.000005	0.000003	0.000003	0.000010	0.000004
	(0.000004)	(0.000002)	(0.000012)	(0.000001)	(0.000003)
α_i	0.057551	0.069248	0.051514	0.097183	0.072531
	(0.008766)	(0.012372)	(0.056051)	(0.007071)	(0.016776)
β_i	0.929596	0.921669	0.943409	0.874143	0.923088
	(0.010211)	(0.013564)	(0.063835)	(0.009700)	(0.018226)
Panel B: June 2, 2006 to June 16, 2011					
μ_i	0.000758	0.000999	-0.000272	0.001240	0.000634
	(0.000599)	(0.000437)	(0.000662)	(0.000642)	(0.000568)
ϕ_i				0.819652	
				(0.095655)	
θ_i				-0.743033	
				(0.111961)	
ω_i	0.000018	0.000003	0.000030	0.000010	0.000010
	(0.000013)	(0.000003)	(0.000014)	(0.000002)	(0.000004)
α_i	0.052156	0.070081	0.067055	0.085517	0.069174
	(0.021722)	(0.016065)	(0.018115)	(0.009920)	(0.004581)
β_i	0.911599	0.923528	0.885697	0.886500	0.914133
	(0.044301)	(0.017053)	(0.036075)	(0.013089)	(0.011326)
Panel C: June 17, 2011 to June 30, 2016					
μ_i	-0.000574	0.000507	-0.001067	0.000579	-0.000287
	(0.000409)	(0.000340)	(0.000458)	(0.000496)	(0.000431)
ϕ_i				0.156408	
				(0.029782)	
ω_i	0.000009	0.000005	0.000004	0.000010	0.000003
	(0.000001)	(0.000002)	(0.000003)	(0.000001)	(0.000004)
α_i	0.079758	0.070717	0.059687	0.105519	0.082122
	(0.006739)	(0.007999)	(0.016452)	(0.009609)	(0.029272)
β_i	0.890516	0.901056	0.929859	0.864721	0.915080
	(0.011189)	(0.011742)	(0.019396)	(0.013999)	(0.030061)

Notes: μ_i, ϕ_i, θ_i, ω_i, α_i, and β_i are the parameters of an ARMA-GARCH model (refer to equations (4.1)-(4.3) in Section 4.3.1). Figures in parentheses are standard errors of the coefficient estimates.

4.4 Empirical Results

This section first reports the estimation results for the marginal distributions for the individual commodity returns. The section then proceeds to present the R-vine copula estimation results. Finally, we discuss the tail dependence results.

4.4.1 Marginal Distribution Estimation

Table 4.2 presents the parameter estimates and standard errors of the selected marginal distribution models for the whole sample period (Panel A), first sub-period (Panel B), and second sub-period (Panel C). For all sample periods, a GARCH(1,1) model with a constant unconditional mean is selected for all commodity return series except for the ethanol return series. In other words, the mean of these series is simply characterized by a constant. For the ethanol return series, the AR(1)-GARCH(1,1) model is chosen for both the whole sample period and the second sub-period, whereas the ARMA(1,1)-GARCH(1,1) model is selected for the first sub-period. This implies that it is necessary to include at least the autoregressive part to capture the strong serial correlation in ethanol return series (see Table 4.1).

It is crucial that the marginal distribution models are well specified as marginal distribution misspecification can result in copula misspecification (Fermanian and Scaillet 2005; Patton 2006). Hence, we apply several goodness-of-fit tests to confirm the adequacy of the chosen marginal distribution models. These tests include the Ljung-Box tests of lack of autocorrelation in the standardized residuals and the squared standardized residuals, the Engle's (1982) Lagrange Multiplier (LM) test of lack of the ARCH effect

in the standardized residuals, the LM tests of serial independence (Patton 2006) of the first four moments of transformed standardized residuals or copula data, and the Kolmogorov-Smirnov test of uniformity of the copula data. The p-values of these tests are reported in Table 4.3. All selected model pass all the tests at the 5% significance level, confirming that the marginal distribution models are appropriately specified.

Table 4.3. Tests of the marginal distribution specifications

	Corn	Soybean	Wheat	Ethanol	Oil
Panel A: June 2, 2006 to June 30, 2016					
$LBQ(10)$ on standardized residuals	0.4082	0.8349	0.6927	0.0743	0.8354
$LBQ(10)$ on squared standardized residuals	0.4045	0.8970	0.7161	0.5112	0.4621
LM on squared standardized residuals	0.4674	0.9999	0.9988	0.8637	0.9999
1st moment LM test on copula data	0.9671	0.9985	0.9875	0.6815	0.9925
2nd moment LM test on copula data	0.8132	0.9988	0.9906	0.9604	0.9992
3rd moment LM test on copula data	0.9950	0.8702	0.9986	0.7620	0.9999
4th moment LM test on copula data	0.8224	0.9999	0.9993	0.9801	0.9996
Kolmogorov-Smirnov test	0.6822	0.7262	0.9980	0.7979	0.9999
Panel B: June 2, 2006 to June 16, 2011					
$LBQ(10)$ on standardized residuals	0.6057	0.7866	0.8894	0.2533	0.9619
$LBQ(10)$ on squared standardized residuals	0.9428	0.9389	0.6479	0.6073	0.9208
LM on squared standardized residuals	0.9985	0.9999	0.8941	0.9715	0.9999
1st moment LM test on copula data	0.9814	0.9999	0.9999	0.8763	0.9987
2nd moment LM test on copula data	0.9996	0.9906	0.8359	0.9222	0.9831
3rd moment LM test on copula data	0.9987	0.9933	0.9998	0.9801	0.9999
4th moment LM test on copula data	0.9975	0.9979	0.9833	0.9001	0.9973
Kolmogorov-Smirnov test	0.8678	0.9077	0.9999	0.9434	0.9999
Panel C: June 17, 2011 to June 30, 2016					
$LBQ(10)$ on standardized residuals	0.6295	0.1879	0.6947	0.3067	0.2957
$LBQ(10)$ on squared standardized residuals	0.6066	0.9984	0.9683	0.2099	0.3586
LM on squared standardized residuals	0.7322	0.9999	0.9999	0.8232	0.9999
1st moment LM test on copula data	0.9481	0.9080	0.9646	0.9073	0.9593
2nd moment LM test on copula data	0.9506	0.9064	0.9868	0.8612	0.9985
3rd moment LM test on copula data	0.9457	0.6591	0.9957	0.9543	0.9808
4th moment LM test on copula data	0.9274	0.9978	0.9976	0.8337	0.9983
Kolmogorov-Smirnov test	0.8678	0.9077	0.9999	0.9434	0.9999

Notes: The table reports the p-values from the Ljung-Box (LBQ) tests on standardized residuals and on squared standardized residuals, the Engle's (1982) Lagrange Multiplier (LM) tests on squared standardized residuals, the LM tests of serial independence (Patton 2006) of the first four moments of copula data or transformed standardized residuals, and the Kolmogorov-Smirnov test of uniformity of the copula data.

Table 4.4. Results for the regular vine copula models

	Pair-Copula	Para1	SE1	Para2	SE2
Panel A: June 2, 2006 to June 30, 2016					
(Corn, Soybean)	t	0.601	0.013	7.035	1.150
(Corn, Wheat)	t	0.651	0.011	7.775	1.241
(Corn, Ethanol)	t	0.602	0.014	4.218	0.451
(Corn, Oil|Ethanol)	Gaussian	0.074	0.020	-	-
(Soybean, Wheat| Corn)	Survival Gumbel	1.072	0.014	-	-
(Soybean, Ethanol| Corn)	Frank	0.680	0.121	-	-
(Soybean, Oil| Corn, Ethanol)	Clayton	0.222	0.027	-	-
(Wheat, Ethanol| Corn, Soybean)	Survival Clayton	0.074	0.021	-	-
(Wheat, Oil| Corn, Soybean, Ethanol)	Frank	0.064	0.119	-	-
(Ethanol, Oil)	Gaussian	0.319	0.017	-	-
Panel B: June 2, 2006 to June 16, 2011					
(Corn, Soybean)	t	0.649	0.017	5.991	1.240
(Corn, Wheat)	t	0.646	0.016	8.437	2.170
(Corn, Ethanol)	t	0.583	0.021	3.091	0.374
(Corn, Oil|Ethanol)	Gaussian	0.137	0.027	-	-
(Soybean, Wheat| Corn)	Survival Gumbel	1.104	0.021	-	-
(Soybean, Ethanol| Corn)	Gaussian	0.117	0.027	-	-
(Soybean, Oil| Corn, Ethanol)	Frank	1.346	0.170	-	-
(Wheat, Ethanol| Corn, Soybean)	Clayton	0.081	0.032	-	-
(Wheat, Oil| Corn, Soybean, Ethanol)	Frank	0.371	0.168	-	-
(Ethanol, Oil)	Survival Gumbel	1.351	0.029	-	-
Panel C: June 17, 2011 to June 30, 2016					
(Corn, Soybean)	BB1	0.240	0.056	1.409	0.044
(Corn, Wheat)	t	0.663	0.015	8.410	1.958
(Corn, Ethanol)	Survival BB1	0.260	0.058	1.547	0.050
(Corn, Oil|Ethanol)	Gumbel	1.005	0.015	-	-
(Soybean, Wheat| Corn)	Gaussian	0.080	0.028	-	-
(Soybean, Ethanol| Corn)	Gumbel	1.054	0.017	-	-
(Soybean, Oil| Corn, Ethanol)	Survival Gumbel	1.102	0.021	-	-
(Wheat, Ethanol| Corn, Soybean)	Survival Clayton	0.098	0.031	-	-
(Wheat, Oil| Corn, Soybean, Ethanol)	Rotated Gumbel (90º)	-1.022	0.018	-	-
(Ethanol, Oil)	Gaussian	0.220	0.026	-	-

4.4.2 Regular Vine Copula Estimation

The selected R-vine copula structure for the whole and two sub-sample periods is presented in Figure 4.1, and the estimated parameters of the corresponding bivariate copulas are given in Table 4.4. While different pair-copula families (i.e., dependence patterns) are chosen for the two sub-sample periods, the R-vine structure – the

connection structure between agricultural and energy commodity markets – remains the same during and after the period of rapid growth of U.S. ethanol production[46]. In particular, we find that the ethanol market has established a link between the corn and crude oil markets (see the first tree in Figure 4.1). This result is consistent with the findings of Tyner (2010) who uses price correlations between (1) corn and crude oil, and (2) corn and ethanol during different time periods to show that the prices of corn and crude oil are connected through the ethanol market. The interaction between corn and crude oil markets through the ethanol market is likely explained by the increased use of corn as ethanol feedstock induced by the Renewable Fuel Standard (RFS) mandate (Schnepf and Yacobucci 2013).

As can be seen from Table 4.4, almost all the parameters of the conditional and unconditional bivariate copulas are statistically significant at the 5% level. The only exception is the parameter of the conditional pair-copula $c_{\text{Wheat, Oil| Corn, Soybean, Ethanol}}$ for the case of the whole sample period. Given the selected unconditional copulas, we find that dependence patterns between the returns of (1) corn and soybean, (2) corn and wheat, and (3) corn and ethanol are all captured by two-parameter copula families. These results indicate that there are strong co-movements between corn and these commodity markets during both extreme market downturns and upturns. In particular, the heavy-tailed Student's t copula is chosen for the three pairs of commodity returns during the period of rapid growth in U.S. ethanol production (June 2, 2006 to June 16,

[46] Recall that the R-vine structure is selected based on maximum spanning trees with the absolute values of pairwise Kendall's tau coefficients as weights.

2011). This implies that the degree of tail dependence is the same in both the upper and lower tails for these commodity pairs. During the period of slowing growth in ethanol production (June 17, 2011 to June 30, 2016), the dependence pattern between corn and wheat is still best characterized by the Student's t copula. However, the BB1 and Rotated BB1 (180 degrees; "Survival BB1") copulas are selected for the corn-soybean and corn-ethanol pairs, respectively. Given the estimated parameters, the upper (lower) tail appears to be somewhat heavier (lighter) than the lower (upper) tail for the corn-soybean (corn-ethanol) pair during the second sub-period[47].

For the unconditional dependence patterns between ethanol and crude oil, the Rotated Gumbel (180 degrees; "Survival Gumbel") copula is selected for the first sub-period whereas the Gaussian copula is chosen for the second sub-period. This implies that, during the period of rapid expansion of ethanol production, ethanol and crude oil returns are more highly correlated in periods of market downturns than in periods of market upturns. Nonetheless, after the period of rapid growth of ethanol production, ethanol and crude oil returns seem to be somewhat independent during extreme market movements. For the other pairs of commodity returns, the (conditional) dependence patterns are all modeled with one-parameter copula families. Because the estimated parameters of these conditional bivariate copulas are difficult to interpret, we derive the easier-to-interpret unconditional estimates of tail dependence coefficients using the

[47] Refer to Example 5.1 in Joe and Hu (1996) for the relationship between copula parameters and tail dependence coefficients of two-parameter families of Archimedean copulas.

simulation-based method described in Section 4.3.3. The results from the simulation exercise are discussed in the next section.

4.4.3 Tail Dependence Coefficients

The upper (lower) tail dependence coefficients are reported in the upper (lower) triangular parts of the matrix in Table 4.5. The upper (lower) tail dependence coefficient measures the probability that we will observe a large price hike (decline) in one commodity market, given that the price of another commodity also has had increased (decreased) significantly. Based on the results for the whole sample period, we find that the upper tail dependence coefficients are statistically significant at the 5% level for only four pairs of commodities: corn-soybean, corn-wheat, corn-ethanol, and ethanol-oil. The lower tail dependence coefficients are all statistically significant at the 5% level. This indicates that all commodity markets are significantly correlated during extreme market downswings. During both extreme market upturns and downturns, the most highly correlated markets are the corn and ethanol markets ($\hat{\lambda}_U = 0.3435;\ \hat{\lambda}_L = 0.3442$), whereas the least highly correlated markets are the wheat and crude oil markets ($\hat{\lambda}_U = 0.0411; \hat{\lambda}_L = 0.0466$).

The results for the two sub-periods show that, during the market upturns, the corn market is significantly linked with the soybean, wheat, and ethanol markets. However, the upper tail dependence coefficients are insignificant for any other pairs of commodity markets. Comparing the upper tail dependent coefficients for the two sub-periods, we find that the degree of comovements between the returns of (1) corn and soybean and (2)

corn and wheat remain relatively stable. Nonetheless, the degree of upper tail dependence between corn and ethanol returns is stronger during the first sub-period than during the second sub-period ($\hat{\lambda}_U = 0.3728$ versus $\hat{\lambda}_U = 0.2741$). This indicates that the probability of simultaneous jumps in the prices of corn and ethanol has fallen as the ethanol market becomes more mature. While insignificant in both sub-periods, it is worth noting that the degree of upper tail dependence between crude oil and other commodity markets becomes even weaker during the period of slowing growth in U.S. ethanol production.

Table 4.5. Upper and lower tail dependence coefficients

	Corn	Soybean	Wheat	Ethanol	Oil
Panel A: June 2, 2006 to June 30, 2016					
Corn		0.2844*	0.3139*	0.3435*	0.0534
Soybean	0.2877*		0.1581	0.1704	0.0445
Wheat	0.3128*	0.2175*		0.1908	0.0411
Ethanol	0.3442*	0.1737*	0.1722*		0.0665*
Oil	0.0487*	0.1150*	0.0466*	0.0600*	
Panel B: June 2, 2006 to June 16, 2011					
Corn		0.3358*	0.3035*	0.3728*	0.0520
Soybean	0.3378*		0.1840	0.2080	0.0573
Wheat	0.3023*	0.2576*		0.1764	0.0447
Ethanol	0.3748*	0.2110*	0.2008*		0.0504
Oil	0.2093*	0.1615*	0.1350*	0.3326*	
Panel C: June 17, 2011 to June 30, 2016					
Corn		0.3696*	0.3153*	0.2741*	0.0349
Soybean	0.2288*		0.1900	0.2063	0.0391
Wheat	0.3176*	0.1383*		0.1772	0.0243
Ethanol	0.4393*	0.1633*	0.2123*		0.0403
Oil	0.0302	0.1111*	0.0222	0.0362	

Notes: Upper and lower tail dependence coefficients are respectively reported in the upper and lower triangular parts of the matrix, where * indicates the rejection of the null hypothesis that the respective tail dependence coefficient is equal to zero at the 5% significance level.

In addition, the lower tail dependence results indicate that all pairs of commodity markets are significantly correlated during the market downturns for the first sub-period but not for the second sub-period. For the second sub-period, the lower tail dependence coefficients are significant at the 5% level for most commodity pairs, except for the oil-corn, oil-wheat, and oil-ethanol pairs. While the lower tail dependence coefficients between oil and soybean markets are statistically significant for both sub-periods, the degree of dependence is weaker during the second sub-period than during the first sub-period. Similar to the results for the upper tail dependence, these findings suggest that the lower tail dependence between crude oil and other commodity markets starts to disappear in the recent years. Furthermore, we find that crude oil and other commodity returns are more dependent during extreme market downturns than during extreme market upturns for the first sub-period. However, during the second sub-period, we find neither asymmetric nor tail dependence between crude oil and most commodity markets (namely, corn, wheat, and ethanol). This empirical evidence regarding the change in the link between crude oil and agricultural commodity markets may be explained by the recent stability and slight drawdowns in ethanol production in the United States.

4.5 Conclusions

In this chapter, we analyze the dependence structure and tail dependence patterns among prices of three agricultural commodity futures (corn, soybean, and wheat futures) and two energy commodity futures (ethanol and crude oil futures) from June 2, 2006 to June 30, 2016. Based on the results for the whole sample period, we find that the prices

of corn and crude oil are linked through the ethanol market, and this is likely explained by the increased demand for corn as an ethanol feedstock. In addition, our empirical results indicate that crude oil and agricultural commodity prices are statistically dependent during the extreme market downturns but independent during the extreme market upturns. This evidence is consistent with Reboredo (2012a) who reported that oil and agricultural commodity prices tend to move independently during market upswings.

We also examine whether and how the dependence structure and the degree of tail dependence evolve over the two periods of ethanol production: rapid growth (June 2, 2006 to June 16, 2011) and slowing growth (June 17, 2011 to June 30, 2016). Based on our sub-sample analysis, we uncover several interesting results. First, crude oil and agricultural commodity markets are connected through the ethanol market during both sub-periods. Second, the connection between the corn and ethanol markets during the extreme market upturns is stronger in the period of rapid growth than the period of slowing growth. Third, during the extreme market upswings, the prices of crude oil and other four commodities tend to move more independently in the slowing growth period. Forth, all commodity prices are likely to move together when markets experience downward movements in the first sub-period, but not in the second sub-period. In particular, in the second sub-period, the lower tail dependence coefficients are statistically significant for most commodity pairs, except for the oil-corn, oil-wheat, and oil-ethanol pairs. Finally, the lower tail dependence between crude oil and other commodity markets starts to disappear in the recent years when the ethanol market became more mature. Our findings regarding the change in the degree of connectedness

between crude oil and agricultural commodity markets during the extreme market upturns and downturns should provide useful information for practitioners, academics and policy makers.

CHAPTER V

SUMMARY

This dissertation consists of three stand-alone but related empirical studies concerning applications of vine copulas – a very flexible tool for modeling complex dependence relationship among multiple data series – in commodity risk management and price analysis. The first study (Chapter II) examines the use of vine copulas in deriving optimal multiproduct hedge ratios for oil refineries in a downside risk framework. The second study (Chapter III) explores the potential of vine copulas in the context of forecasting the distributions of energy commodity returns. The third study (Chapter IV) analyzes the dependence patterns among prices of three agricultural commodity futures (corn, soybean, and wheat futures), and two energy commodity futures (ethanol and crude oil futures) using a regular vine copula approach.

The first study, titled "Hedging Downside Risk of Oil Refineries with Vine Copulas," focuses on the use of vine copulas in the context of hedging downside risk of oil refineries. As their financial health greatly depends on their refining margin (the difference between the selling prices of refined products – typically, gasoline and heating oil – and the purchasing price of crude oil), the refineries may hedge against the risk of refining margin erosion – the downside risk facing oil refineries – using crude oil, gasoline, and heating oil futures. This study purposes a vine copula approach, a relatively new class of multivariate copula approach, to estimate multiproduct hedge ratios that minimize the risk of refining margin erosion. The proposed approach allows

us to capture important characteristics of petroleum price changes such as an asymmetry in their marginal distributions and heterogeneous (tail) dependence between different pairs of price changes. Through an extensive out-of-sample hedging exercise, hedging effectiveness of two popular classes of vine copula models – canonical and drawable vine copula models – are evaluated and compared with that of a widely used nonparametric method and three standard multivariate copula models (namely, standard Gaussian, Student's t, and Clayton copula models). The empirical findings reveal that the drawable vine copula model seems to be a good and safe choice in managing the downside risk of the refineries. The results are consistent across all downside risk measures considered: Semivariance, Lower Partial Moment, Value at Risk, and Expected Shortfall.

The second study, titled "Forecasting the Distributions of Energy Commodity Returns: An Importance of Modeling Heterogeneous Dependence Structures," considers the potential of vine copulas in forecasting the distributions of multiple energy commodity returns. Because energy traders typically involve exposure to price risks in multiple related energy commodities, they often need knowledge of joint density forecasts of price changes for the purpose of risk assessment and management. This study explores the importance of modeling heterogeneous dependence structures between different pairs of energy commodity returns using vine copulas in improving one-step-ahead density forecasts of these returns. In this study, three vine copula models – the canonical vine copula, drawable vine copula, and regular vine copula models – are considered. The value of modeling heterogeneous dependence structures is measured by

comparing the performance of density forecasts based on vine copulas with density forecasts based on standard copulas that assume homogeneous dependence structures. Calibration and equal predictive accuracy test results indicate that modeling heterogeneous dependence structures using vine copula models (with mixed pair-copulas) does not help improve quality of multivariate density forecasts of energy commodity returns.

The third study, titled "Measuring Tail Dependence between Agricultural and Energy Commodity Markets: A Regular Vine Copula Method," employs a regular vine copula approach to investigate the multivariate dependence structure of agricultural and energy commodity markets. In particular, the regular vine copula method is used to analyze the dependence structure and tail dependence patterns of daily prices of three agricultural commodities – corn, soybean, and wheat – and two energy commodities – ethanol and crude oil from June 2, 2006 to June 30, 2016. The empirical results indicate that the corn and crude oil markets are connected through the ethanol market. This is consistent with the results from previous studies. The findings also show that crude oil and agricultural commodity prices are statistically dependent during the extreme market downswings but independent during the extreme market upswings. In addition, the results from the sub-sample analysis suggest that both the upper and lower tail dependence between crude oil and the other four commodity markets become weaker in the recent years when the ethanol market became more mature.

REFERENCES

Aas, K., and D. Berg. 2011. "Modeling Dependence between Financial Returns Using Pair-Copula Constructions." In D. Kurowicka and H. Joe, eds. *Dependence Modeling: Vine Copula Handbook.* Singapore: World Scientific, pp. 305-328.

Aas, K., C. Czado, A. Frigessi, and H. Bakken. 2009. "Pair-Copula Constructions of Multiple Dependence." *Insurance: Mathematics and Economics* 44(2):182-198.

Adam, A., M. Houkari, and J.-P. Laurent. 2008. "Spectral Risk Measures and Portfolio Selection." *Journal of Banking & Finance* 32(9):1870-1882.

Agarwal, V., and N.Y. Naik. 2004. "Risks and Portfolio Decisions Involving Hedge Funds." *Review of Financial Studies* 17(1):63-98.

Alexander, C., M. Prokopczuk, and A. Sumawong. 2013. "The (De)Merits of Minimum-Variance Hedging: Application to the Crack Spread." *Energy Economics* 36:698-707.

Allen, D.E., M.A. Ashraf, M. McAleer, R.J. Powell, and A.K. Singh. 2013. "Financial Dependence Analysis: Applications of Vine Copulas." *Statistica Neerlandica* 67(4):403-435.

Aloui, R., M.S.B. Aïssa, S. Hammoudeh, and D.K. Nguyen. 2014. "Dependence and Extreme Dependence of Crude Oil and Natural Gas Prices with Applications to Risk Management." *Energy Economics* 42:332-342.

Ammann, M., and S. Süss. 2009. "Asymmetric Dependence Patterns in Financial Time Series." *The European Journal of Finance* 15(7-8):703-719.

Ang, A., and G. Bekaert. 2002. “International Asset Allocation with Regime Shifts.” *Review of Financial Studies* 15(4):1137-1187.

Ang, A., and J. Chen. 2002. “Asymmetric Correlations of Equity Portfolios.” *Journal of Financial Economics* 63(3):443-494.

Artzner, P., F. Delbaen, J.-M. Eber, and D. Heath. 1999. “Coherent Measures of Risk.” *Mathematical Finance* 9(3):203-228.

Awudu, I., William W., and B. Dahl. 2016. “Hedging Strategy for Ethanol Processing with Copula Distributions.” *Energy Economics* 57:59-65.

Barbi, M., and S. Romagnoli. 2014. “A Copula-Based Quantile Risk Measure Approach to Estimate the Optimal Hedge Ratio.” *Journal of Futures Markets* 34(7):658-675.

Bartlett, M.S. 1950. “Tests of Significance in Factor Analysis.” *British Journal of Mathematical and Statistical Psychology* 3(2):77-85.

Baumeister, C., and L. Kilian. 2014. “Do Oil Price Increases Cause Higher Food Prices?” *Economic Policy* 29(80):691-747.

Bedford, T., and R.M. Cooke. 2001. “Probability Density Decomposition for Conditionally Dependent Random Variables Modeled by Vines.” *Annals of Mathematics and Artificial Intelligence* 32(1):245-268.

___. 2002. “Vines: A New Graphical Model for Dependent Random Variables.” *Annals of Statistics* 30(4):1031-1068.

Bekiros, S.D., and D.A. Georgoutsos. 2005. “Estimation of Value-at-Risk by Extreme Value and Conventional Methods: A Comparative Evaluation of Their Predictive

Performance." *Journal of International Financial Markets, Institutions and Money* 15(3):209-228.

Bekiros, S., J.A. Hernandez, S. Hammoudeh, and D.K. Nguyen. 2015. "Multivariate Dependence Risk and Portfolio Optimization: An Application to Mining Stock Portfolios." *Resources Policy* 46:1-11.

Berkowitz, J. 2001. "Testing Density Forecasts, with Applications to Risk Management." *Journal of Business & Economic Statistics* 19(4):465-474.

Bouyé, E., and M. Salmon. 2009. "Dynamic Copula Quantile Regressions and Tail Area Dynamic Dependence in Forex Markets." *European Journal of Finance* 15(7-8):721-750.

Brechmann, E.C. and U. Schepsmeier. 2013. "Modeling Dependence with C- and D-Vine Copulas: The R Package CDVine." *Journal of Statistical Software* 52(3):1-27.

Brechmann, E., C. Czado, and S. Paterlini. 2014. "Flexible Dependence Modeling of Operational Risk Losses and Its Impact on Total Capital Requirements." *Journal of Banking & Finance* 40:271-285.

Campiche, J.L., H.L. Bryant, J.W. Richardson, and J.L. Outlaw. 2007. "Examining the Evolving Correspondence Between Petroleum Prices and Agricultural Commodity Prices." Paper presented at AAEA annual meeting, Portland, OR, 29 July-1 August.

Cao, Z., R.D.F. Harris, and J. Shen. 2010. "Hedging and Value at Risk: A Semi-Parametric Approach." *Journal of Futures Markets* 30(8):780-794.

Carchano, Ó., and Á. Pardo. 2009. "Rolling over Stock Index Futures Contracts." *Journal of Futures Markets* 29(7):684-694.

Chang, C.-L., M. McAleer, and R. Tansuchat. 2010. "Analyzing and Forecasting Volatility Spillovers, Asymmetries and Hedging in Major Oil Markets." *Energy Economics* 32(6):1445-1455.

Charpentier, A., J.-D. Fermanian, and O. Scaillet. 2007. "The Estimation of Copulas: Theory and Practice." In J. Risk, ed. *Copulas: From Theory to Application in Finance*. London: Risk Books, pp. 35-60.

Chen, X., and Y. Fan. 2006. "Estimation and Model Selection of Semiparametric Copula-Based Multivariate Dynamic Models under Copula Misspecification." *Journal of Econometrics* 135(1-2):125-154.

Chen, S.-S., C.-F. Lee, and K. Shrestha. 2004. "An Empirical Analysis of the Relationship between the Hedge Ratio and Hedging Horizon: A Simultaneous Estimation of the Short- and Long-Run Hedge Ratios." *Journal of Futures Markets* 24(4):359-386.

Chollete, L., A. Heinen, and A. Valdesogo. 2009. "Modeling International Financial Returns with a Multivariate Regime-Switching Copula." *Journal of Financial Econometrics* 7(4):437-480.

Chu, B. 2011. "Recovering Copulas from Limited Information and an Application to Asset Allocation." *Journal of Banking and Finance* 35(7):1824-1842.

Clarke, K.A. 2007. "A Simple Distribution-Free Test for Nonnested Model Selection." *Political Analysis* 15(3):347-363.

Collins, R.A. 2000. "The Risk Management Effectiveness of Multivariate Hedging Models in the U.S. Soy Complex." *Journal of Futures Markets* 20(2):189-204.

Conlon, T., and J. Cotter. 2012. "An Empirical Analysis of Dynamic Multiscale Hedging Using Wavelet Decomposition." *Journal of Futures Markets* 32(3):272-299.

___. 2013. "Downside Risk and the Energy Hedger's Horizon." *Energy Economics* 36:371-379.

Czado, C. 2010. "Pair-Copula Constructions of Multivariate Copulas." In P. Jaworski, F. Durante, W. Härdle, and T. Rychlik, eds. *Copula Theory and Its Applications*. New York: Springer, pp. 93-109

Czado, C., U. Schepsmeier, and A. Min. 2012. "Maximum Likelihood Estimation of Mixed C-Vines with Application to Exchange Rates." *Statistical Modelling* 12(3):229-255.

D'Agostino, R.B., and M.A. Stephens. 1986. *Goodness-of-Fit Techniques*. New York: Marcel Dekker.

Danielsson, J., and C.G. De Vries. 2000. "Value-at-Risk and Extreme Returns." *Annales d'Économie et de Statistique* 60:239-270.

Dawid, A.P. 1984. "Statistical Theory: The Prequential Approach." *Journal of Royal Statistical Society* 147(2):278-292.

Demirer, R., and D. Lien. 2003. "Downside Risk for Short and Long Hedgers." *International Review of Economics & Finance* 12(1):25-44.

Diebold, F.X., T.A. Gunther, and A.S. Tay. 1998. "Evaluating Density Forecasts with Applications to Financial Risk Management." *International Economic Review* 39(4):863-883.

Diebold, F.X., J. Hahn, and A.S. Tay. 1999. "Multivariate Density Forecast Evaluation and Calibration in Financial Risk Management: High-Frequency Returns on Foreign Exchange." *Review of Economics and Statistics* 81(4):661-673.

Diebold, F.X., R.S. Mariano. 1995. "Comparing Predictive Accuracy." *Journal of Business and Economic Statistics* 13:253-265.

Diks, C., V. Panchenko, and D. van Dijk. 2010. "Out-of-Sample Comparison of Copula Specifications in Multivariate Density Forecasts." *Journal of Economic Dynamics & Control* 34:1596-1609.

Dißmann, J., E.C. Brechmann, C. Czado, and D. Kurowicka. 2013. "Selecting and Estimating Regular Vine Copulae and Application to Financial Returns." *Computational Statistics & Data Analysis* 59:52-69.

Du, X., and L.L. McPhail. 2012. "Inside the Black Box: the Price Linkage and Transmission between Energy and Agricultural Markets." *Energy Journal* 33(2):171-194.

Ederington, L.H. 1979. "The Hedging Performance of the New Futures Markets." *Journal of Finance* 34(1):157-170.

Engle, R.F. 1982. "Autoregressive Conditional Heteroskedasticity with Estimates of the Variance of United Kingdom Inflation." *Econometrica* 50:987-1007.

Fernandez, C., and M.F.J. Steel. 1998. "On Bayesian Modeling of Fat Tails and Skewness." *Journal of the American Statistical Association* 93(441):359-371.

Fermanian, J.-D., and O. Scaillet. 2005. "Some Statistical Pitfalls in Copula Modeling for Financial Applications." In E. Klein, ed. *Capital Formation, Governance and Banking*. New York: Nova Science Publishers, pp. 59-74.

Fishburn, P.C. 1977. "Mean-Risk Analysis with Risk Associated with Below-Target Returns." *American Economic Review* 67(2):116-126.

Gaivoronski, A.A., and G. Pflug. 2005. "Value-at-Risk in Portfolio Optimization: Properties and Computational Approach." *Journal of Risk* 7(2):1-31.

Garratt, A., K. Lee, M.H. Pesaran, and Y. Shin. 2003. "Forecast Uncertainties in Macroeconomic Modeling: An Application to the UK Economy." *Journal of the American Statistical Association* 98(464):829-838.

Genest, C., K. Ghoudi, and L.-P. Rivest. 1995. "A Semiparametric Estimation Procedure of Dependence Parameters in Multivariate Families of Distributions." *Biometrika* 82(3):543-552.

Giacomini, R., and H. White. 2006. "Tests of Conditional Predictive Ability." *Econometrica* 74(6):1545-1578.

Gilbert, C.L. 2010. "How to Understand High Food Prices." *Journal of Agricultural Economics* 61(2):398-425.

Grégoire, V., C. Genest, and M. Gendron. 2008. "Using Copulas to Model Price Dependence in Energy Markets." *Energy Risk* 5(5):58-64.

Grothe, O., and J. Schnieders. 2011. "Spatial Dependence in Wind and Optimal Wind Power Allocation: A Copula-Based Analysis." *Energy Policy* 39(9):4742-4754.

Haigh, M.S., and M.T. Holt. 2000. “Hedging Multiple Price Uncertainty in International Grain Trade.” *American Journal of Agricultural Economics* 82(4):881-896.

___. 2002. “Crack Spread Hedging: Accounting for Time-Varying Volatility Spillovers in the Energy Futures Markets.” *Journal of Applied Econometrics* 17(3):269-289.

Hammoudeh, S., H. Li, and B. Jeon. 2003. “Causality and Volatility Spillovers among Petroleum Prices of Wti, Gasoline and Heating Oil in Different Locations.” *North American Journal of Economics and Finance* 14(1):89-114.

Han, L., Y. Zhou, and L. Yin. 2015. “Exogenous Impacts on the Links between Energy and Agricultural Commodity Markets.” *Energy Economics* 49:350-358.

Harlow, W.V. 1991. “Asset Allocation in a Downside-Risk Framework.” *Financial Analysts Journal* 47(5):28-40.

Harris, R.D.F., and J. Shen. 2006. “Hedging and Value at Risk.” *Journal of Futures Markets* 26(4):369-390.

Hernandez, J.A. 2014. “Are Oil and Gas Stocks from the Australian Market Riskier than Coal and Uranium Stocks? Dependence Risk Analysis and Portfolio Optimization.” *Energy Economics* 45:528-536.

Hertel, T.W., and J. Beckman. 2012. “Commodity Price Volatility in the Biofuel Era: An Examination of the Linkage Between Energy and Agricultural Markets.” In J.S.G. Zivin and J.M. Perloff, eds. *The Intended and Unintended Effects of U.S. Agricultural and Biotechnology Policies*. Chicago: University of Chicago Press for NBER, pp. 189-221.

Hofmanna, M., and C. Czadob. 2010. “Assessing the Var of a Portfolio Using D-Vine Copula Based Multivariate Garch Models.” Working paper, Zentrum Mathematik, Technische Universtät München.

Høg, E., and L. Tsiaras. 2011. “Density Forecasts of Crude-Oil Prices Using Option-Implied and ARCH-Type Models.” *Journal of Futures Markets* 31(8):727-754.

Hsu, C.-C., C.-P. Tseng, and Y.-H. Wang. 2008. “Dynamic Hedging with Futures: A Copula-Based Garch Model.” *Journal of Futures Markets* 28(11):1095-1116.

Ji, Q., and Y. Fan. 2011. “A Dynamic Hedging Approach for Refineries in Multiproduct Oil Markets.” *Energy* 36(2):881-887.

Joe, H. 1996. “Families of M-Variate Distributions with Given Margins and M (M-1)/2 Bivariate Dependence Parameters.” *Lecture Notes-Monograph Series* 28:120-141.

___. 1997. *Multivariate Models and Multivariate Dependence Concepts*. New York: CRC Press.

Joe, H., and T. Hu. 1996. “Multivariate Distributions from Mixtures of Max-Infinitely Divisible Distributions.” *Journal of Multivariate Analysis* 57(2):240-265.

Kling, J.L., and D.A. Bessler. 1989. “Calibration-based Predictive Distributions: An Application of Prequential Analysis to Interest Rates, Money, Prices, and Output.” *Journal of Business* 62(4):477-499.

Kristoufek, L., K. Janda, and D. Zilberman. 2012. “Correlations Between Biofuels and Related Commodities Before and During the Food Crisis: A Taxonomy Perspective.” *Energy Economics* 34(5):1380-1391.

Kullback, S., and R.A. Leibler. 1951. "On Information and Sufficiency." *Annals of Mathematical Statistics* 22(1):79-86.

Kurowicka, D., and R.M. Cooke. 2005. "Distribution-Free Continuous Bayesian Belief Nets." In A. Wilson, N. Limnios, S. Keller-McNulty and Y. Armijo, eds. *Modern Statistical and Mathematical Methods in Reliability*. Singapore: World Scientific, 309-323.

___. 2006. *Uncertainty Analysis with High Dimensional Dependence Modelling*. Sussex: John Wiley & Sons.

Kurowicka, D., and H. Joe. 2011. *Dependence Modeling: Vine Copula Handbook*. Singapore: World Scientific.

Lee, H.-T. 2009. "A Copula-Based Regime-Switching Garch Model for Optimal Futures Hedging." *Journal of Futures Markets* 29(10):946-972.

Leuthold, R.M., and P.E. Peterson. 1987. "A Portfolio Approach to Optimal Hedging for a Commercial Cattle Feedlot." *Journal of Futures Markets* 7(2):119-133.

Lien, D., and Y.K. Tse. 1998. "Hedging Time-Varying Downside Risk." *Journal of Futures Markets*, 18(6): 705-722.

___. 2000. "Hedging Downside Risk with Futures Contracts." *Applied Financial Economics* 10(2):163-170.

___. 2001. "Hedging Downside Risk: Futures Vs. Options." *International Review of Economics & Finance* 10(2):159-169.

Loaiza Maya, R.A., J.E. Gomez-Gonzalez, and L.F. Melo Velandia. 2015. "Latin American Exchange Rate Dependencies: A Regular Vine Copula Approach." *Contemporary Economic Policy* 33(3):535-549.

Low, R.K.Y., J. Alcock, R. Faff, and T. Brailsford. 2013. "Canonical Vine Copulas in the Context of Modern Portfolio Management: Are They Worth It?" *Journal of Banking & Finance* 37(8):3085-3099.

Lucotte, Y. 2016. "Co-movements Between Crude Oil and Food Prices: A Post-Commodity Boom Perspective." *Economics Letters* 147:142-147.

McNeil, A.J., and R. Frey. 2000. "Estimation of Tail-Related Risk Measures for Heteroscedastic Financial Time Series: An Extreme Value Approach." *Journal of Empirical Finance* 7(3-4):271-300.

Meade, N. 2010. "Oil Prices – Brownian Motion or Mean Reversion? A Study Using a One Year Ahead Density Forecast Criterion." *Energy Economics* 32(6):1485-1498.

Mitchell, J., and K.F. Wallis. 2011. "Evaluating Density Forecasts: Forecast Combinations, Model Mixtures, Calibration and Sharpness." *Journal of Applied Econometrics* 26:1023-1040.

Morales-Nápoles, O., R.M. Cooke, and D. Kurowicka. 2010. "About the Number of Vines and Regular Vines on n Nodes." Working Paper, Delft University of Technology.

Morana, C., 2001. "A Semiparametric Approach to Short-Term Oil Price Forecasting." *Energy Economics* 23:325-338.

Muhammad, A., and E. Kebede. 2009. "The Emergence of an Agro-Energy Sector: Is Agriculture Importing Instability from the Oil Sector?" *Choices* 24(1):12-15.

Nelder, J.A., and R. Mead. 1965. "A Simplex Method for Function Minimization." *The Computer Journal* 7(4):308-313.

Nelson, R.B. 2006. An Introduction to Copulas. 2nd edition. Berlin: Springer-Verlag.

Nikoloulopoulos, A.K., H. Joe, and H. Li. 2012. "Vine Copulas with Asymmetric Tail Dependence and Applications to Financial Return Data." *Computational Statistics & Data Analysis* 56(11):3659-3673.

Noussinov, M.A., and R.M. Leuthold. 1999. "Optimal Hedging Strategies for the U.S. Cattle Feeder." *Journal of Agribusiness* 17(1):1-19.

Patton, A.J. 2004. "On the Out-of-Sample Importance of Skewness and Asymmetric Dependence for Asset Allocation." *Journal of Financial Econometrics* 2(1):130-168.

___. 2006. "Modelling Asymmetric Exchange Rate Dependence." *International Economic Review* 47(2):527-556.

___. 2012. "A Review of Copula Models for Economic Time Series." *Journal of Multivariate Analysis* 110:4-18.

Power, G.J., and D. Vedenov. 2010. "Dealing with Downside Risk in a Multi-Commodity Setting: A Case for a "Texas Hedge"?" *Journal of Futures Markets* 30(3):290-304.

Pritsker, M. 2006. "The Hidden Dangers of Historical Simulation." *Journal of Banking & Finance* 30(2):561-582.

Quaranta, A.G., and A. Zaffaroni. 2008. "Robust Optimization of Conditional Value at Risk and Portfolio Selection." *Journal of Banking & Finance* 32(10):2046-2056.

Reboredo, J.C. 2012a. "Do Food and Oil Prices Co-Move?" Energy Policy 49:456-467.

___. 2012b. "Modelling Oil Price and Exchange Rate Co-Movements." *Journal of Policy Modeling* 34(3):419-440.

Reeves, J.J. 2005. "Bootstrap Prediction Intervals for ARCH Models." International *Journal of Forecasting* 21(2):237-248.

Riccetti, L. 2013. "A Copula–Garch Model for Macro Asset allocation of a Portfolio with Commodities." *Empirical Economics* 44(3):1315-1336.

Rockafellar, R.T., and S. Uryasev. 2002. "Conditional Value-at-Risk for General Loss Distributions." *Journal of Banking & Finance* 26(7):1443-1471.

Roy, A.D. 1952. "Safety First and the Holding of Assets." *Econometrica* 20(3):431-449.

Sarassoro, G.F., and R.M. Leuthold. 1991. "Managing Multiple International Risks Simultaneously with an Optimal Hedging Model." *Agricultural Economics* 6(1):31-47.

Schnepf, R., and B.D. Yacobucci. 2013. *Renewable Fuel Standard (RFS): Overview and Issues*. Washington DC: Congressional Research Service, CRS Report for Congress 7-5700, 14 March 2013.

Seillier, F.M., and A.P. Dawid. 1993. "On Testing the Validity of Sequential Probability Forecasts." *Journal of the American Statistical Association* 88(421):355-359.

Serra, T., and J.M. Gil. 2012. "Biodiesel as a Motor Fuel Price Stabilization Mechanism." *Energy Policy* 50:689-698.

Serra, T., and D. Zilberman. 2013. "Biofuel-Related Price Transmission Literature: A Review." *Energy Economics* 37:141-151.

Siburg, K.F., P. Stoimenov, and G.N.F. Weiß. 2015. "Forecasting Portfolio-Value-at-Risk with Nonparametric Lower Tail Dependence Estimates." *Journal of Banking & Finance* 54:129-140.

Silverman, B.W. 1986. *Density Estimation*. London: Chapman and Hall.

Sklar, A. 1959. "Fonctions de Répartition à n Dimensions et Leurs Marges." *Publications de l' Institut Statistique de l'Université de Paris* 8:229-231.

Stephens, M.A. 1974. "EDF Statistics for Goodness of Fit and Some Comparisons." *Journal of American Statistical Association* 69(347):730-737.

Sukcharoen, K., H. Choi, and D.J. Leatham. 2015. "Optimal Gasoline Hedging Strategies Using Futures Contracts and Exchange-Traded Funds." *Applied Economics* 47(32):3482-3498.

Tejeda, H.A., and B.K. Goodwin. 2014. "Dynamic Multiproduct Optimal Hedging in the Soybean Complex – Do Time-Varying Correlations Provide Hedging Improvements?" *Applied Economics* 46(27):3312-3322.

Tejeda, H., and D. Feuz. 2014. "Determining the Effectiveness of Optimal Time-Varying Hedge Ratios for Cattle Feeders under Multiproduct and Single Commodity Settings." *Agricultural Finance Review* 74(2):217-235.

Tong, B., C. Wu, and C. Zhou. 2013. "Modeling the Co-Movements between Crude Oil and Refined Petroleum Markets." *Energy Economics* 40:882-897.

Tyner, W.E. 2010. "The Integration of Energy and Agricultural Markets." *Agricultural Economics* 41(1):193-201.

Tzang, D.-N., and R.M. Leuthold. 1990. "Hedge Ratios under Inherent Risk Reduction in a Commodity Complex." *Journal of Futures Markets* 10(5):497-504.

Unser, M. 2000. "Lower Partial Moments as Measures of Perceived Risk: An Experimental Study." *Journal of Economic Psychology* 21(3):253-280.

U.S. Energy Information Administration. 2011. "Growth Slows in U.S. Ethanol Production and Consumption". *Today in Energy* (September 14, 2011), Washington DC. Internet site: https://www.eia.gov/todayinenergy/detail.php?id=3070 (Accessed February 12, 2017).

Veld, C., and Y.V. Veld-Merkoulova. 2008. "The Risk Perceptions of Individual Investors." *Journal of Economic Psychology* 29(2):226-252.

Vuong, Q.H. 1989. "Likelihood Ratio Tests for Model Selection and Non-Nested Hypotheses." *Econometrica* 57(2):307-333.

Wei, W., J. Li, L. Cao, J. Sun, C. Liu, and M. Li. 2013. "Optimal Allocation of High Dimensional Assets through Canonical Vines." In J. Pei, V.S. Tseng, L. Cao, H. Motoda and G. Xu, eds. *Advances in Knowledge Discovery and Data Mining*. Berlin-Heidelberg: Springer, pp. 366-377.

Weiß, G.N.F., and H. Supper. 2013. "Forecasting Liquidity-Adjusted Intraday Value-at-Risk with Vine Copulas." *Journal of Banking & Finance* 37(9):3334-3350.

Wilson, W.W., W.E. Nganje, and R. Wagner. 2006. "Hedging Strategies for Grain Processors." *Canadian Journal of Agricultural Economics* 54(2):311-326.

Zhang, B., Y. Wei, J. Yu, X. Lai, and Z. Peng. 2014. "Forecasting Var and Es of Stock Index Portfolio: A Vine Copula Method." *Physica A: Statistical Mechanics and its Applications* 416:112-124.

Zhang, D. 2014. "Vine Copulas and Applications to the European Union Sovereign Debt Analysis." *International Review of Financial Analysis* 36:46-56.

Zilberman, D., G. Hochman, D. Rajagopal, S. Sexton, and G. Timilsina. 2013. "The Impact of Biofuels on Commodity Food Prices: Assessment of Findings." *American Journal of Agricultural Economics* 95(2):275-281.

Zimmer, D.M. 2015. "Analyzing Comovements in Housing Prices Using Vine Copulas." *Economic Inquiry* 53(2):1156-1169.

APPENDIX A

SUPPLEMENTARY RESULTS FOR CHAPTER II

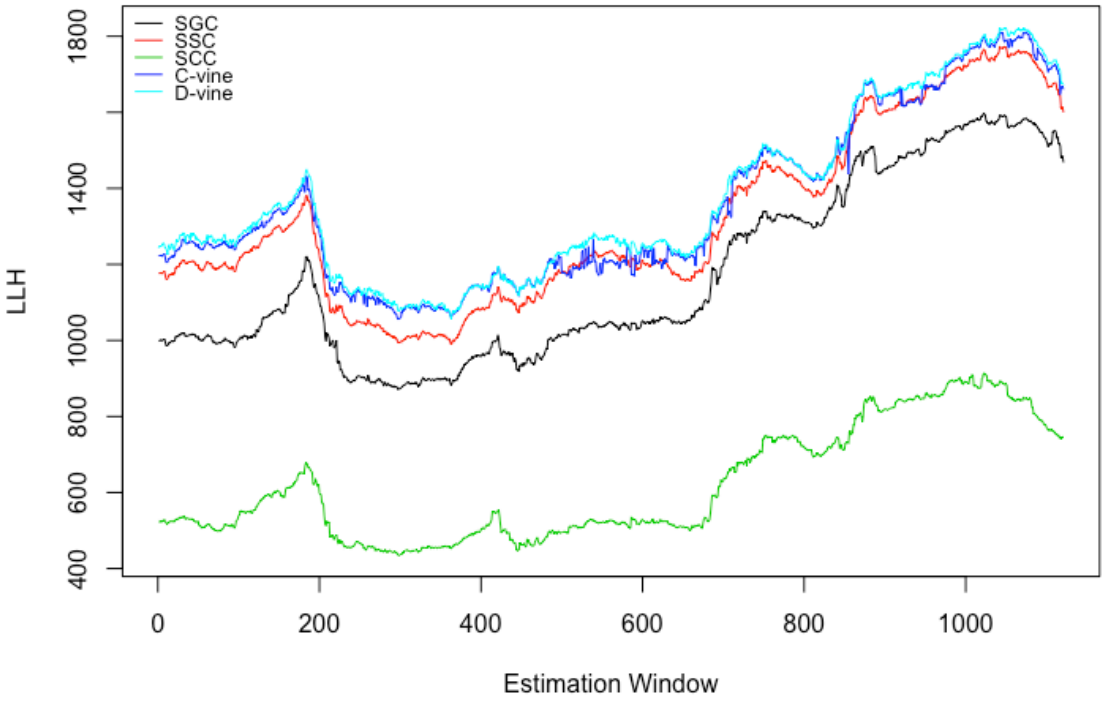

Figure A.1. In-sample log-likelihood (LLH) across 1,121 estimation windows

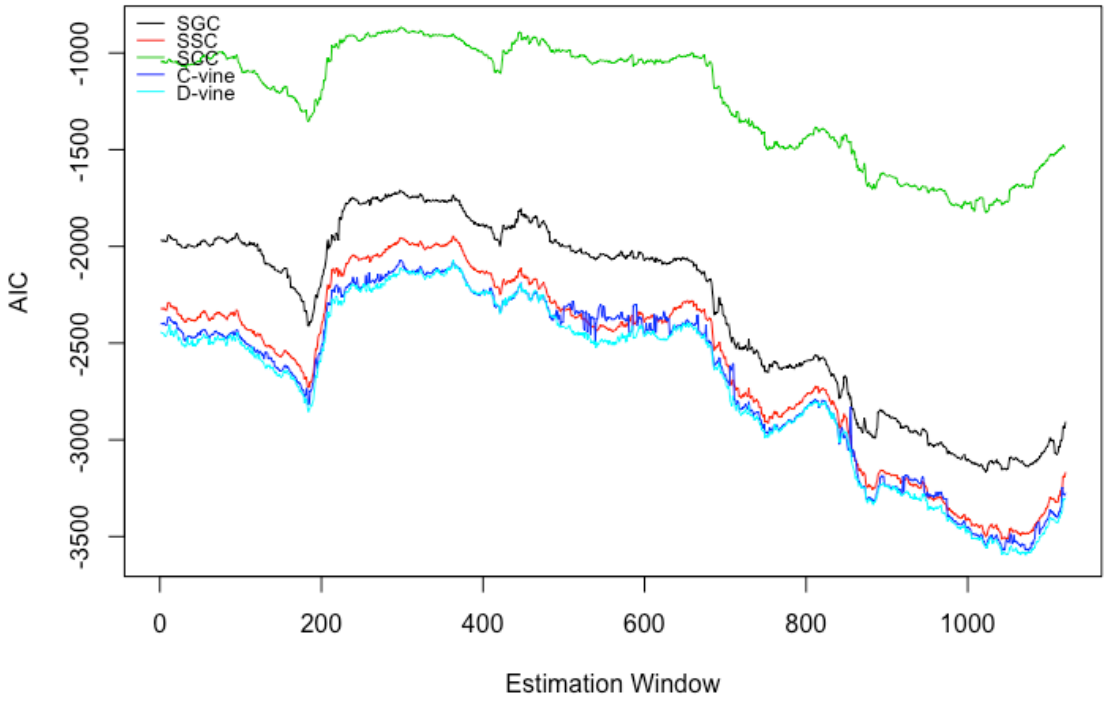

Figure A.2. In-sample Akaike Information Criterion (AIC) across 1,121 estimation windows

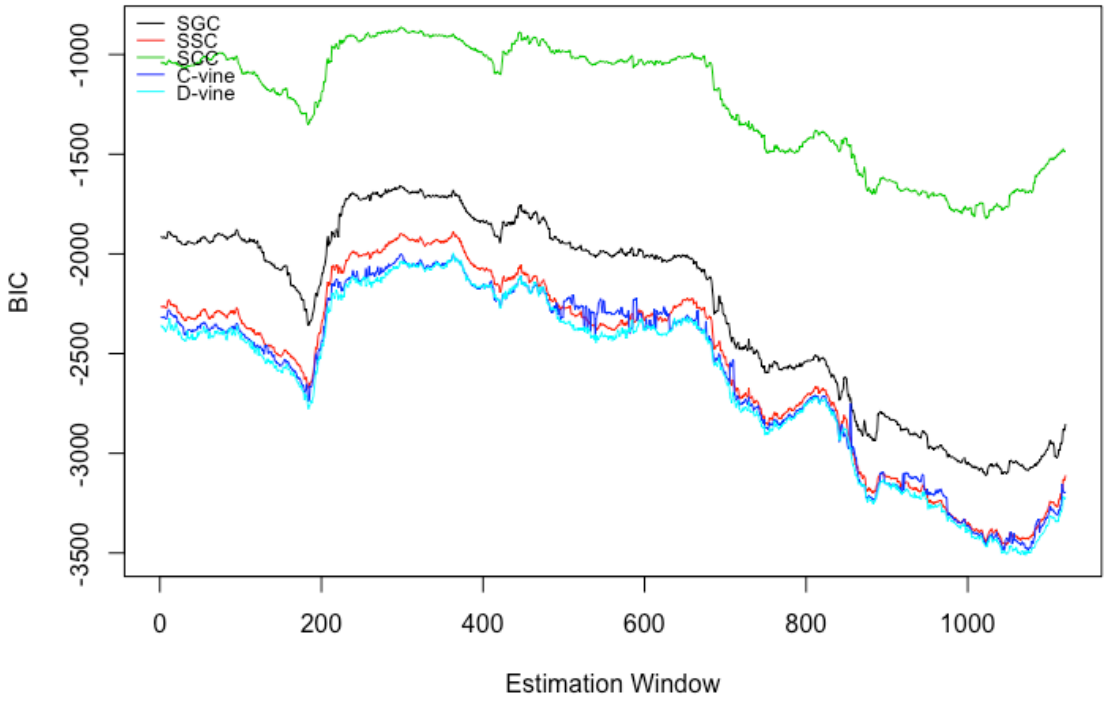

Figure A.3. In-sample Bayesian Information Criterion (BIC) across 1,121 estimation windows

APPENDIX B

SUPPLEMENTARY RESULTS FOR CHAPTER III

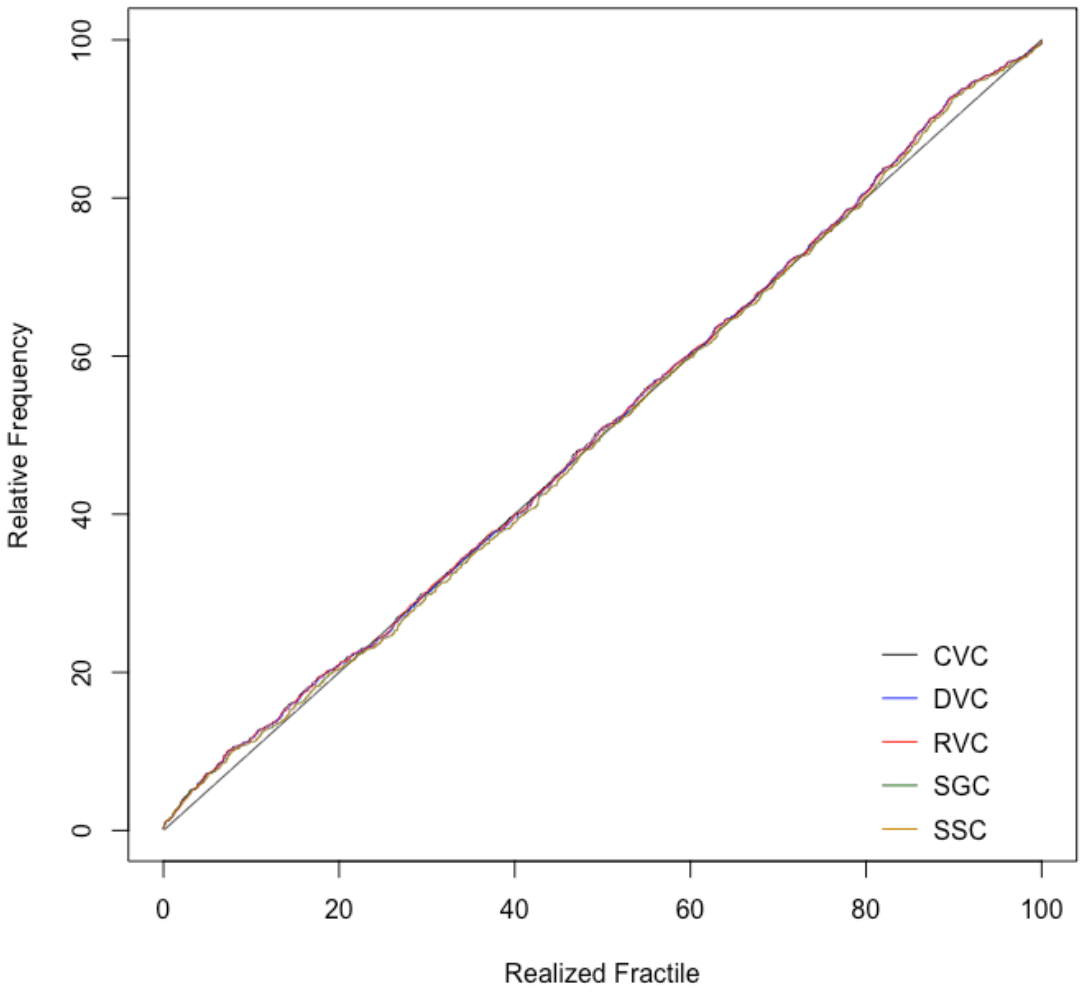

Figure B.1. Calibration plots for the density forecasts of crude oil returns based on the canonical vine copula (CVC), drawable vine copula (DVC), regular vine copula (RVC), standard Gaussian copula (SGC), and standard Student's t copula (SSC) models with normal marginal distributions

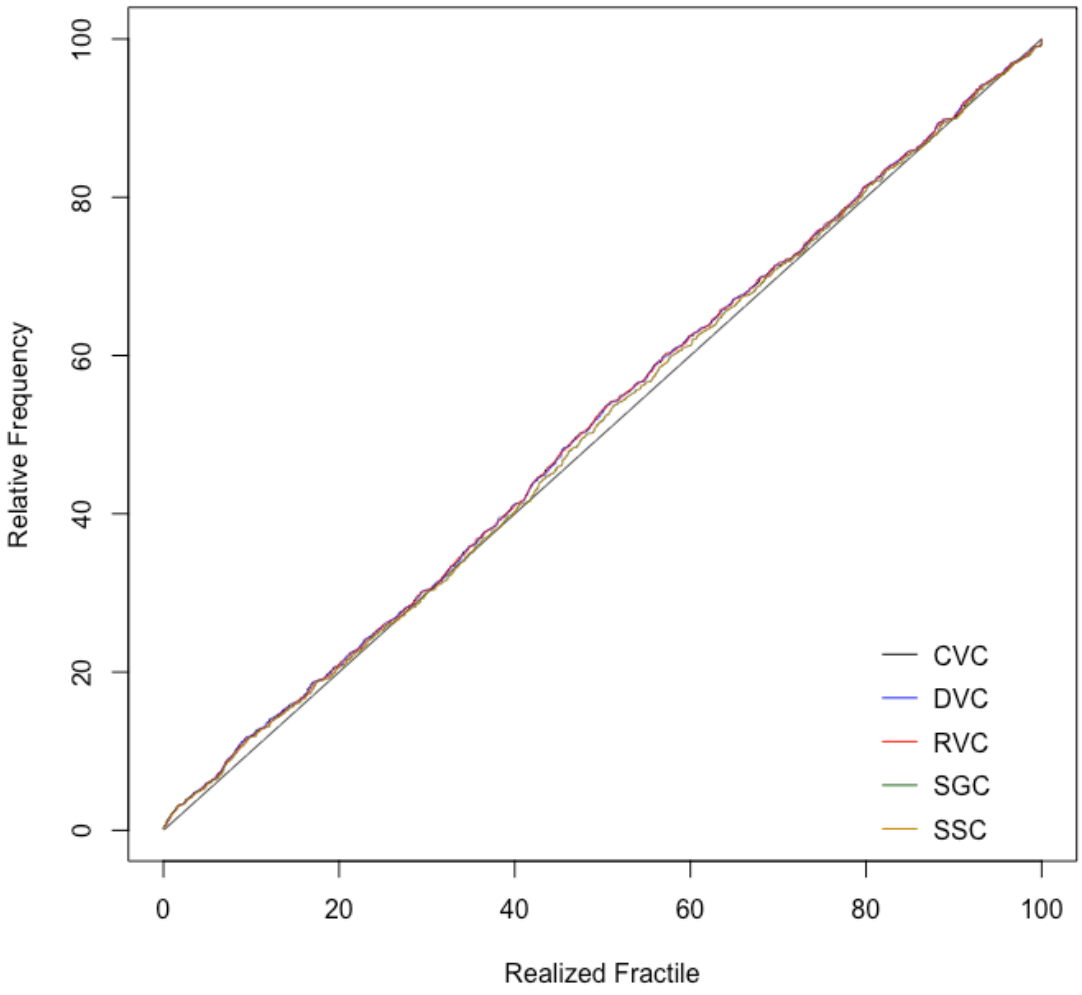

Figure B.2. Calibration plots for the density forecasts of diesel fuel returns based on the canonical vine copula (CVC), drawable vine copula (DVC), regular vine copula (RVC), standard Gaussian copula (SGC), and standard Student's t copula (SSC) models with normal marginal distributions

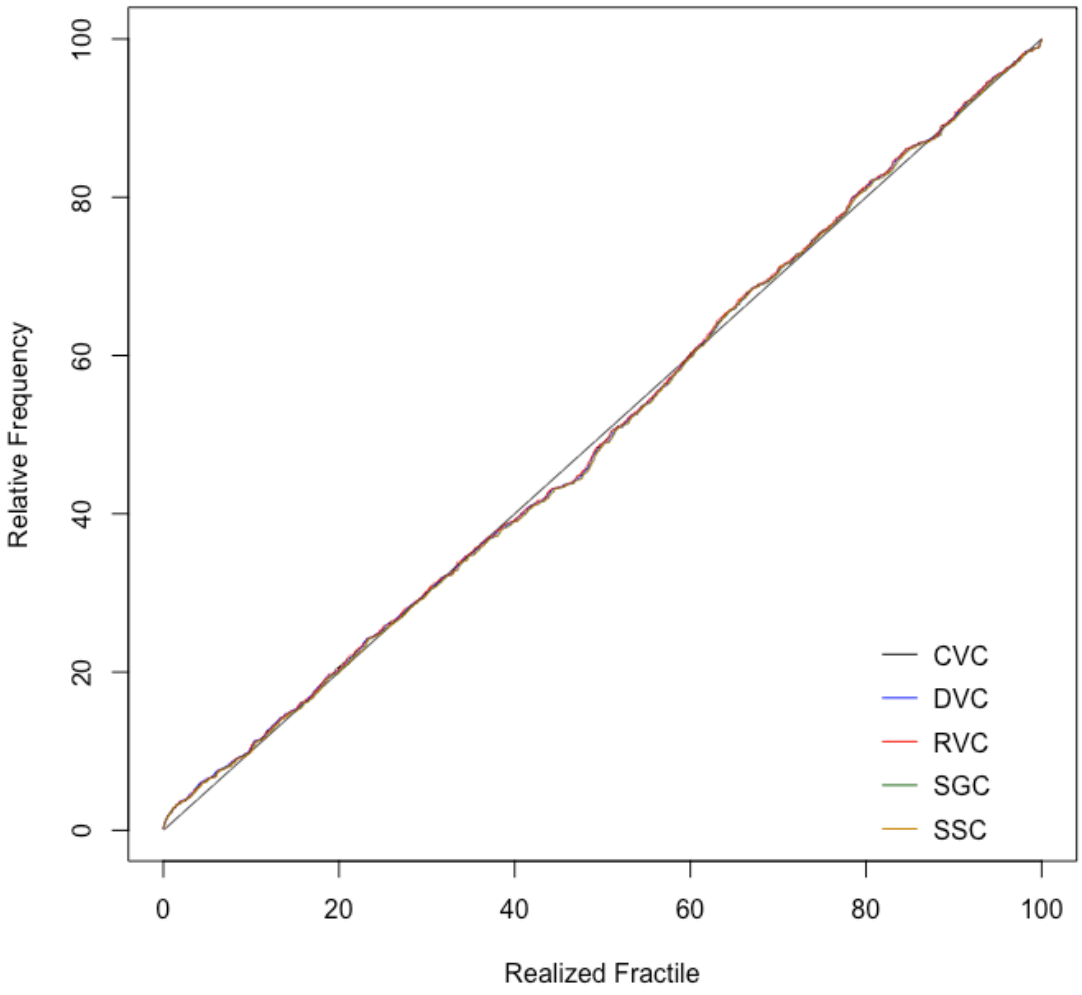

Figure B.3. Calibration plots for the density forecasts of gasoline returns based on the canonical vine copula (CVC), drawable vine copula (DVC), regular vine copula (RVC), standard Gaussian copula (SGC), and standard Student's t copula (SSC) models with normal marginal distributions

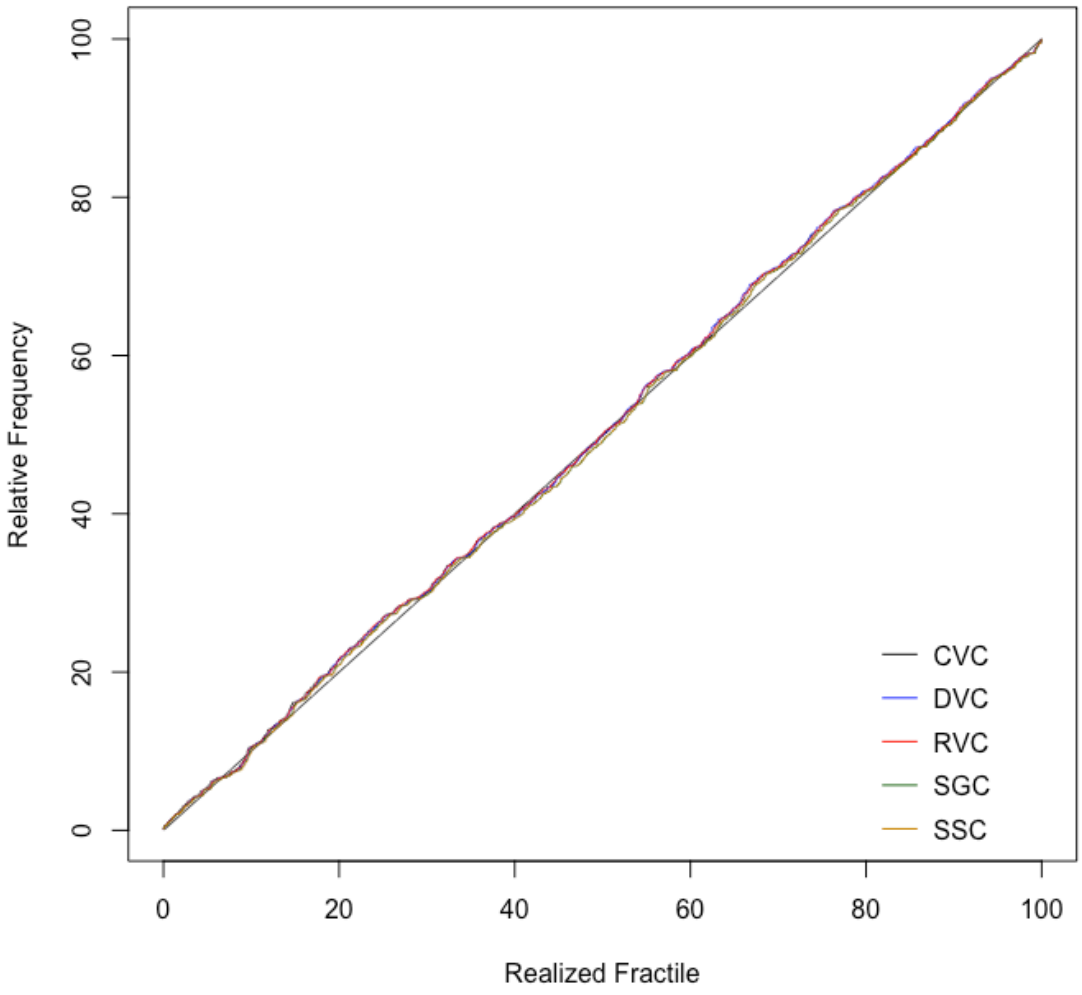

Figure B.4. Calibration plots for the density forecasts of heating oil returns based on the canonical vine copula (CVC), drawable vine copula (DVC), regular vine copula (RVC), standard Gaussian copula (SGC), and standard Student's t copula (SSC) models with normal marginal distributions

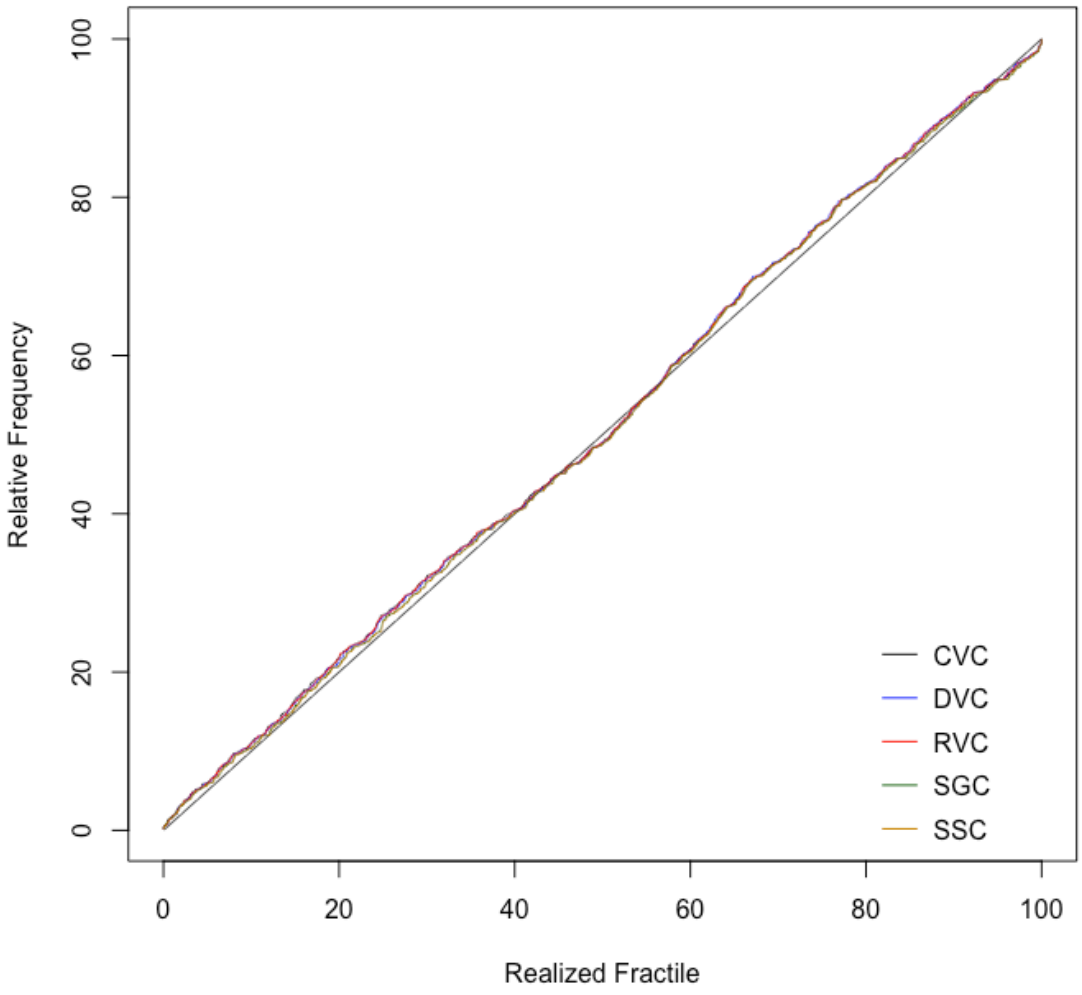

Figure B.5. Calibration plots for the density forecasts of jet fuel returns based on the canonical vine copula (CVC), drawable vine copula (DVC), regular vine copula (RVC), standard Gaussian copula (SGC), and standard Student's t copula (SSC) models with normal marginal distributions

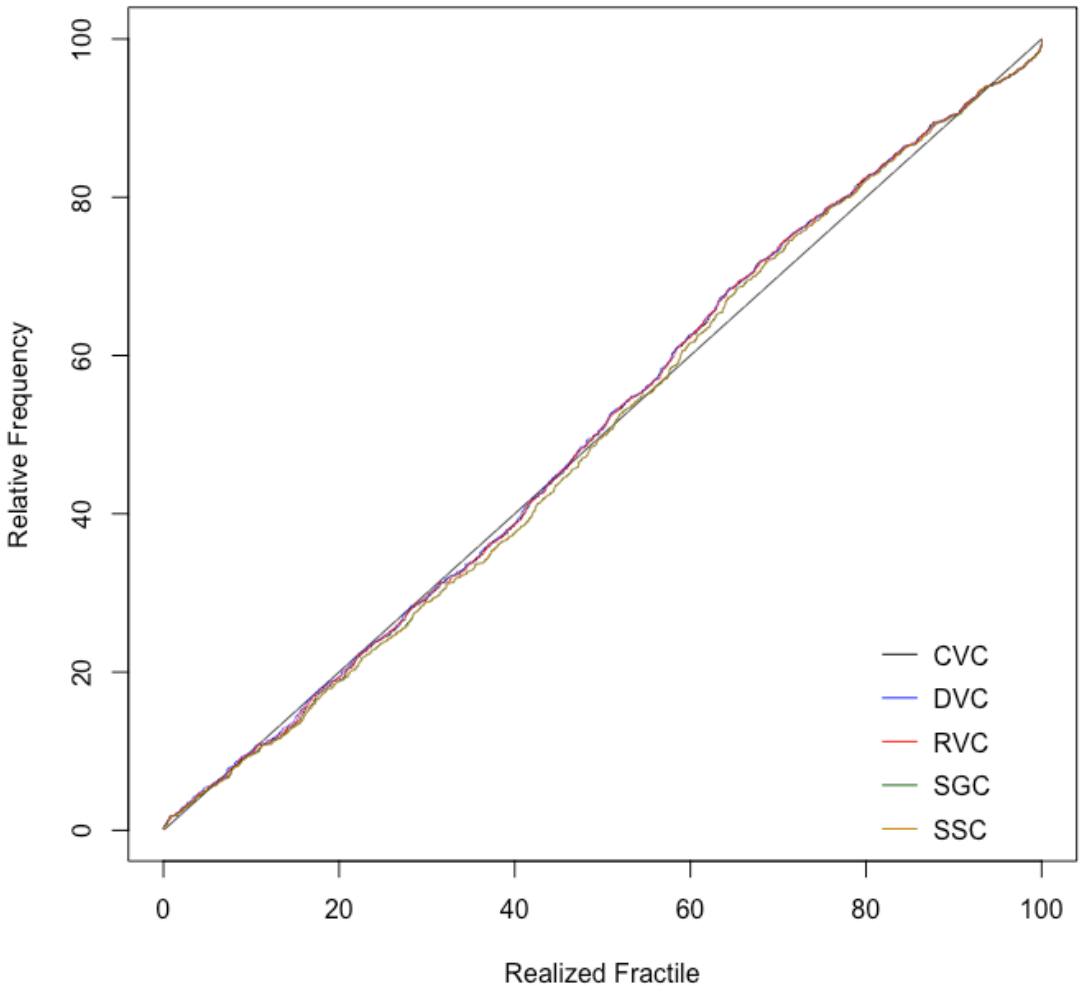

Figure B.6. Calibration plots for the density forecasts of natural gas returns based on the canonical vine copula (CVC), drawable vine copula (DVC), regular vine copula (RVC), standard Gaussian copula (SGC), and standard Student's t copula (SSC) models with normal marginal distributions

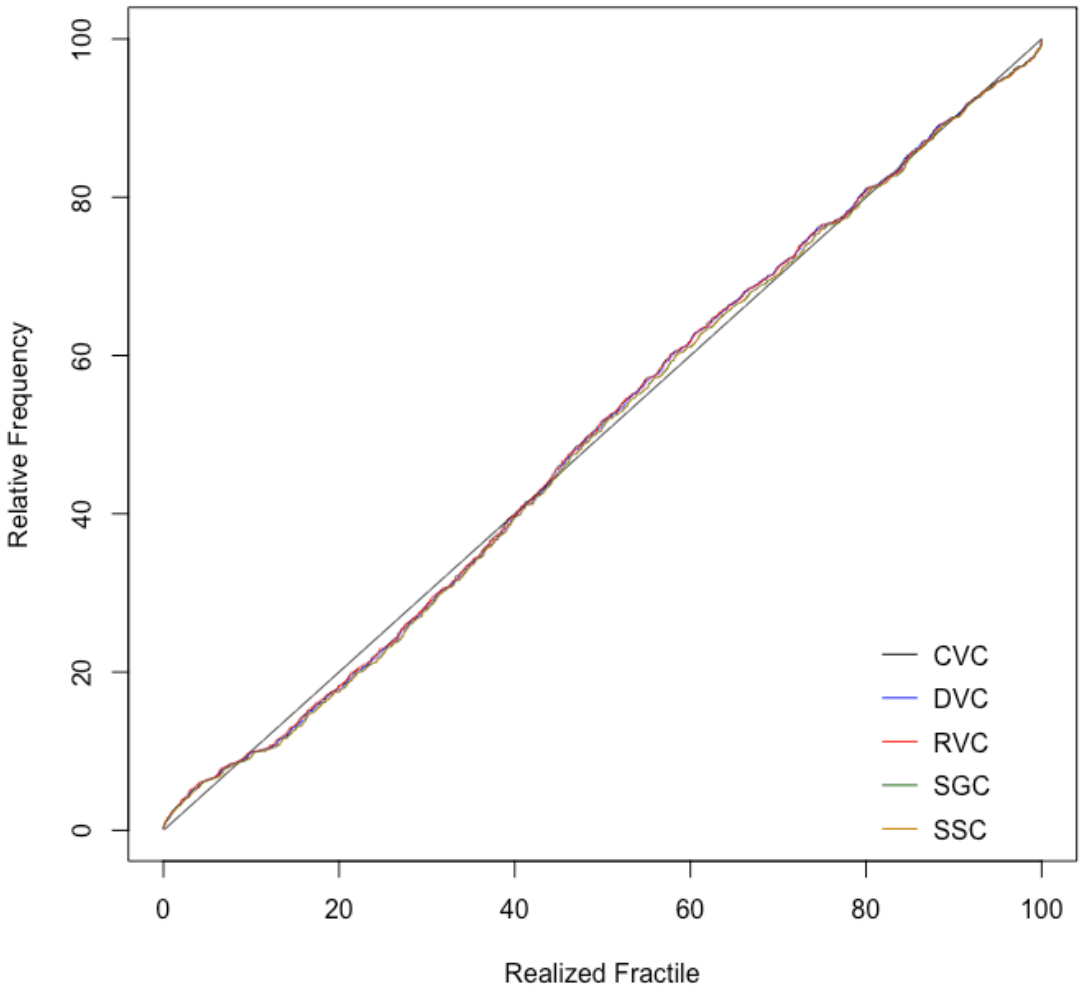

Figure B.7. Calibration plots for the density forecasts of propane returns based on the canonical vine copula (CVC), drawable vine copula (DVC), regular vine copula (RVC), standard Gaussian copula (SGC), and standard Student's t copula (SSC) models with normal marginal distributions

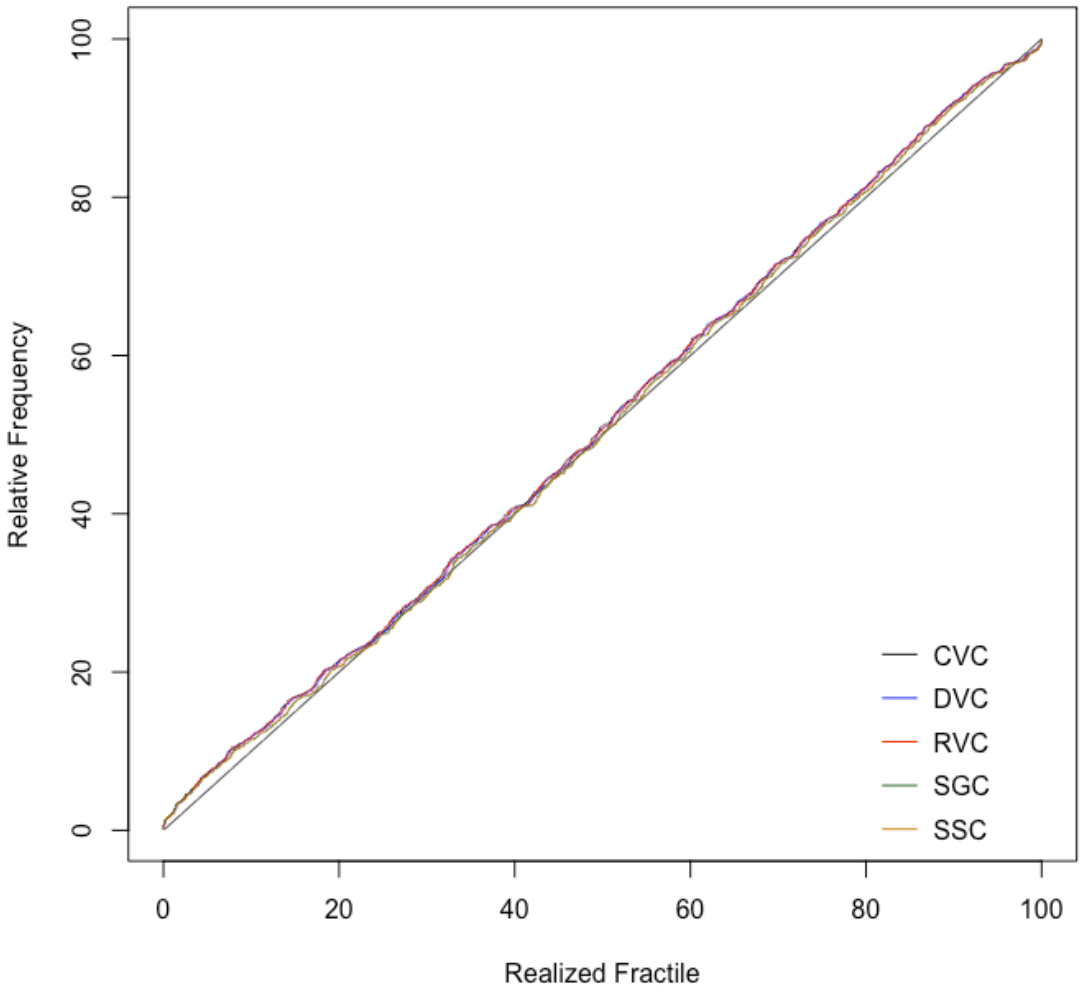

Figure B.8. Calibration plots for the density forecasts of crude oil returns based on the canonical vine copula (CVC), drawable vine copula (DVC), regular vine copula (RVC), standard Gaussian copula (SGC), and standard Student's t copula (SSC) models with skewed normal marginal distributions

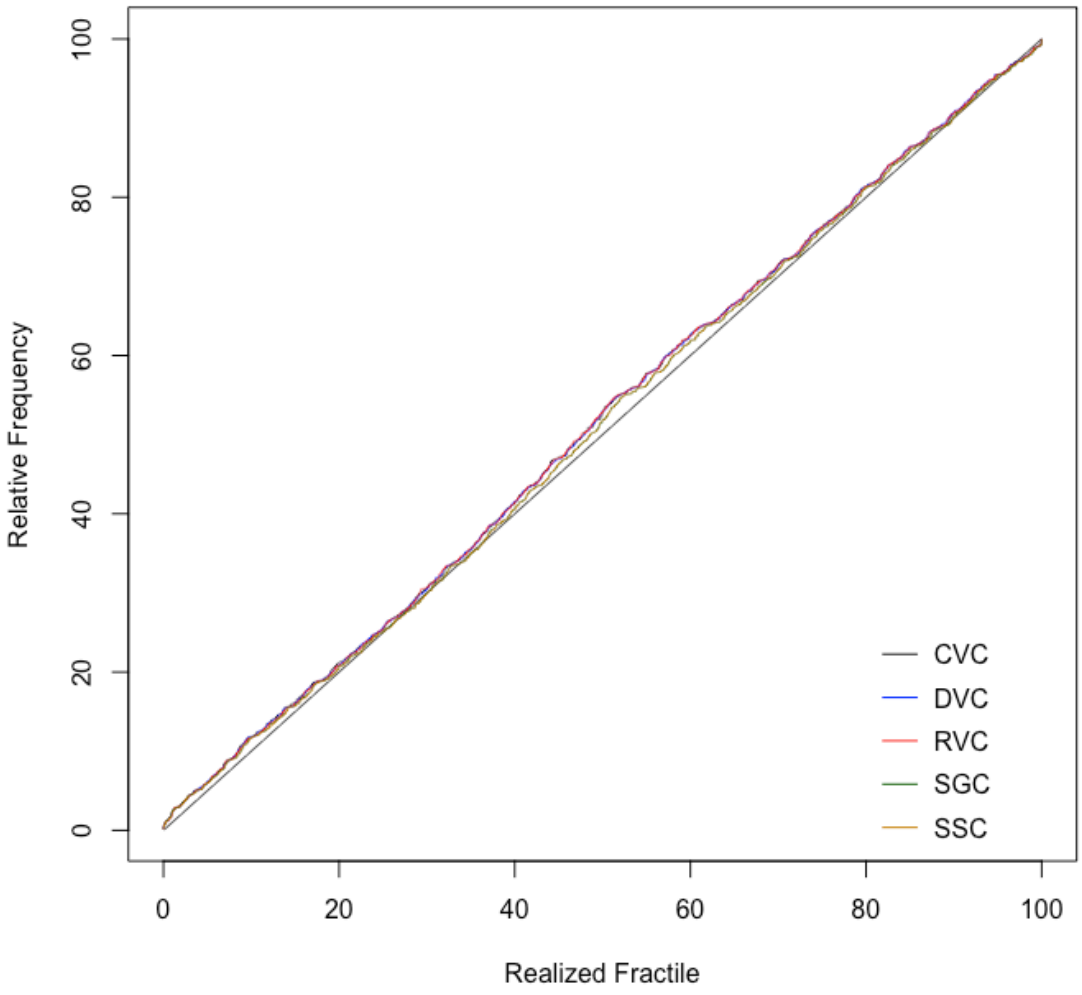

Figure B.9. Calibration plots for the density forecasts of diesel fuel returns based on the canonical vine copula (CVC), drawable vine copula (DVC), regular vine copula (RVC), standard Gaussian copula (SGC), and standard Student's t copula (SSC) models with skewed normal marginal distributions

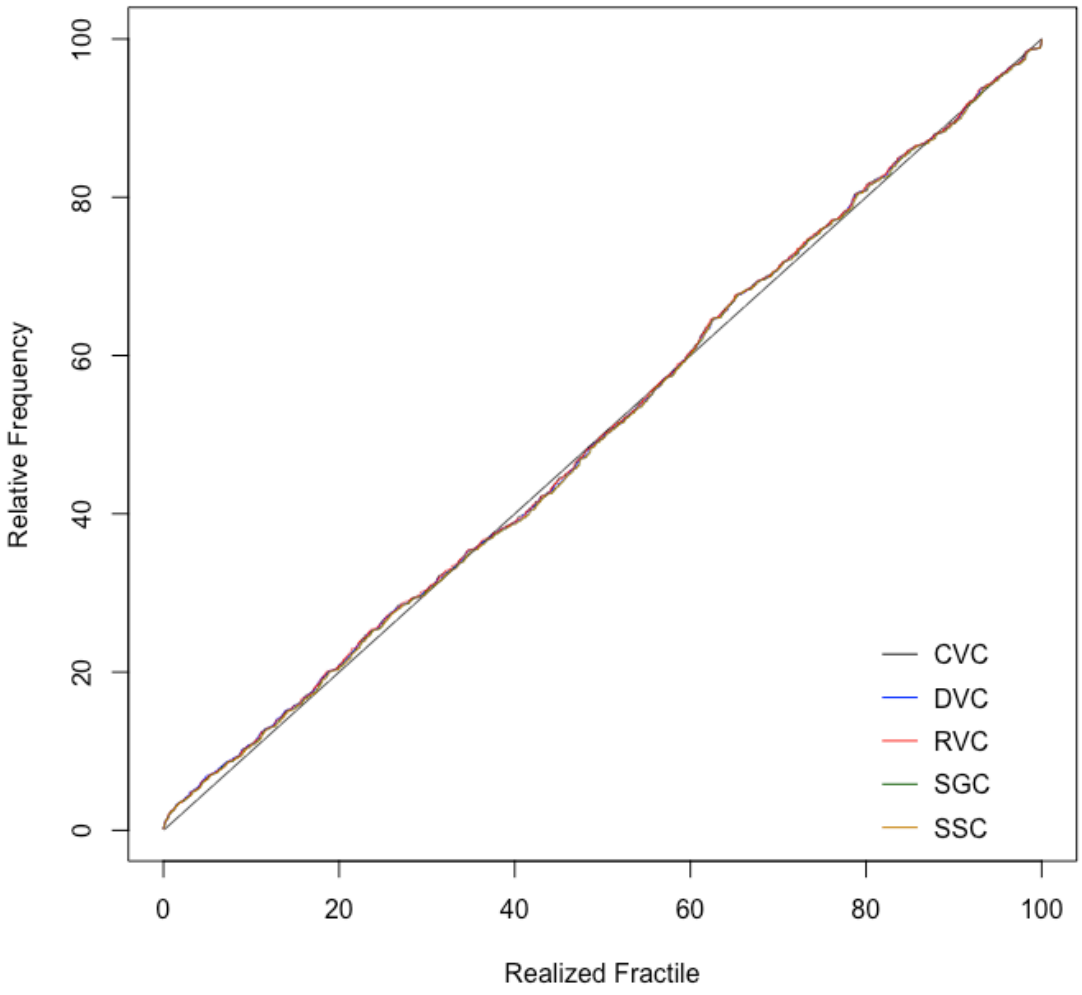

Figure B.10. Calibration plots for the density forecasts of gasoline returns based on the canonical vine copula (CVC), drawable vine copula (DVC), regular vine copula (RVC), standard Gaussian copula (SGC), and standard Student's t copula (SSC) models with skewed normal marginal distributions

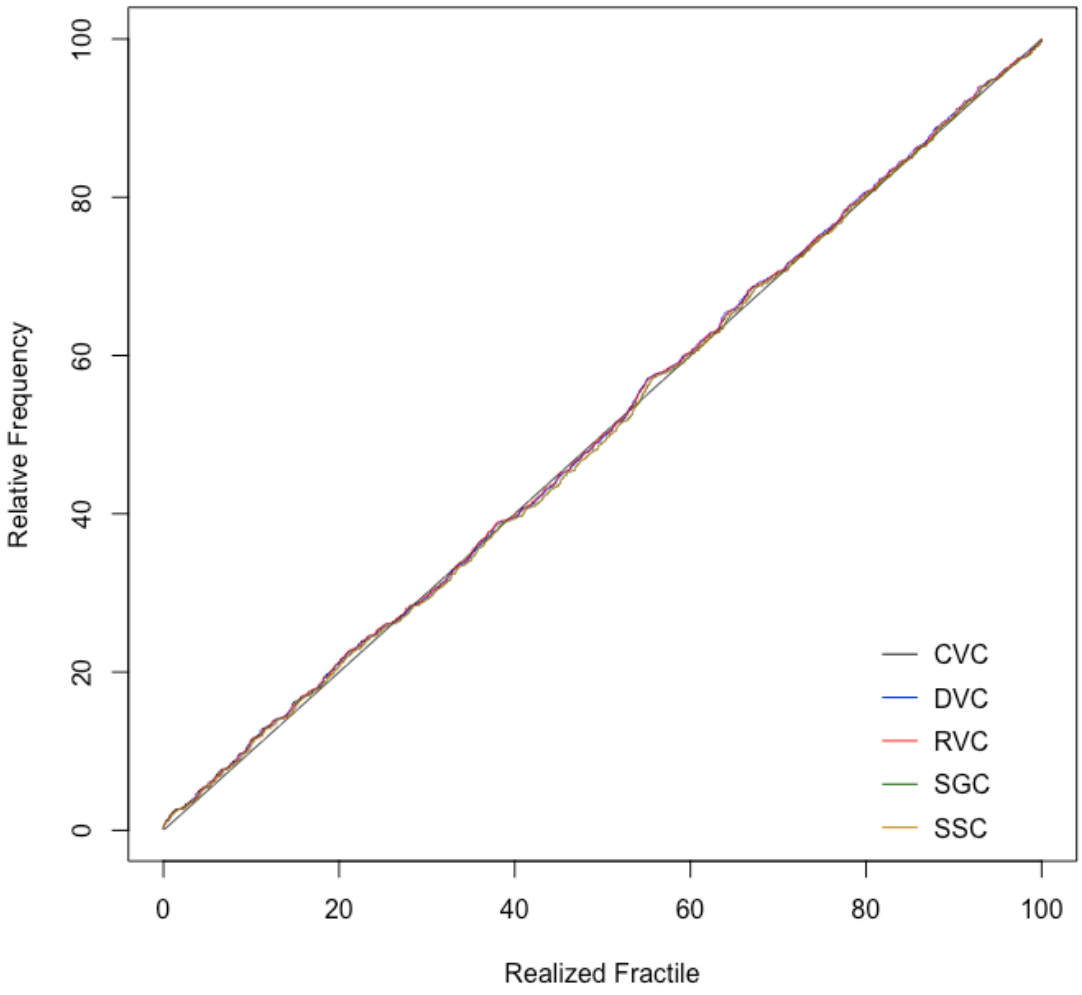

Figure B.11. Calibration plots for the density forecasts of heating oil returns based on the canonical vine copula (CVC), drawable vine copula (DVC), regular vine copula (RVC), standard Gaussian copula (SGC), and standard Student's t copula (SSC) models with skewed normal marginal distributions

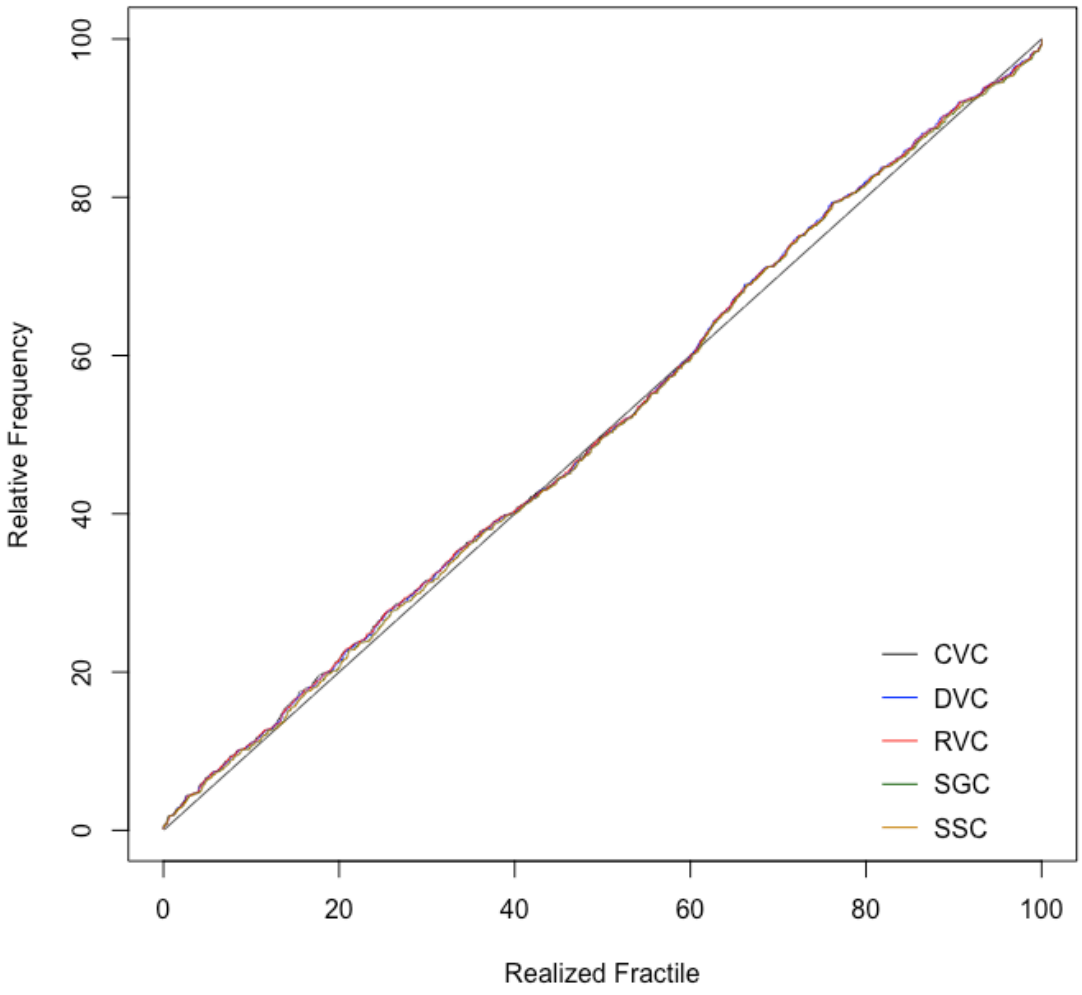

Figure B.12. Calibration plots for the density forecasts of jet fuel returns based on the canonical vine copula (CVC), drawable vine copula (DVC), regular vine copula (RVC), standard Gaussian copula (SGC), and standard Student's t copula (SSC) models with skewed normal marginal distributions

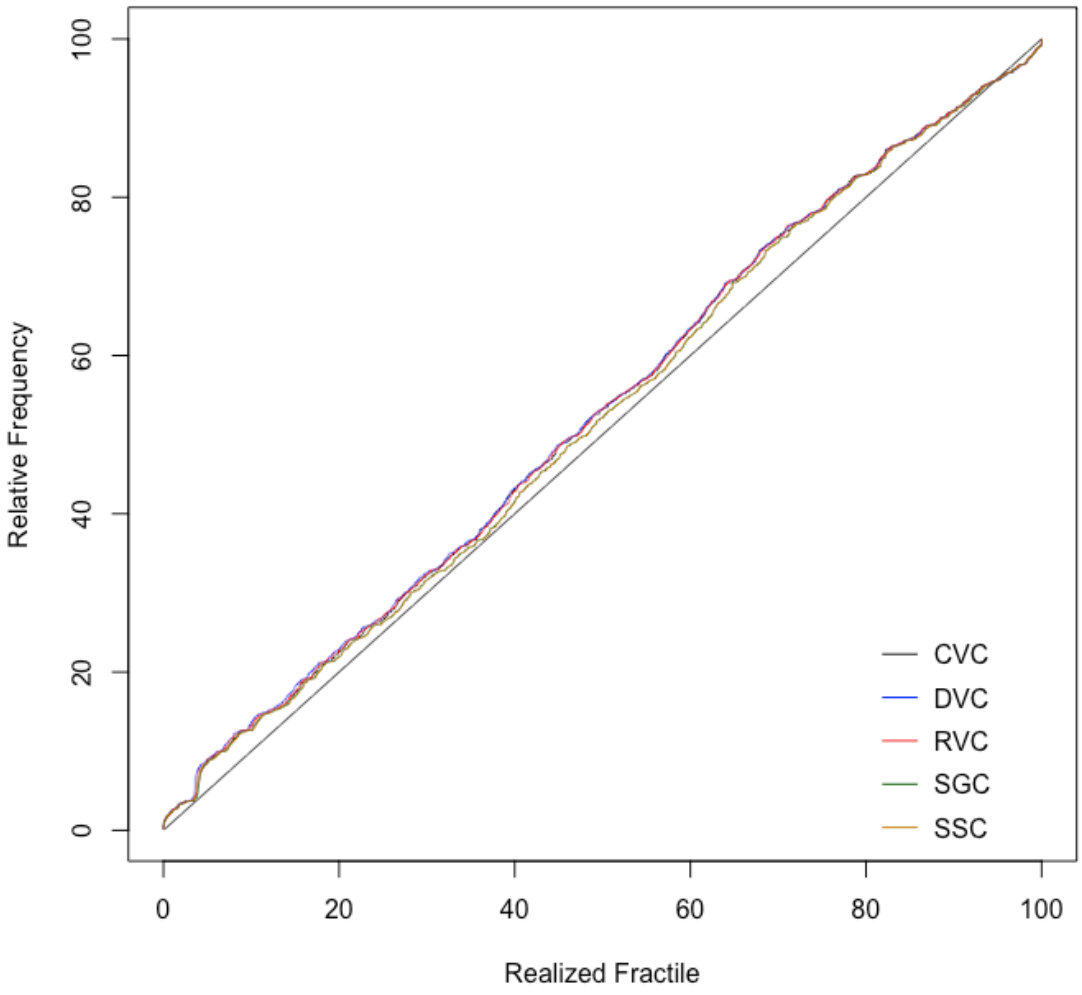

Figure B.13. Calibration plots for the density forecasts of natural gas returns based on the canonical vine copula (CVC), drawable vine copula (DVC), regular vine copula (RVC), standard Gaussian copula (SGC), and standard Student's t copula (SSC) models with skewed normal marginal distributions

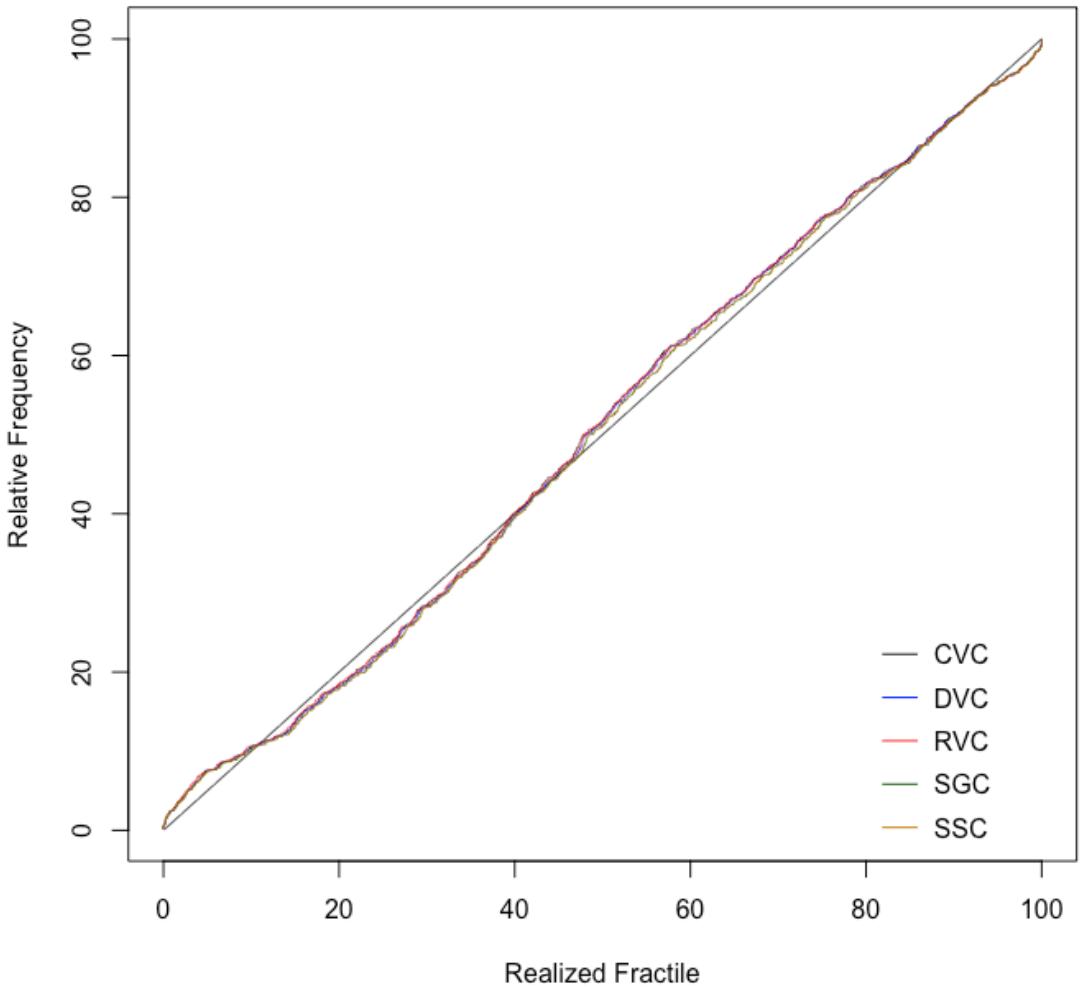

Figure B.14. Calibration plots for the density forecasts of propane returns based on the canonical vine copula (CVC), drawable vine copula (DVC), regular vine copula (RVC), standard Gaussian copula (SGC), and standard Student's t copula (SSC) models with skewed normal marginal distributions

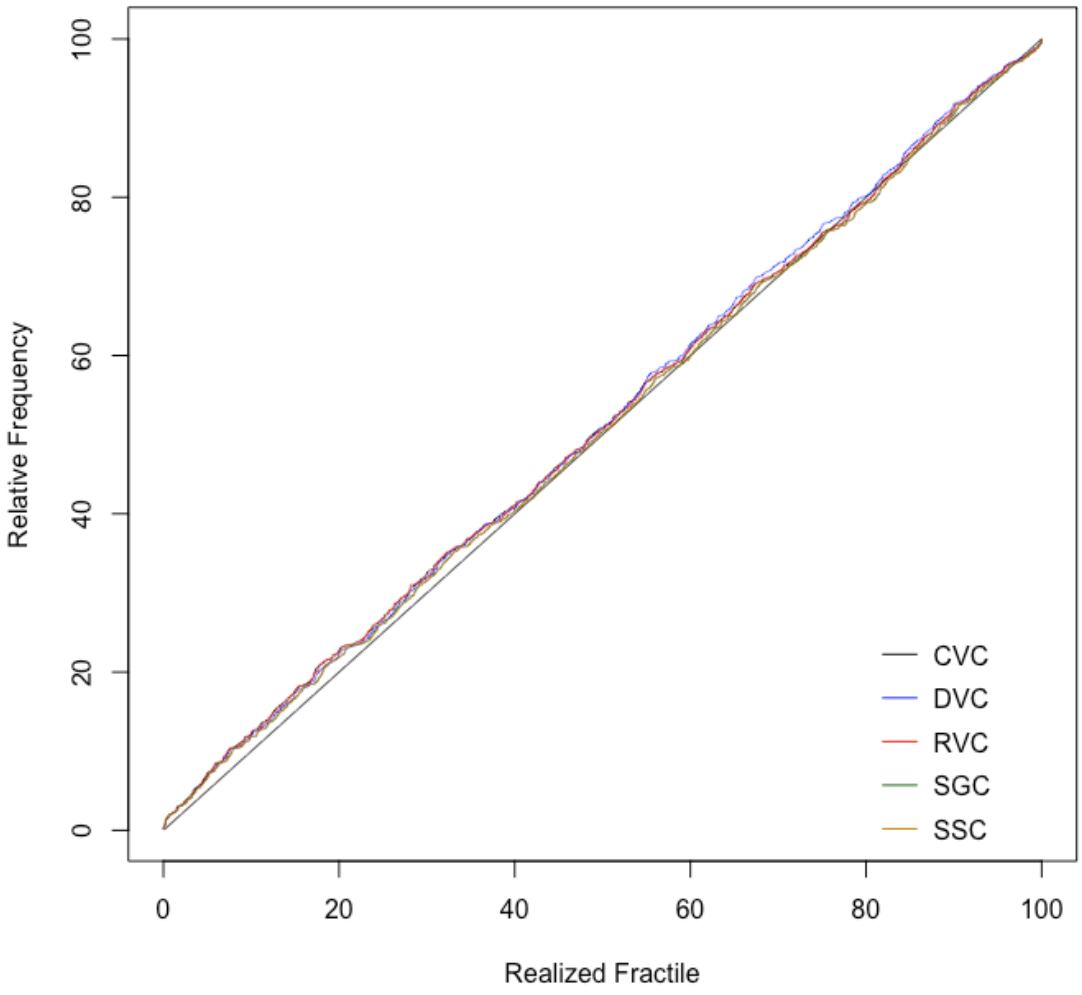

Figure B.15. Calibration plots for the density forecasts of crude oil returns based on the canonical vine copula (CVC), drawable vine copula (DVC), regular vine copula (RVC), standard Gaussian copula (SGC), and standard Student's t copula (SSC) models with skewed Student's t marginal distributions

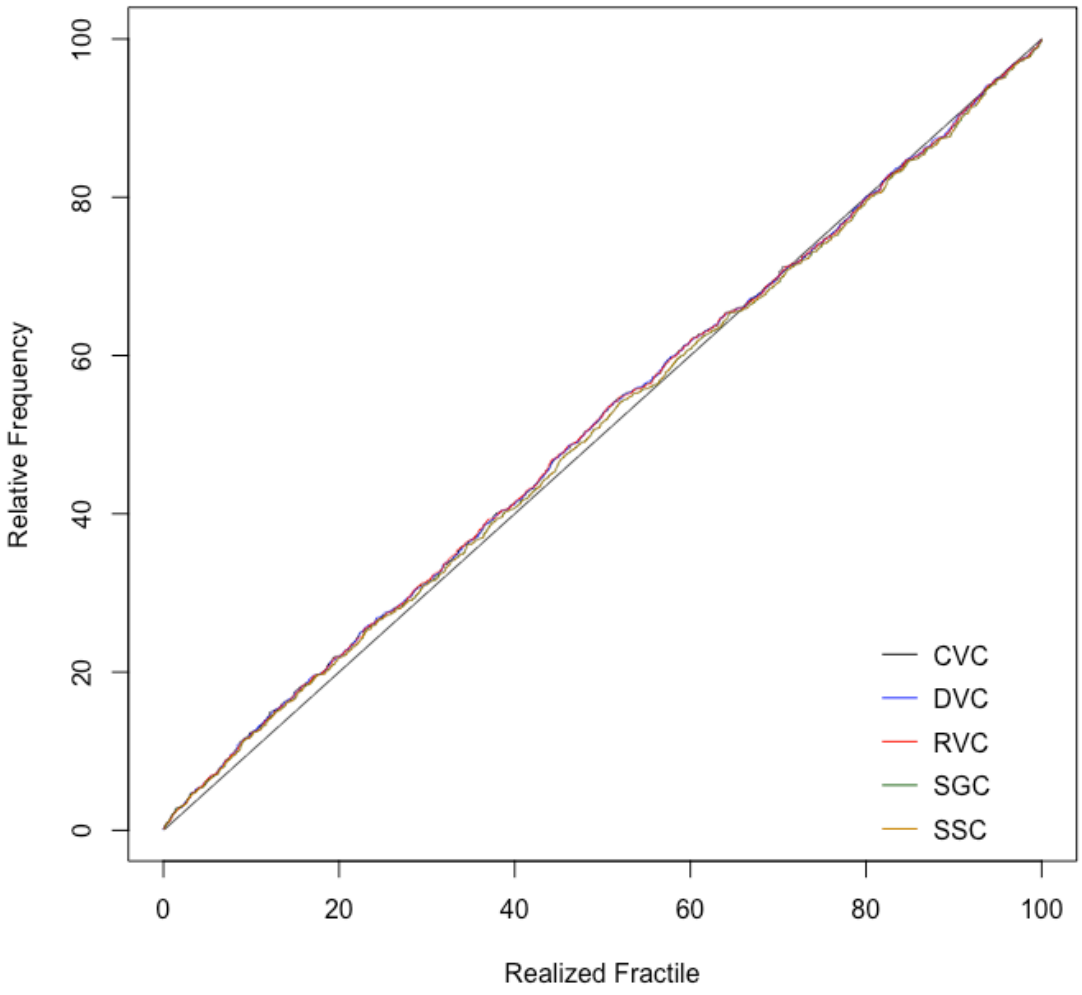

Figure B.16. Calibration plots for the density forecasts of diesel fuel returns based on the canonical vine copula (CVC), drawable vine copula (DVC), regular vine copula (RVC), standard Gaussian copula (SGC), and standard Student's t copula (SSC) models with skewed Student's t marginal distributions

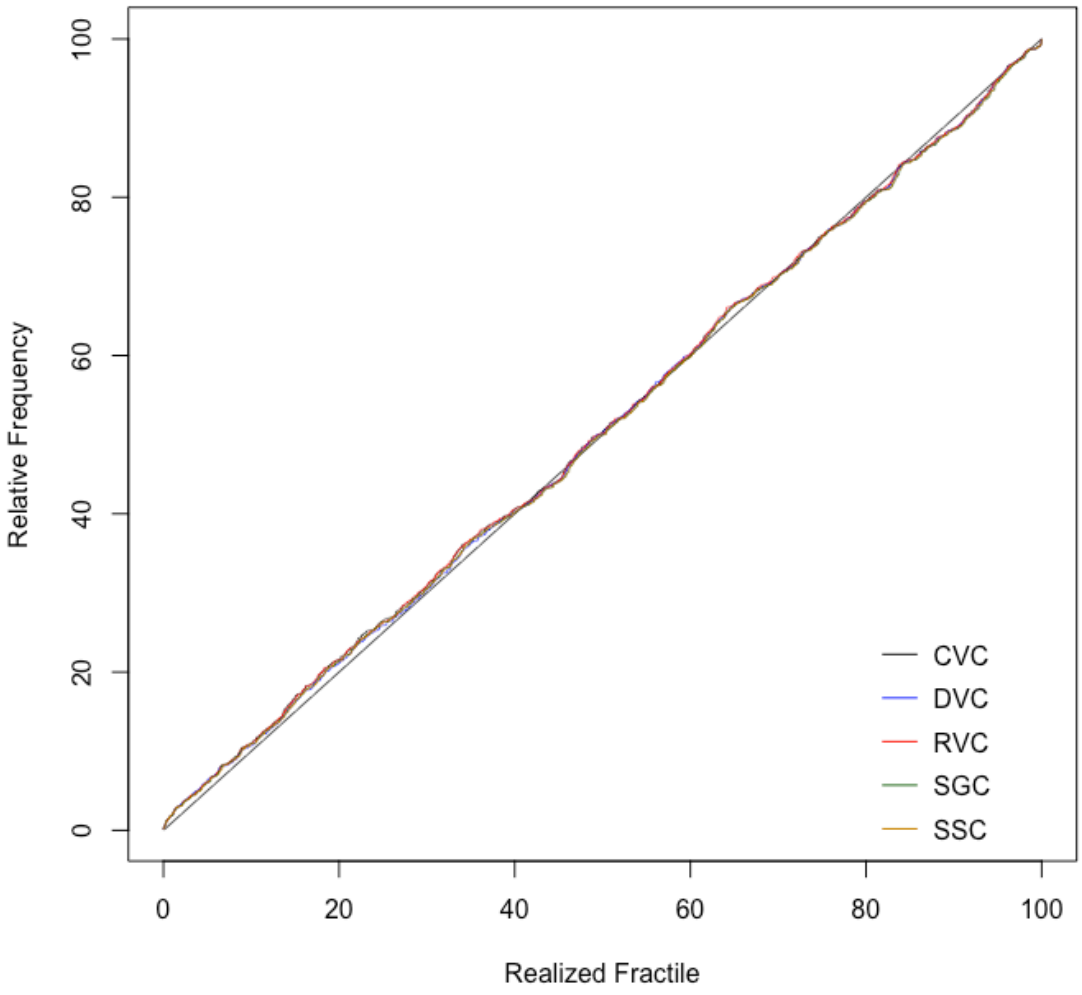

Figure B.17. Calibration plots for the density forecasts of gasoline returns based on the canonical vine copula (CVC), drawable vine copula (DVC), regular vine copula (RVC), standard Gaussian copula (SGC), and standard Student's t copula (SSC) models with skewed Student's t marginal distributions

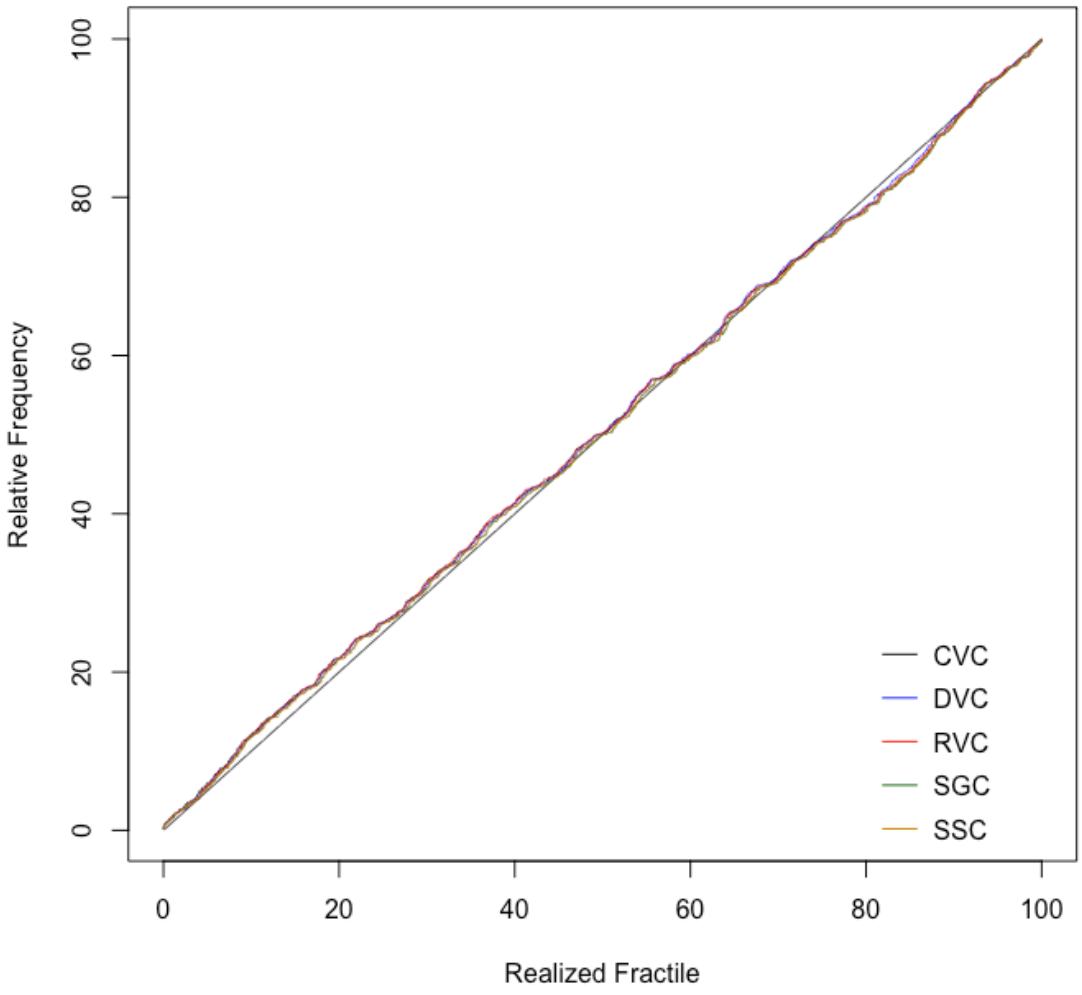

Figure B.18. Calibration plots for the density forecasts of heating oil returns based on the canonical vine copula (CVC), drawable vine copula (DVC), regular vine copula (RVC), standard Gaussian copula (SGC), and standard Student's t copula (SSC) models with skewed Student's t marginal distributions

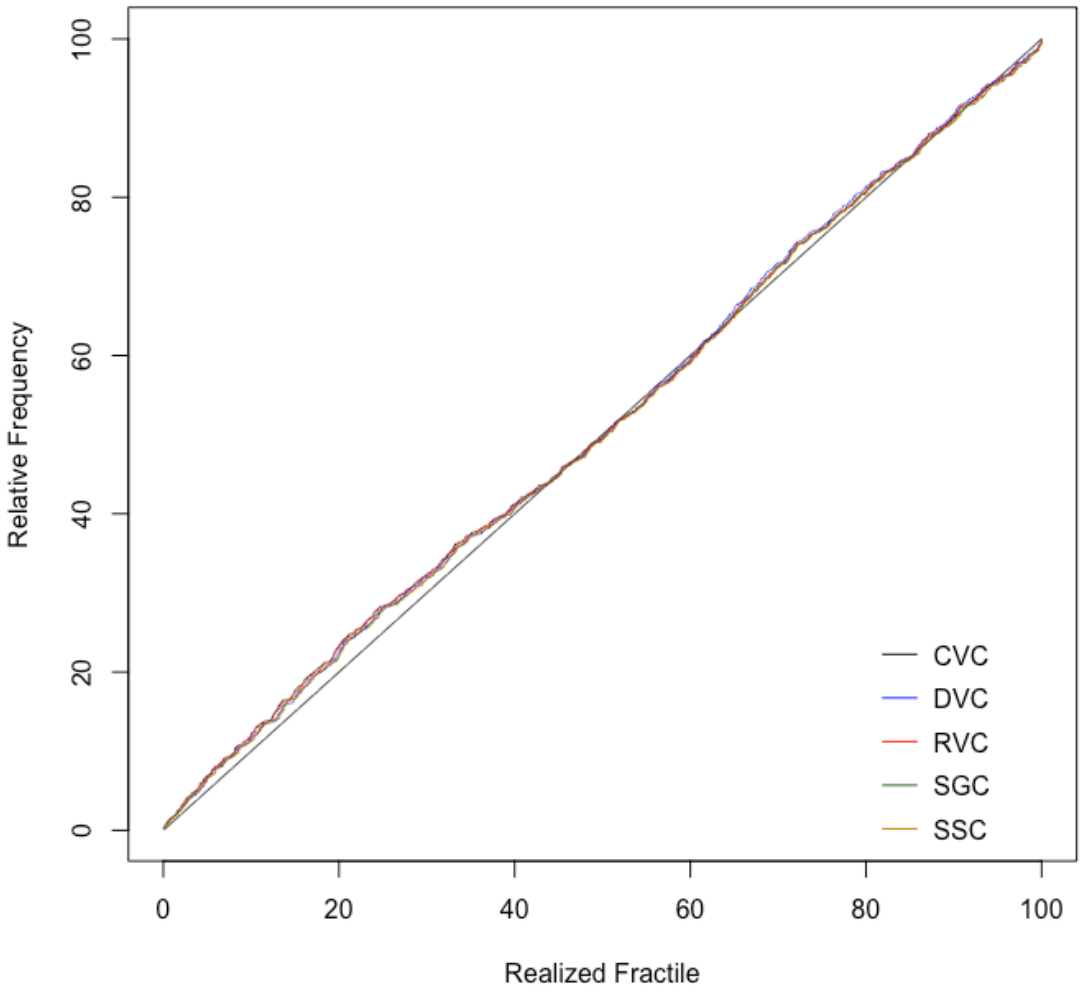

Figure B.19. Calibration plots for the density forecasts of jet fuel returns based on the canonical vine copula (CVC), drawable vine copula (DVC), regular vine copula (RVC), standard Gaussian copula (SGC), and standard Student's t copula (SSC) models with skewed Student's t marginal distributions

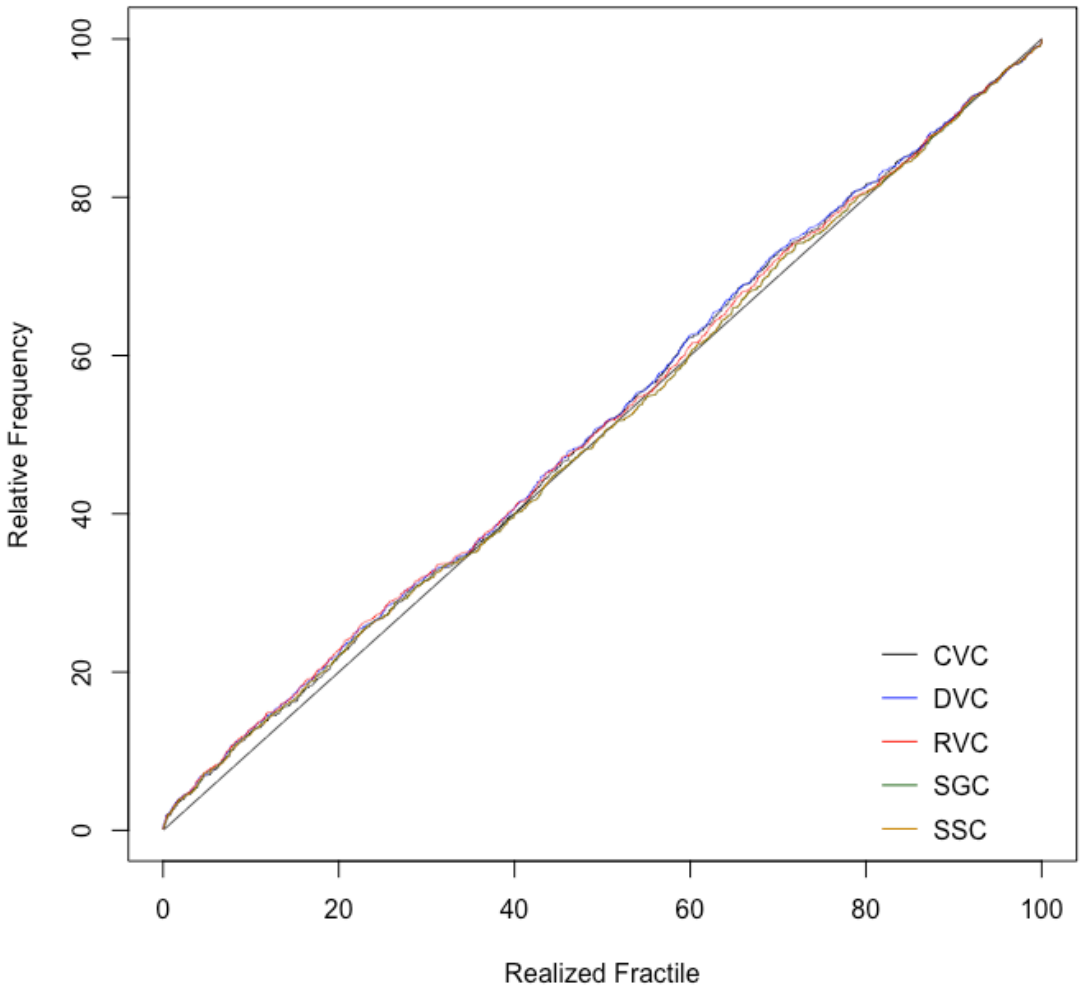

Figure B.20. Calibration plots for the density forecasts of natural gas returns based on the canonical vine copula (CVC), drawable vine copula (DVC), regular vine copula (RVC), standard Gaussian copula (SGC), and standard Student's t copula (SSC) models with skewed Student's t marginal distributions

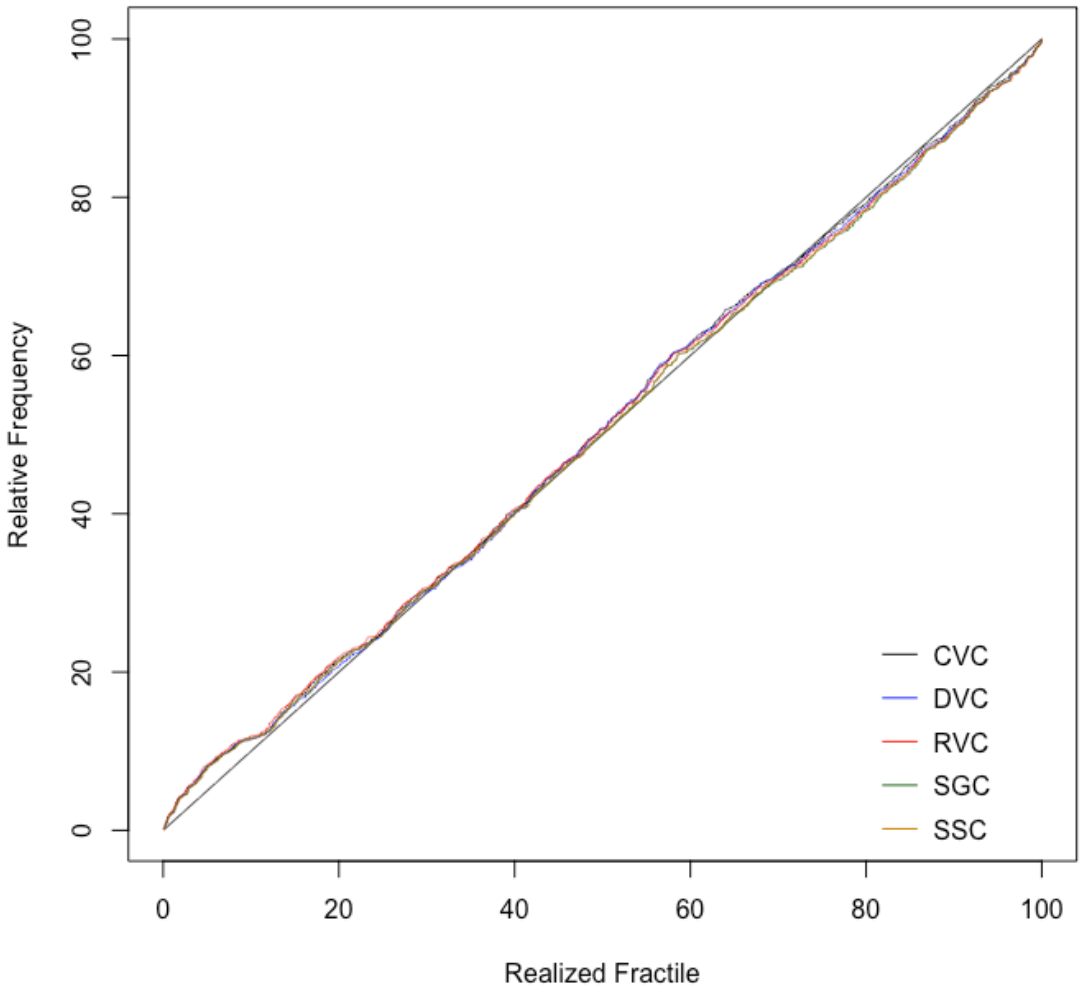

Figure B.21. Calibration plots for the density forecasts of propane returns based on the canonical vine copula (CVC), drawable vine copula (DVC), regular vine copula (RVC), standard Gaussian copula (SGC), and standard Student's t copula (SSC) models with skewed Student's t marginal distributions